

**BILE SALT HYDROXYLATION AS A MECHANISM FOR
DETOXIFICATION IN SPGP KNOCKOUT MICE**

by

DANA NICHOLE FORREST

B.Sc., The University of Regina, 2000

A THESIS SUBMITTED IN PARTIAL FULFILMENT OF
THE REQUIREMENTS FOR THE DEGREE OF

MASTER OF SCIENCE

in

THE FACULTY OF GRADUATE STUDIES
(Department of Biochemistry and Molecular Biology)

We accept this thesis as conforming

to the required standard

THE UNIVERSITY OF BRITISH COLUMBIA

April 2003

© Dana Nichole Forrest, 2003

In presenting this thesis in partial fulfilment of the requirements for an advanced degree at the University of British Columbia, I agree that the Library shall make it freely available for reference and study. I further agree that permission for extensive copying of this thesis for scholarly purposes may be granted by the head of my department or by his or her representatives. It is understood that copying or publication of this thesis for financial gain shall not be allowed without my written permission.

Department of Biochemistry and Molecular Biology

The University of British Columbia
Vancouver, Canada

Date 04/23/03

Abstract

In humans, mutations in the Sister of P-glycoprotein (*spgp*) gene involved in bile salt transport lead to progressive familial intrahepatic cholestasis type 2 (PFIC2). Generation of the *spgp*^{-/-} mice demonstrated that the mice are not affected as severely as humans. Analysis of the biliary bile salt pool of the *spgp*^{-/-} mice indicated the presence of tetrahydroxylated bile salts. However, the transport rate of the hydrophilic bile salts was unaffected. Examination of tetrahydroxylated bile salts as a possible detoxification mechanism requires identification and characterization of the enzyme involved. Development of an HPLC bile salt separation method generated bile salt profiles of *spgp*^{-/-} and wild-type mice fed a normal or 0.5% cholic acid (CA) enriched diet. Analysis of the profiles suggested the 2-day change in diet had little effect on the already elevated levels of tetrahydroxylated bile salt levels in the *spgp*^{-/-} mice. However, wild-type mice produced increased levels of the tetrahydroxylated bile salt when fed the 0.5% CA diet. Three tetrahydroxylated bile salt species were present in the HPLC profiles. Expression analysis of the CYP3A family, the three major enzymes in bile salt synthesis, and five of the main nuclear receptors involved in the regulation of cholesterol and bile salt metabolism was performed using Northern Blot analysis and real-time PCR. When tetrahydroxylated bile salt levels were compared to the mRNA expression levels, there was little correlation to the candidate genes tested. Furthermore, the reduction in CYP7A1 and CYP8B1 expression levels under the 0.5% CA supplemented diet indicated substrates from these pathways are not involved in the synthesis of the tetrahydroxylated bile salts. Consequently, it is believed that bile salt tetrahydroxylation is either regulated at the protein level or is due to expression of a gene not tested.

Table of Contents

ABSTRACT	ii
TABLE OF CONTENTS	iii
LIST OF TABLES	v
LIST OF FIGURES	vi
GLOSSARY OF ABBREVIATIONS	vii
ACKNOWLEDGEMENTS	viii
PUBLICATIONS	ix
1 INTRODUCTION	1
1.1 LIVER PHYSIOLOGY AND FUNCTION BACKGROUND	2
1.2 BILE SALTS	5
1.2.1 <i>Cholesterol Homeostasis</i>	6
1.2.2 <i>Bile Salt Structure</i>	8
1.2.3 <i>Bile Salt Synthesis</i>	11
1.2.4 <i>Bile Salt Function</i>	14
1.2.5 <i>Regulation of Bile Salt Synthesis</i>	14
1.3 BILE FORMATION	15
1.4 SISTER OF P-GLYCOPROTEIN	17
1.5 PROGRESSIVE FAMILIAL INTRAHEPATIC CHOLESTASIS TYPE 2	18
1.6 SPGP ^{-/-} MICE	18
1.7 CYTOCHROME P450 ENZYMES	21
1.7.1 <i>Background to the CYP System</i>	21
1.7.2 <i>Mouse CYP3A Enzymes</i>	23
1.7.3 <i>Regulation of CYP by Nuclear Receptors</i>	25
1.7.4 <i>CYP Interaction with Bile Salts</i>	26
1.7.5 <i>Bile Salts as CYP Substrates</i>	28
1.8 HYPOTHESIS	30
2 MATERIALS AND METHODS	31
2.1 MICE AND ANIMAL TREATMENT	31
2.2 HIGH PERFORMANCE LIQUID CHROMATOGRAPHY OF MOUSE BILE	32
2.3 IDENTITY CONFIRMATION THROUGH MASS SPECTROMETRY	33
2.4 NORTHERN BLOT ANALYSIS	34
2.5 REAL-TIME PCR	38
2.6 STATISTICS	42
3 RESULTS	42

3.1	HIGH PERFORMANCE LIQUID CHROMATOGRAPHY TO DETECT TETRAHYDROXYLATED BILE SALTS	43
3.1.1	<i>Method Optimization</i>	44
3.1.2	<i>Biliary Bile Salt Profile</i>	46
3.1.3	<i>Identification of unknown HPLC peaks using Mass Spectrometry</i>	51
3.2	MRNA EXPRESSION ANALYSIS	53
3.2.1	<i>Control Gene Choice</i>	55
3.2.2	<i>CYP3A mRNA Expression Profile</i>	57
3.2.3	<i>Bile Salt Synthesis CYP mRNA Expression Profile</i>	65
3.2.4	<i>Nuclear Receptor mRNA Expression Profile</i>	69
4	DISCUSSION	72
5	FUTURE WORK	79
6	REFERENCES	84
	APPENDIX	105
	MOUSE DIET	105

List of Tables

Table 1: Summary of primers designed for probe synthesis in the Northern Blot procedure.....	36
Table 2: A BLAST analysis of the probes used for Northern analysis.....	37
Table 3: Summary of primers designed for real-time PCR analysis.	40
Table 4: A BLAST analysis of amplicons and indicate differences in the primers.	41
Table 5: Quantification of bile salts via HPLC.	45
Table 6: Total biliary bile salt levels and the relative levels of biliary tetrahydroxylated bile salts in FVB/NJ mouse bile as determined by HPLC.	50
Table 7: Summary of the frequency of common housekeeping genes as determined from SAGE analysis on 4-day old C57BL mice.....	56
Table 8: Correlation of RPS15 and Cyclophilin to CYP3A mRNA expression in FVB/NJ mice.....	56

List of Figures

Figure 1: A diagram of potential sources of bile salts and their interaction with nuclear receptors to affect gene expression in the hepatocyte	4
Figure 2: The core structure of bile salts with some of the common variations in mice and humans listed in the table	7
Figure 3: Space-filling structure demonstrating the hydrophobicity of bile salts	10
Figure 4: Bile salt biosynthesis	12
Figure 5: Bile flow rate, Bile acid output in wild-type and <i>spgp</i> ^{-/-} mice.	20
Figure 6: Multiple sequence alignment of the mouse CYP3A family	24
Figure 7: Chromatographs of bile salt separation on a Spherisorb S5 ODS2 C-18 reverse phase analytical column.	47
Figure 8: HPLC of <i>spgp</i> ^{-/-} mouse bile revealed peaks not present in the wild-type mouse bile.	48
Figure 9: Taurine-conjugated tetrahydroxylated bile salt isolated from <i>spgp</i> ^{-/-} mice via HPLC and detection through LC/MS/MS	52
Figure 10: Northern Blot Analysis of β -actin and Cyclophilin mRNA levels of FVB/NJ mice	56
Figure 11: Northern Blot Analysis of CYP3A mRNA levels of C57BL/6J mice on a normal diet	58
Figure 12: Northern Blot Analysis of CYP3A mRNA levels from mice of a FVB/NJ background on a normal diet and 0.5% CA diet for two days prior to sacrifice	59
Figure 13: Real-time PCR Analysis of CYP3A mRNA levels from mice of a FVB/NJ background	64
Figure 14: Northern Blot Analysis of bile salt biosynthesis CYP mRNA levels of C57BL/6J mice on a normal diet, FVB/NJ mice on a normal diet, and FVB/NJ mice fed a 0.5% CA supplemented diet for two days prior to sacrifice.	66
Figure 15: Real-time PCR Analysis of mRNA levels of enzymes involved in bile salt synthesis from mice of a FVB/NJ background	67
Figure 16: Real-time PCR Analysis of mRNA levels of nuclear receptors affected by bile salts from mice of a FVB/NJ background	71

Glossary of Abbreviations

ABC	ATP binding cassette transporter
ACAT	acyl-CoA:cholesterol acyltransferase
Acetyl CoA	acetyl-Co enzyme A
BADF	bile acid dependent bile flow
BAIF	bile salt independent bile flow
BFR	bile flow rate
β MCA	β -muricholate
BSEP	bile salt export protein
CA	cholic acid
CDCA	chenodeoxycholic acid
CTX	Cerebrotendinous xanthomatosis
CYP	cytochrome P450
CYP27	sterol 27-hydroxylase
CYP7A1	cholesterol 7 α -hydroxylase
CYP8B1	sterol 12 α -hydroxylase
DCA	deoxycholic acid
EHC	enterohepatic circulation
FXR	farnesol X-activated receptor
GUDCA	glycoursodeoxycholic acid
HMG-CoA	3-hydroxy-3-methylglutaryl CoA
HPLC	high performance liquid chromatography
LCA	lithocholic acid
LCAT	lecithin cholesterol acyl transferase
LRH-1	liver receptor homolog 1
LXR	liver orphan receptor
MCA	muricholic acid
MS	mass spectrometry
NTCP	sodium dependant taurocholate co-transporting protein
PFIC2	Progressive familial intrahepatic cholestasis type 2
PPAR	peroxisome proliferator-activated receptor
PXR	pregnane X receptor
RXR	retinoid X receptors
SHP-1	short heterodimer partner
Spgp	sister of P-Glycoprotein
SREBPs	sterol regulatory element binding proteins
T β MCA	tauro- β -muricholate
TCA	taurocholic acid
TCDCa	taurochenodeoxycholic acid
TDCA	taurodeoxycholic acid
TLCA	tauroolithocholic acid
TMCA	tauromuricholic acid
TUDCA	tauroursodeoxycholic acid
UDCA	ursodeoxycholic acid

Acknowledgements

I would like to thank my supervisor Dr. Victor Ling for his help, insight, and questions. Sincere thanks also go out to all members of the Ling lab. I also have deep appreciation for the technical advice from Dr Renxue Wang, Ping Lam, and Lin Liu.

Special thanks goes to Dr Alan Hofmann and Dr. Lee Hagey for their assistance in the development of the HPLC method and for answering so many of my questions. A thanks also goes to my committee members Dr. Roger Brownsey and Dr. Stelvio Bandiera who always had advice and interesting questions.

Gratitude and thanks to my mother, Patricia Rourke and my grandmother, Margaret Rourke, for their emotional and financial support. Finally, thanks to my husband, Greg, who always provided emotional support and a sense of humor.

Publications

Perwaiz, S., D. Forrest, D. Mignault, B. Tuchweber, M.J. Phillip, R. Wang, V. Ling, and I.M. Yousef, *Appearance of atypical 3 α ,6 β ,7 β ,12 α -tetrahydroxy-5 β -cholan-24-oic acid in spgp knockout mice*. J Lipid Res, 2003. **44**(3): p. 494-502.

Wang, R., P. Lam, L. Liu, D. Forrest, I.M. Yousef, D. Mignault, B. Tuchweber, M.J. Phillips, and V. Ling, *Severe cholestasis induced by cholic acid feeding in knockout mice of Sister of P-glycoprotein*. J Clin Invest, 2003 (Submitted).

1 Introduction

Sister of P-glycoprotein (Spgp) has been identified as the bile salt export pump in the canalicular membrane of the hepatocyte [1, 2]. Mutations in human *spgp* are linked to progressive familial intrahepatic cholestasis type 2 (PFIC2) where bile salt transport in patients is only 1% of normal. Although PFIC2 is fatal in infancy or childhood, generation of *spgp*^{-/-} mice demonstrated the mice are viable and fertile [3]. The study of the *spgp*^{-/-} mice provides insight into potential PFIC2 therapies. Furthermore, they also allow the study of biotransformations in cholestasis that may be detoxification mechanisms and alternate canalicular bile salt transporters.

Unlike humans, the *spgp*^{-/-} mice were still able to transport 25% the bile salt of the wild-type mice. The bile salt pool of the *spgp*^{-/-} mice was more hydrophilic than that of the wild-type mice, with the notable presence of a tetrahydroxylated bile salt. The altered bile salt composition is interesting as hydrophilic bile salts are often administered in the treatment of cholestasis [4]. While hydrophobic bile salts like chenodeoxycholic acid (CDCA) can induce cellular damage, result in membrane perturbations, and cause reduction of cytochrome P450 (CYP) levels, concurrent administration of hydrophilic bile salts mitigate the damaging effects [4-6]. Hydroxylation of bile salts has also been shown to provide recovery from lithocholic acid (LCA) induced cholestasis [7]. These factors make the presence of the tetrahydroxylated bile salt the result of a potential detoxification mechanism and may help explain the viability of the *spgp*^{-/-} mice. A target of CYP3A was identified due to the subfamily's role in bile salt synthesis and bile salt hydroxylation [8-10]. Some inducers of CYP3A differ between mouse and humans, possibly leading to protection in mice against a phenotype displayed in humans [11, 12]. Consequently,

levels of tetrahydroxylated bile salts were examined to observe a potential correlation to CYP3A expression.

1.1 Liver Physiology and Function Background

The liver is a well-vascularized organ within the abdominal cavity beneath and attached to the diaphragm [13]. A high degree of vascularization in the liver is necessary as it filters blood to help detoxify compounds in the body. The liver parenchymal cells (hepatocytes) represent about 70% of the total number of cells in the liver and these form a one cell thick layer, lining the sinusoids [14]. Hepatocytes are polarized with a sinusoidal membrane facing the blood and a canalicular membrane facing the canaliculi. The canalicular domain is rich in microvilli and is separated from the plasma membrane by tight junctions. Liver endothelial cells cover the hepatocytes, forming a barrier between blood and the hepatocytes. Consequently, blood must go through pores in the endothelial layer to reach the hepatocytes.

The blood in the portal vein has just passed through the capillary bed of the alimentary tract, so it is rich in nutrients and other compounds absorbed from the intestine. However, portal vein blood is low in oxygen. Oxygenated blood enters the liver from the hepatic artery. The blood from the portal vein and hepatic artery mixes in the sinusoids and leaves the liver through the central vein.

The hepatocytes closest to the portal vein are known as periportal hepatocytes while those closest to the central vein are perivenous hepatocytes. The periportal hepatocytes are the first hepatocytes to receive the nutrients and toxins from the blood. These cells are specialized in oxidative energy metabolism including fatty acid oxidation and cholesterol synthesis. In comparison, the perivenous hepatocytes are specialized in lipogenesis, glycolysis, and

biotransformation activities [15]. Basal CYP levels are higher in the perivenous hepatocytes than in the periportal hepatocytes and the perivenous hepatocytes experience faster induction of CYPs [15]. The zonation of the hepatocytes is thought to be a combination of various factors including the decrease in the O₂ concentration in the perivenous region and hormone gradients.

Bile is secreted from hepatocytes into the bile canaliculi, small channels formed by the plasma membrane between two hepatocytes [13]. The canaliculi form a branching network that drain the bile into the canals of Hering, which then drain into the bile ducts [13]. Due to the lipophilic composition of bile, bile is involved with the removal of hydrophobic compounds from the liver and aids in their elimination *via* fecal excretion. Bile may be stored in the gallbladder before being secreted into the intestine. Once in the intestine, bile aids digestion and facilitates fat absorption.

Since the liver is involved in the uptake and secretion of a large variety of compounds, the basolateral and canalicular membranes contain many transport proteins. On the basolateral membrane, several transporters have been identified including the small organic cation transporter (oct1), sodium dependant taurocholate co-transporting protein (NTCP), and the organic anion transporting polypeptides (oatp-1 and oatp-2) [16]. The canalicular membrane contains transporters to transport compounds for bile formation. Most of the identified canalicular transporters belong to the ATP binding cassette (ABC) transporter super family and consequently, share many common structural features [17]. The canalicular multispecific organic

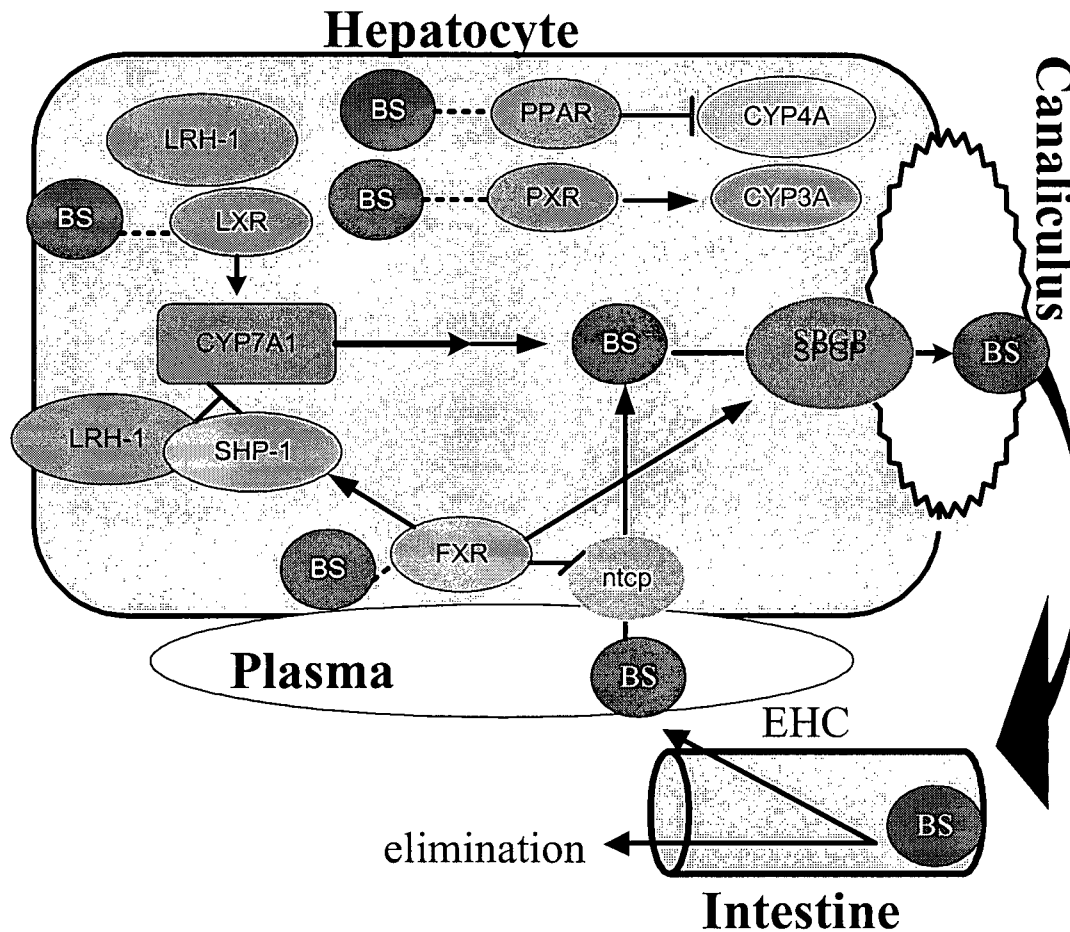


Figure 1: A diagram of potential sources of bile salts (BS) and their interaction with nuclear receptors to affect gene expression in the hepatocyte. Cholesterol (Chl) may be obtained through dietary absorption or through synthesis from Acetyl-Coenzyme A (Ac). High cholesterol levels lead to increased levels of oxysterols (OX). Oxysterols are capable of binding to SREBPs, which decreases cholesterol uptake and synthesis. The oxysterols also affect cholesterol homeostasis through activation of LXR. In combination with LRH-1, LXR induces expression of one of the main bile synthesis enzymes, CYP7A1, to convert some of the cholesterol into bile salts. Besides de novo synthesis from cholesterol, bile salts may also be obtained through uptake from the plasma by NTCP on the basolateral membrane. Increased bile salt levels within the hepatocyte leads to activation of FXR. FXR induces expression of Sgpp to increase transport of bile salts out of the hepatocyte into the canaliculi. FXR also induces SHP-1, which represses CYP7A1 expression through antagonism of LRH-1. Finally, FXR can inhibit NTCP expression, thus decreasing the amount of bile salt reabsorbed by the hepatocyte from the blood. Bile salts may also activate PXR, which induces expression of the CYP3A family of enzymes as a detoxification mechanism. Once bile salts are transported into the canaliculi, they are stored in the gall bladder and released to aid in the absorption of dietary lipids. Most bile salts are transported out of the intestine, back into the blood through enterohepatic circulation (EHC). However, very toxic bile salts are not reabsorbed and are eliminated through fecal excretion.

anion transporter cMOAT/MRP2 eliminates anions, glutathione, glucuronide, and sulfate conjugates while MDR3 transports phosphatidylcholine [16, 18]. Finally, the major bile salt transporter is the bile salt export pump (BSEP) also known as Spgp [1, 2].

An important function of the liver is detoxification of compounds filtered from the blood. The main detoxification pathways include chemical modification through oxidoreductases, hydrolases, and transferases, and the synthesis and secretion of bile to remove fat-soluble compounds from the body. Oxidoreductases and hydrolases are often used in Phase I metabolism to generate sites that may be used in Phase II metabolism for conjugation. Phase I reactions tend to increase the polarity of the compounds, thus enhancing their potential to be excreted. However, this process may create active or toxic metabolites. In Phase II reactions, groups such as acetate, amino acids, sulfate, glucuronic acid, or glutathione may be added to the metabolically active sites through reactions catalyzed by transferases. Phase II metabolism produces products that are usually less toxic, more water soluble and less biologically active than the parent compound.

1.2 Bile salts

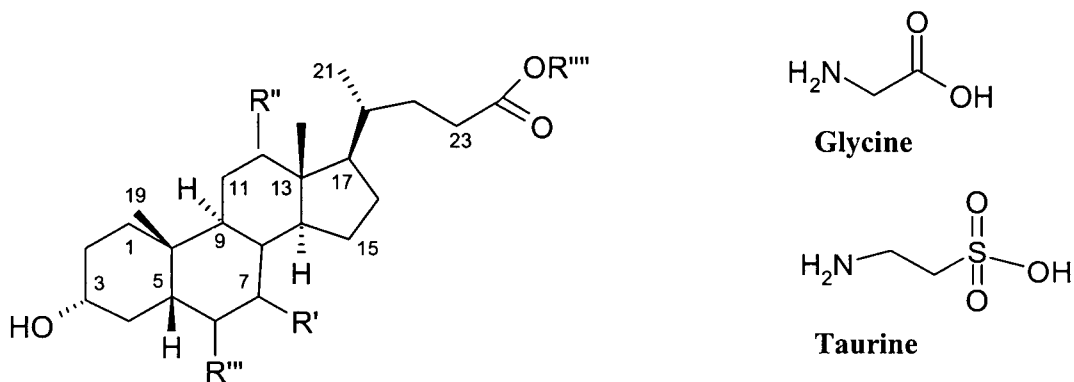
As demonstrated in Figure 1, bile salts are synthesized and conjugated in the liver, secreted into the bile, stored in the gallbladder, released into the intestine, re-absorbed into the blood from the intestine, and returned to the liver *via* the portal vein in a process known as enterohepatic circulation (EHC). During periods of fasting, bile salts are removed from the blood by the periportal hepatocytes and then secreted into the bile [16]. Feeding periods require more bile salts than are available through periportal uptake so bile salts are actively synthesized in the perivenous hepatocytes [19]. Although periportal hepatocytes are capable of bile salt synthesis,

the intracellular bile salt levels resulting from uptake inhibit synthesis [20]. Both periportal and perivenous hepatocytes secrete bile salts resulting in the main driving force for bile acid dependent bile flow (BADF) [21]. The total amount of bile salt in EHC is defined as the circulating bile salt pool.

1.2.1 Cholesterol Homeostasis

Besides being an important component of biological membranes, cholesterol is also the sole precursor of bile salts, steroid hormones, and some vitamins. The cholesterol pool is maintained through uptake of dietary cholesterol and *de novo* synthesis from acetyl-Coenzyme A (Acetyl CoA) in a series of enzymatic steps, mainly confined to the endoplasmic reticulum in the periportal region of the liver [22]. The rate-controlling enzyme in cholesterol synthesis from acetyl-CoA is 3-hydroxy-3-methylglutaryl CoA (HMG-CoA) reductase [22]. Many of the genes involved in cholesterol biosynthesis like HMG-CoA reductase and the LDL receptor are regulated by the sterol regulatory element binding proteins (SREBPs) [23].

Animals are incapable of degrading the steroid nucleus of cholesterol so free cholesterol reduction must occur through bile salt synthesis, biliary excretion, or cholesterol storage. Although animals cannot degrade the steroid nucleus, they can hydroxylate the steroid nucleus and shorten the side chain to create bile salts. Besides being an end product of cholesterol metabolism, bile salts also promote the secretion of free cholesterol from hepatocytes into the bile. Those bile salts and cholesterol that are not reabsorbed in the intestine are eliminated through fecal excretion. A less significant method is to store cholesterol by esterifying the free cholesterol [24]. Since this is a storage form, the rate of interconversion between free cholesterol and the esterified form is important and is regulated by either lecithin cholesterol acyl transferase



R'	R''	R'''	Name
α -OH	α -OH	H	Cholic acid
α -OH	H	H	Chenodeoxycholic acid
H	α -OH	H	Deoxycholic acid
β -OH	H	H	Ursodeoxycholic acid
H	H	H	Lithocholic acid
β -OH	H	β -OH	β -muricholic acid
α -OH	H	β -OH	α -muricholic acid
β -OH	H	α -OH	Ω -muricholic acid
β -OH	α -OH	β -OH	3 α , 6 β , 7 β , 12 α -tetrahydroxy-5 β chol-24-oic acid
α -OH	α -OH	β -OH	3 α , 6 β , 7 α , 12 α -tetrahydroxy-5 β chol-24-oic acid

Figure 2: The core structure of bile salts with some of the common variations in mice and humans listed in the table. All bile salts have a 3 α hydroxy group. In some forms of cholestasis, there is also potential for tetrahydroxylated bile salts to form that are hydroxylated at the 1C [25]. The numbering system follows the standard numbering system for a steroid nucleus. R''' may consist of a H, a glycine residue or a taurine residue.

(LCAT) or acyl-CoA: cholesterol acyltransferase (ACAT)[26, 27]. To obtain free cholesterol again, there are two esterases that recognize cholesterol esters, one in lysosomes and one that is membrane associated and in the cytosol [28].

1.2.2 Bile Salt Structure

The common bile salt structure is indicated in Figure 2 and consists of a 19 carbon saturated sterol nucleus, an α -orientated hydroxyl group at C3, and a branched five carbon saturated side chain, ending in a carboxylic acid [29]. Both the acid and the salt form are present at physiological pH, and while the salt is predominant, “bile acid” and “bile salt” may be used interchangeably. Unlike the planar ring system of cholesterol, bile salts have a β -orientated hydrogen at C5 resulting in a bend in the steroid nucleus.

Free bile salts have pKa values around 5.0. The pKa values are significantly lowered upon conjugation to an amino acid. Since conjugation reduces the pKa of a bile salt, at a given pH, a larger fraction will be in the ionized form leading to increased solubility [30]. Glycine conjugates have a pKa values around 3.9 while taurine conjugates have pKa values less than 1 [31]. As conjugation results in the complete ionization of the bile salts, they are impermeable to membranes.

The addition of polar moieties onto the steroid nucleus through Phase II detoxification causes a reduction in the transport of the bile salts across the intestinal mucosa while enhancing the urinary excretion. Sulfation and glucuronidation are common additions to hydroxyl groups on the steroid nucleus and lead to the accelerated loss of bile salts from EHC. However, only LCA tends to be sulfated in humans [29].

The common bile salts differ from each other primarily in the number, position, and orientation of the hydroxyl groups on the sterol ring. Common bile salt structures are listed in Figure 2 with the structural differences in the bile salts resulting in different properties [32]. As the number of hydroxyl groups decreases, the toxicity of the bile salt increases. This relationship leads to the hypothesis that bile salt hydroxylases act as a method of detoxification. All bile salts have at least one hydroxyl group at the 3α position with hydroxylations common at C6, C7, and C12. Common mammalian bile salts are mono-, di-, or tri-hydroxylated.

In some forms of intrahepatic cholestasis in humans, tetrahydroxylated bile salts may be produced [33, 34]. When radiolabeled CA was administered to mildly cholestatic males, 10% of the radioactivity was recovered as tetrahydroxylated bile salts in the urine [33]. Five metabolites were detected with the major metabolite of the fraction being $3\alpha,6\alpha,7\alpha,12\alpha$ -tetrahydroxy- 5β -cholanoic acid and a minor component in the form of $1\beta,3\alpha,7\alpha,12\alpha$ -tetrahydroxy- 5β -cholanoic acid. These two forms of tetrahydroxylated bile salts have also been identified during pregnancy [34]. In normal pregnant women, the relative amount of tetrahydroxylated bile salt was 1-2% while during the recurrent cholestasis of pregnancy, the value increased to 10% [34].

The orientation of the hydroxyl group is also important as it may be in the α or β conformation on the steroid nucleus. When visualized in three dimensions, the polar groups appear to be asymmetrically distributed on the steroid nucleus [35]. If the polar groups are located on the same face of the molecule, these groups will become hydrated in aqueous solution causing that face to become hydrophilic and the opposite side to be hydrophobic as seen in Figure 3.

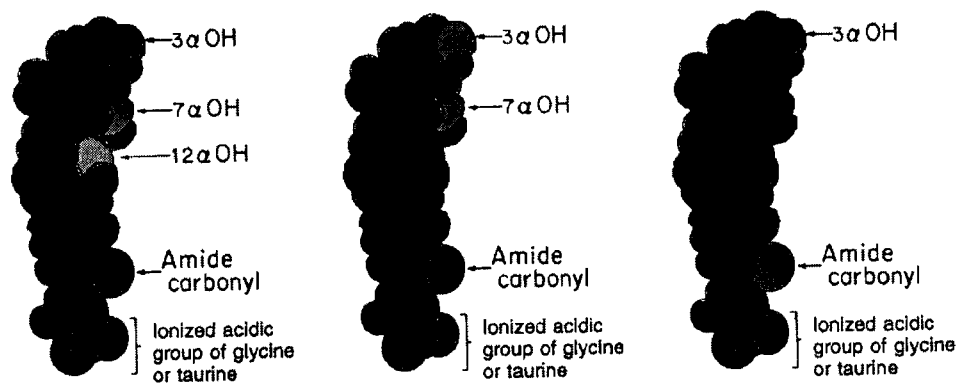


Figure 3: Space-filling structure demonstrating the hydrophobicity of bile salts. The hydrophilic hydroxy groups conjugated groups are indicated in red [35]. The more hydrophilic atoms there are on one face of the molecule, the more hydrophilic the molecules.

Conversely, when the polar groups are scattered, a hydrophilic face is not formed, and, they exhibit poor solubility in aqueous solutions and are toxic to the organism. The amphipathic nature of the bile salts provides them with many properties of detergents, resulting in aggregation of bile salts as micelles in aqueous solutions, which aid in the solubilization of more hydrophobic compounds.

Micelle formation occurs above a threshold termed the critical micellar concentration [29]. At concentrations slightly greater than the critical micellar concentration, bile salts interact *via* their hydrophobic surfaces to form micelles consisting of 2-13 molecules. Biological property differences in the various bile salts results from their different relative affinities for the aqueous versus lipid environments; a property termed hydrophilic-hydrophobic balance. The relative hydrophobic activity decreases as the number of hydroxyl groups increase and the hydroxyl group orientation forms a hydrophilic face [29]. Ionization of the bile salt also results in decreased hydrophobic activity [36]. It is also possible to increase the hydrophobic activity through elevation of the ionic strength of the solution since the positively charged ions partially neutralize the negative charge of the bile salt [36].

1.2.3 Bile Salt Synthesis

Bile salts are synthesized in the pericentral hepatocytes from the sole precursor of cholesterol through a multi-enzyme process illustrated in Figure 4 involving hydroxylation of the steroid nucleus and oxidative cleavage of the side chain [29]. Mammals possess two separate pathways for bile salt biosynthesis: a neutral microsomal pathway and an acidic mitochondrial pathway [37]. The bile salts produced *de novo* in the liver are called primary bile salts. The neutral route is initiated by the rate limiting reaction of the conversion of cholesterol to 7α -cholesterol by

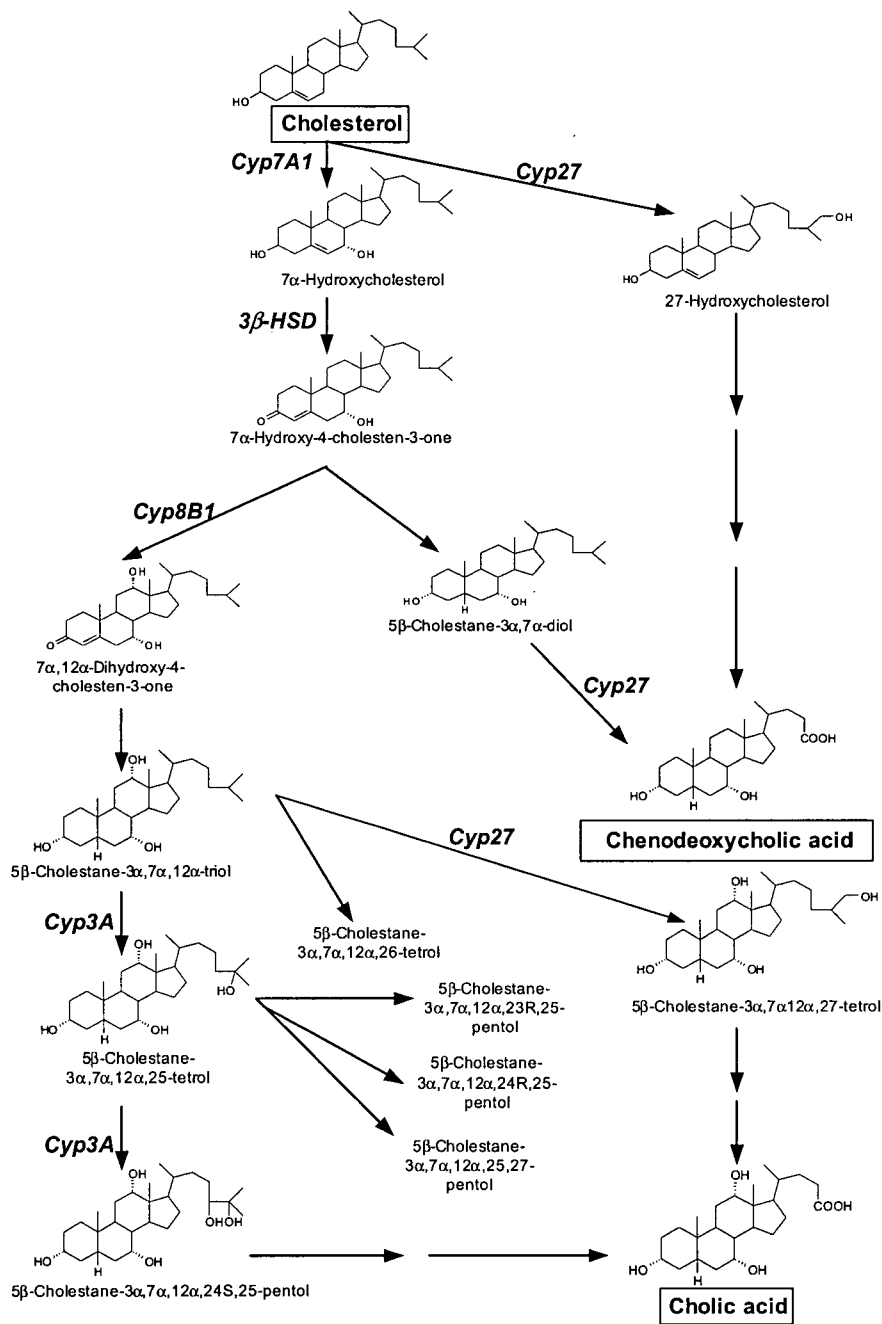


Figure 4: Bile salt biosynthesis [11]. The classic pathway is regulated by CYP7A1. CYP27 is the enzyme at the beginning of the alternative pathway. Although the CYP3A family is involved with side chain hydroxylation, they may also be involved in hydroxylation of the steroid nucleus [9].

hydroxylation of the steroid nucleus by cholesterol 7 α -hydroxylase (CYP7A1) [38]. The acidic pathway begins with hydroxylation of the side chain by sterol 27-hydroxylase (CYP27) [39].

While the classic pathway preferentially produces CA, the acidic pathway preferentially produces CDCA [37, 40]. CA is a trihydroxy bile salt that has α -hydroxy groups at C3, C7, and C12 while CDC is a dihydroxy bile salt with α -hydroxyl groups at C3 and C7. Levels of sterol 12 α -hydroxylase (CYP8B1) affect the ratio of primary bile salts as high levels of CYP8B1 lead to increased production of CA [41]. Rats and mice convert the majority of their CDCA to the trihydroxy muricholic acids (MCAs) [40, 42]. Most human bile salts are conjugated to glycine or taurine residues in a ratio of approximately 3:1 although the ratio may be affected by taurine dietary intake [43]. The preferred conjugated form is species dependent as human bile salts are preferentially conjugated to glycine while mouse bile salts are usually conjugated to taurine.

As the bile salts enter the intestine, transformations by the intestinal bacteria can generate at least 15-20 metabolites from the primary bile salts [40]. Bile salts produced by modification of the primary bile salts are known as secondary bile salts. Known microbial biotransformations of bile salts include deconjugation yielding free bile salts, oxidation of hydroxyl groups at C3, C7, and C12, reduction of oxo groups yielding epimer bile salts, and 7 α -dehydroxylation [44, 45]. The most common reactions are 7 α -dehydroxylation that produces deoxycholic acid (DCA) and LCA and epimerization of the 7 α -hydroxyl group to generate ursodeoxycholic acid (UDCA). These unconjugated bile salts may be reabsorbed into the liver to undergo conjugation again. LCA is often conjugated to a sulfate group at C3 that inhibits reabsorption from the small intestine and aids in elimination of the highly toxic bile salt.

1.2.4 Bile Salt Function

Bile salts play an important role in cholesterol homeostasis through several mechanisms. First, approximately 50% of cholesterol is eliminated by metabolic conversion to bile salts [46, 47]. The remaining cholesterol is eliminated through the bile where bile salts solubilize cholesterol through the formation of micelles [48]. EHC of bile salts is significant as this movement helps generate bile flow [29]. Bile salts also act as ligands for several nuclear receptors involved in the regulation of cholesterol synthesis, hepatic uptake, and excretion [49, 50]. Besides cholesterol homeostasis, bile salts are also necessary for the biliary elimination of various toxins and aid in the intestinal absorption of dietary fats and fat-soluble vitamins.

1.2.5 Regulation of Bile Salt Synthesis

Although bile salts are transported out of the liver, 90% of them are re-absorbed in the intestine and return to the liver through EHC. Increased hepatic bile salt levels appear to result in negative feedback of CYP7A1 expression [19, 51]. Structural features of bile salts are likely important as CYP7A1 expression is down-regulated by hydrophobic but not hydrophilic bile salts [52, 53]. Likely this effect is due to bile salts acting as ligands for the farnesol X-activated receptor (FXR) [54]. CYP27 mRNA is down-regulated by hydrophobic bile salts feeding, possibly by inhibiting the recruitment of coactivators for the peroxisome proliferator-activated receptor (PPAR α) [55]. CYP8B1, which determines the ratio of CA to CDCA, is regulated through FXR and may also be regulated by PPAR α binding to an imperfect recognition site [56].

The liver orphan receptor (LXR) exerts positive regulation on CYP7A1 [57, 58]. Figure 1 demonstrates that elevated cholesterol levels result in an upregulation of the CYP7A1 pathway, probably due to the increased levels of oxysterols acting as ligands for LXR [59, 60].

Furthermore, naturally occurring 6 α -hydroxylated bile salts act as ligands for LXR α to induce CYP7A1 expression [61]. Although cholesterol impacts CYP7A1 expression, elevated cholesterol levels only appear to impact CYP27 expression after prolonged exposure [62]. One theory is that bile salt synthesis from the mitochondrial pathway is regulated by cholesterol transport into the mitochondria [63]. In CYP27 overexpressing mice, there was altered biliary bile salt composition and increased fecal levels of neutral steroids in females but not in males [64].

1.3 Bile Formation

Bile is an aqueous solution containing bile salts, phospholipids, cholesterol, various proteins, bilirubin, various electrolytes, and some trace metals [18, 65]. When hepatocytes take up endogenous and exogenous compounds from the blood, many of these compounds will be secreted into the bile. Bile formation serves as a mechanism to remove toxic compounds through fecal excretion. Biliary phospholipids combine with bile salts to form micelles and aid in lipid absorption and the biliary elimination of hydrophobic compounds [48, 66].

Cholestasis is a condition in which bile excretion is blocked, either in the liver or bile ducts [16, 17]. There are several causes of cholestasis including genetic defects, infection, and bile duct obstruction by gallstones [67]. When bile excretion is inhibited, the accumulation of bile salts in the liver may have damaging effects on the hepatocytes due to their detergent effects [68]. Steatorrhea and hypoprothrombinemia may also result due to poor fat and vitamin K absorption from the intestine. Clinically, cholestasis is suspected if the patient experiences jaundice, digestive problems, nausea, or dark urine. Liver function indicators may be used to diagnose the patient as many cholestatic patients have elevated levels of bilirubin, gamma-glutamyl

transferase, and alkaline phosphatase. Progressive cholestasis occurs when there is a significant blockage of bile secretion into the intestine and no compensatory mechanism is available.

Bile formation is an osmotic process generated by the active transport of compounds across the canalicular membrane. Canalicular secretion of bile salts and other organic compounds are rate-limiting steps in hepatobiliary transport. There are two components in bile formation: BADF and bile salt independent bile flow (BAIF). BAIF is driven by organic anions and glutathione with the magnitude of the flow varying between species [21, 69, 70]. In healthy mice, BAIF is the major contributor to bile flow. It is essential that bile salts are efficiently conserved through EHC as the transport of bile salts through periportal hepatocytes is the driving force for BADF [29].

Up to 98% of some bile salt species may be returned to the liver during one passage of the blood through the liver [32]. Uptake of conjugated bile salts is highly efficient and the conjugation to glycine or taurine appears to be more important to uptake than the hydroxylation status [71, 72]. The charge of the side chain may also influence hepatic uptake as monoanionic and uncharged bile salts are taken up more rapidly than zwitterionic and cationic bile salts [72]. Usually the highest uptake into the liver occurs for the bile salt that predominates a given species [29].

Bile salt uptake by the hepatocytes occurs against a chemical and electric gradient. Most of the hepatic uptake of bile salts is accomplished by a carrier mediated sodium dependant energy requiring system [73]. Following hepatic uptake, the bile salts are translocated from the sinusoidal membrane to the canalicular membrane through a poorly understood mechanism.

Once at the canalicular membrane, bile salts are transported out of the hepatocyte through an active transport process mediated by Spgp, probably the rate limiting step in EHC [1, 73].

Large variations in hepatic bile salt levels have minor effects on the expression of murine NTCP and Spgp suggesting that these transporters are abundantly expressed and able to accommodate a wide range of physiological bile salt fluxes [74]. Although Spgp and NTCP are homogeneously distributed along the liver acinus, bile transport is predominantly localized to the periportal zone leading to the potential for excess transport capacity at higher bile salt levels [74]. After TCA feeding, Spgp was upregulated 65% at the mRNA and protein level [74]. Upregulation of Spgp is probably due to FXR regulation as *spgp* mRNA in *FXR*^{-/-} mice was only at 30% of the control mice [56]. Apparently, minimal levels of Spgp expression are necessary for normal liver function and Spgp expression may be induced by bile salts in the promoter region in a FXR mediated manner [75].

1.4 Sister of P-Glycoprotein

Most ABC proteins are transporters that utilize the energy from ATP hydrolysis to transport compounds across a plasma membrane against a concentration gradient. In their active form, these transporters are comprised of two hydrophobic membrane-spanning domains and two nucleotide-binding domains on the cytosolic side to the membrane [76]. Low stringency screening identified a cDNA with high homology to MDR1 that was called Spgp [2]. Functional analysis of this protein identified it as BSEP with analysis demonstrating expression limited to the liver [1].

Unlike many of the other ABC transporters, Spgp appears to be a high affinity bile salt transporter and has little or no transport activity with non-bile salt compounds [77]. Major substrates for murine Spgp are glycine and taurine conjugated bile salts with the highest affinity occurring with TCDCA [78]. The relative affinities for the major bile salts vary between species, reflecting the different composition of the bile salt pool [79]. Cyclosporin A, rifampicin, and glibenclamide are competitive inhibitors of Spgp [80].

1.5 Progressive Familial Intrahepatic Cholestasis type 2

Progressive familial intrahepatic cholestasis (PFIC) encompasses a number of inherited childhood liver diseases that are characterized by cholestasis and jaundice leading to cirrhosis [67]. Cholestasis results from the accumulation of bile salts and other toxic bile components in plasma and hepatocytes while jaundice results from a build up of bilirubin [16, 17]. Mutations in Spgp are linked to PFIC2 [81]. This disease is characterized by normal gamma-glutamyl transferase levels, increased serum bile salt levels and biliary bile salt levels that are 1% of normal [81]. PFIC2 is fatal in infancy or childhood and liver transplants are currently the only therapy available to cure the patient.

1.6 *Spgp*^{-/-} Mice

Spgp^{-/-} mice were generated in an attempt to create a disease model for PFIC2 [3]. Unlike humans with PFIC2, *spgp*^{-/-} mice exhibited only mild symptoms of non-progressive cholestasis, suggesting the presence of a compensatory mechanism. Many common indicators of liver function such as gamma-glutamyl transferase, alkaline phosphatase, aspartate aminotransferase, alanine aminotransferase, 5' nucleotidase, plasma albumin, and bilirubin were not significantly different between *spgp*^{-/-} and the wild-type mice.

Although the *spgp*^{-/-} mice experienced growth retardation, they were viable. While *spgp*^{-/-} mice were fertile, female *spgp*^{+/-} mice were bred with male *spgp*^{-/-} mice to increase breeding efficiency. Although breeding efficiency was increased, approximately 50% of the *spgp*^{-/-} mice did not survive until they were weaned. The high infant mortality rate appeared to be correlated to poor absorption of lipids and lipid-soluble vitamins. Those mice that did survive until they were weaned did not experience further health problems.

Bile flow was reduced approximately 2-fold in the *spgp*^{-/-} mice (Figure 5). While PFIC2 patients experience biliary bile salt secretion 1% of normal, *spgp*^{-/-} mice have biliary bile salt secretion 25% of normal [3]. Analysis of the biliary bile salt composition indicated the ratio of the individual bile salt species was different between the wild-type and the *spgp*^{-/-} mice [3]. There was a significant decrease in the CA concentration, an increase in the percentage of MCA, and the presence of a tetrahydroxylated bile salt species not detected in wild-type mice [3, 82]. The changes to the bile salt pool make it more hydrophilic, possibly reducing toxicity and allowing transport by an alternate transporter.

Challenging the *spgp*^{-/-} mice with a 0.5% CA enriched diet resulted in rapid weight loss and hypoactivity [83]. While male *spgp*^{-/-} mice were terminally ill or dead within 5-9 days of commencing 0.5% CA, female *spgp*^{-/-} mice survived over a 100 days of 0.5% CA feeding without showing signs of terminal illness. Feeding *spgp*^{-/-} mice the 0.5% CA diet for several days resulted in the levels of biochemical indicator liver function resembling those demonstrated by PFIC2 patients that reflected severe hepatocellular but mild ductular damage.

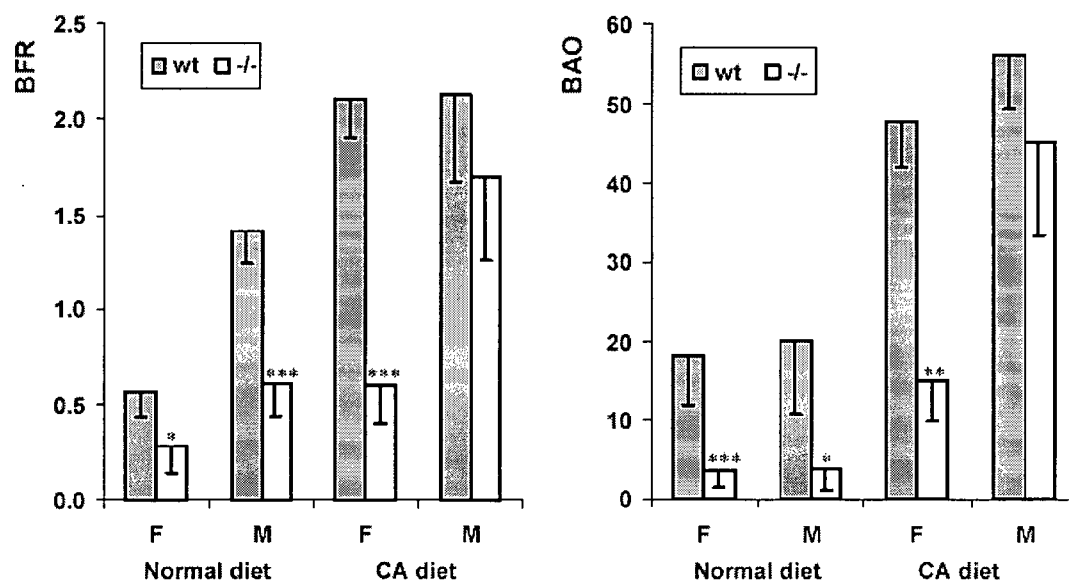


Figure 5: Bile flow rate (BFR), Bile acid output (BAO) in wild-type and *spgp*^{-/-} mice. (a) BFR ($\mu\text{L}/\text{min}/\text{g}$ Liver Weight) and (b) BAO ($\text{nmol}/\text{min}/\text{g}$ Liver Weight) in mice on the normal or 0.5% CA-supplemented diet for 2 days [83]. Asterisks indicate statistical significance between wild-type and *spgp*^{-/-} mice of same sex. *, $0.05 > P > 0.01$; **, $0.01 > P > 0.001$; ***, $0.001 > P$; no asterisks, no statistical significance.

Under normal dietary conditions, the bile flow rate (BAF) for the *spgp*^{-/-} mice was approximately half the wild-type BAF [83]. However, a sexual dimorphism occurs in the *spgp*^{-/-} mice fed the 0.5% CA supplemented diet as female *spgp*^{-/-} mice maintain a similar BAF as on the normal diet while the male *spgp*^{-/-} mice have an increased BAF that is not significantly different than the wild-type mice. Biliary bile salt analysis indicated *spgp*^{-/-} mice fed the 0.5% CA supplemented diet had a total bile salt level not significantly different than the wild-type mice fed the supplemented diet. While prolonged 0.5% CA feeding did promote increased BFR, a bolus injection of TCA failed to cause any changes in the biliary bile salt levels of the *spgp*^{-/-} mice.

1.7 Cytochrome P450 enzymes

1.7.1 Background to the CYP System

The cytochrome P450 (CYP) super family is comprised of over 2000 different genes in animals, plants, lower eukaryotes, and bacteria¹ [84]. The CYPs are the key components in the Phase 1 detoxification of endogenous and exogenous compounds and also have a major role in the synthesis of steroid hormones and bile salts. If a compound has more than one reactive centre, it may undergo reaction at any, all, or some combination of the reactive sites. CYP expression levels are determined through a variety of physiological, environmental, dietary and genetic factors. Many CYPs have polymorphic sites that are associated with altered enzyme activity or gene expression [85]. These sites can lead to considerable variation in expression within a species.

¹ Updated at <http://drnelson.utmem.edu/CytochromeP450.html>

The CYP oxidation system is an electron transport chain, primarily associated with the ER and other intracellular membranes. The key protein in the CYP electron transport chain is the cytochrome P450 where "P" stands for pigment and 450 stands for the wavelength of a characteristic absorption peak [86]. Besides a substrate, the CYP system also requires electrons and molecular oxygen. The primary source of electrons is NADPH using NADPH cytochrome P450 reductase. Although the P450 system is most prominent in the liver, it is also present in other organs.

The super family is designated CYP, the family with a number, the subfamily with a letter, and each member is numbered consecutively as identified. The families are comprised of forms exhibiting at least 40% sequence identity while those family members over 55-60% sequence identity are within the same subfamily [87].

So far, subfamily members form clusters on the chromosomes where they are adjacent to each other [85, 88]. For example, the CYP3A locus in humans contains four genes and three pseudogenes [85]. These genes have a high degree of similarity and often have overlapping substrate spectra. Since the subfamily members are adjacent to each other, it is likely that there is shared regulation and also the potential for intergenic splicing [89].

Most of the CYPs identified in humans have homologs in mice. Mice have more CYPs than humans, likely due to increased gene duplication. While many of the mouse CYPs have similar substrate profiles as human CYPs, there are often differences in regulation [12].

1.7.2 Mouse CYP3A Enzymes

Expression of the CYP3A family was examined since it is known to be involved in bile salt hydroxylation and is one of the major families involved in Phase I detoxification. Furthermore, the CYP3A family comprises a significant portion of the total CYP pool in the liver [90]. CYP3A4, the human equivalent of CYP3A11, represents 30% of the total cytochrome P450 content in the liver and is implicated in the biotransformation of over 50% of the pharmaceutical agents oxidized by CYP enzymes [91, 92]. Increased expression of the CYP3A enzymes is not unexpected as this family is involved in drug metabolism and is easily induced by a variety of naturally occurring and synthetic compounds. Figure 6 demonstrates the high level of homology at the protein level between the murine CYP3A members.

Although six inducers (dexamethasone, 3-methylcholanthrene, phenobarbital, polychlorinated biphenyl, pregnenolone 16 α -carbonitrile, and rifampicin) were found to increase expression of CYP3A11 and CYP3A13, CYP3A11 was expressed at higher levels and was induced more than CYP3A13 [93]. Maximal levels of CYP3A11 and CYP3A13 were reached between 4 and 8 weeks, suggesting that they are similarly controlled by hormones (sex, growth) [93]. In comparison, CYP3A16 is developmentally regulated and its levels decrease between week 2 and week 5 after birth [94].

CYP3A41 is a female specific enzyme and is a major 3A form in female mice [95]. The classic inducers of the CYP3A family did not induce CYP3A41 and in some cases, it was suppressed by other common CYP inducers [95]. Minimal CYP3A41 is expressed at infancy in both genders but by adulthood, CYP3A41 is almost exclusively produced by the females [95].

```

1 Cyp3A11      1 [ HDLVSRAL SLETWVLLRAI SLVLLIYRYGTREKHELEKKQGITP GPKPLPELGT VLNYYTKGLWKEDRE SYKKYQK 70
2 Cyp3A13      HDLIPNF SHETWMLLAT SLVLLIYLYGTHSHGIEKKL GIPGPKPLPEL GTLLAYQKGFWECDIQ SHKKYQK
3 Cyp3A16      HMLF SRA SLDTLVLLRAIILVLLIYRYGTYYHGLEKKQGITP GPKPLPELGT VLNYYTKGLWKEDRE SYKKYQK
4 Cyp3A25      HMLIPML SLETWVLLVT SLVLEFYLYGTYSHGLEKKL GIPGPKPLPEL GTIFENYYDGHMKRDED SYKKYQK
5 Cyp3A41      HMLF SRA SLDTWVLLRAIILVLLIYRYGTETHGLEKKQGITP GFTPLPELGT VLNYYTKGLWKEDRE SYKKYQK
consensus/ 80%  MSLhssLSL-TWVLLAK LULLYLYGTHSHGLEKK. GIPGPKPLPEL GTLLNYYTKGLWKEDR-SYcKYQK
consensus/ 100% HpLhssRSh-ThALLsh. LVLLRYLYGTThpHGLEKK. GIPGFPPLPELGTLLhSY. cGLWchD. p0acKYQK

71      1      140
1 Cyp3A11      TWGLEDDGQTPLLAVTDPETIKQVLVKEEF SVETNRERDF GPVGINSKKALICISKDDEWIKRYRALL SPTFTSG
2 Cyp3A13      HWGLYDGRQPVLAITDPPDIIRKTVLVEE SYSTFTNRERDF GPVGIILKKALISISENEEWIKRIEALL SPTFTSG
3 Cyp3A16      TWGLEDDGQIPLEFVITDPEIKQVLVKEEF SVETNRQDFFPVGIHKKALISLAKDEWIKRYRALL SPTFTSG
4 Cyp3A25      TWGFEYGDQPIILAHNDPBIIRKTVLVEE SYSVETNRERDF GPVGENKKALITISEDEWIKRLRLL SPTFTSG
5 Cyp3A41      TWGLEDDGQMPLEFVITDPEIKQVLVKEEF SVETNRERDF GPVGIHKKALISISKDDEWIKRYRALL SPTFTSG
consensus/ 80%  HWGLaDcp. Pllh0ITDPEIRIK0VLVKEE0SVETNRER0DF GPVGIN0KKALISIS0cDDEWIKR0RALL SPTFTSG
consensus/ 100% HWGha-G. Pllh0hADP-hIK. VLVKEE0as0SVETNR0p. Fh0PVGhhpKul0oluc0-EWIKR0h0LL SPTFTSG

141      2      210
1 Cyp3A11      KLKEHFPIEQYGDILLVKYLRQKAKKKEPVTMHDVL GAYSHDVITST SF GVMVD SLNMPDPEFVEKAKKL
2 Cyp3A13      RLKEHFPIINQFTDVLVNRHRQGLGEGKPT SHKDIF GAYSHDVITAT SF GVMVD SLNMPDPEFVEKIKKL
3 Cyp3A16      MLKEHFPIEQYGDILLVKYLRQERAKKGPVAVKDVLGAYSHDVII STFGVMVD SLNMPDPEFVENAKKV
4 Cyp3A25      KLKEHFPIHRQYGDILLVNLEREREKGEPI SHKDIF GAYSHDVITGT SF GVMVD SLNMPDPEFVQKAKKI
5 Cyp3A41      KLKEHFPIEQYGDILLVKYLRQERAKKGPVTMHDVL GAYSIDVITST SF GVMVD SLNMPDPEFVEKAKGI
consensus/ 80%  +LKEHFPIEQYGDILLV+. LRQctcKAKKPL0SHKDL0hGAYSHDVITat SF GVMVD SLNMP0pDPEFVEKAKKI
consensus/ 100% pLKEHFPIhpQasDILLV+. hhp0t. teGcPh0hKDL0hGAYSHDVIT0hT0cF GVMVD SLNMP0pDPEFVpphKtL

211      280
1 Cyp3A11      LRFDFDPLLESVVLEPPLTPVYEMLMECHFPKDSIEFFKKEVDRHKE SRLDSKQKHEVDELQLMGN0SHY
2 Cyp3A13      LKFDIEDELEL SVTLEPPLTPVEDALNVSLEPRDVI SEFTTSVERHKENRHKKEKQRVDELQLMINS0QN
3 Cyp3A16      LRFDYFDPLSLSVALPPLTPVYEMLMECHFPKDSIEFFKKEVDRHTEWRLDSKQKHEVDEIYLMHEAYN
4 Cyp3A25      LKFKIEDELEL SVTLEPPLTPVYEMLMECHFPKDSIEPRDSHNEFFKKEVDRHKKERLAS0NQKHEVDELQLMONT0QN
5 Cyp3A41      LRVDIEFDPLVE SVVLEPPLTPVYEMLMECHFPKDSIEFFKKEVDRHKE SRLDSKQKHEVDELQLMGN0MAHY
consensus/ 80%  L+R0DFDELEL0hSV0LEPPLTPVYEMLME0CHFP+D0SI0p0FFKKEV0c0RHKE0hRL0c0SKQ0p0RVDELQLMGN0ap0N
consensus/ 100% L+R0h0DFD0p0. h0SL0LEPPLTPV0a0-h0L0h0s0h0FP+D0sh0p0FF0pp. Vp0R0h0cp0R0h0tp0pp0K0p0RVDELQLM0h0s0.N

```

Figure 6: Multiple sequence alignment of the mouse CYP3A family. Amino acids are coloured by type using mView [96].

Hypophysectomy and growth hormone replacement studies indicate that expression of CYP3A41 is dependant upon the feminine plasma growth hormone profile [90].

1.7.3 Regulation of CYP by Nuclear Receptors

Many physiological processes in the adult liver are regulated by nuclear receptors that require heterodimerization with the retinoid X receptors (RXRs). The RXRs are unique among the nuclear receptors as they bind DNA as a homodimer but are heterodimer partners for numerous other nuclear receptors to bind to DNA [97]. For the maintenance of bile salt homeostasis, the proteins involved in the synthesis, metabolism and transport of bile salts are tightly regulated. When plasma bile salt levels increase, the hepatic uptake of bile salts decreases while the canalicular bile salt transport increases [49]. Bile salts are found in high concentrations in the hepatic nuclei where they regulate gene expression through FXR, the pregnane X receptor (PXR), and LXR α [58, 61, 98, 99].

FXR is believed to be the major bile salt sensor that regulates the major enzymes in bile salt synthesis, and transport [58]. FXR is active as a heterodimer with RXR, and is expressed in the liver, intestine, and kidney [100]. Bile salts bind to FXR in the hepatic nuclei, leading to an upregulation of proteins involved in bile salt trafficking and the down-regulation of some enzymes involved in bile salt biosynthesis [56, 101, 102]. Activated FXR also induces transcription of the short heterodimer partner (SHP-1), leading to the repression of NTCP as well as self-repression [103]. Furthermore, elevated SHP levels inactivates liver receptor homolog 1 (LRH-1), thus repressing transcription of CYP7A1 [103, 104].

Loss of Spgp expression leads to decreased biliary bile salt secretion and can result in elevated levels of hepatic bile salts. Elevated levels of bile salts in the liver results in increased expression of many ABC transporters, including MDR1a/b, MRP2, MRP3, and MRP4 [101, 105]. Furthermore, expression levels of CYP3A11 was found to increase in *FXR*^{-/-} mice, which experienced a significant decrease in Spgp expression [101]. Increased expression of the transporters and CYP3A11 are thought to be regulated by PXR in response to monohydroxy bile salt binding, in particular LCA [106].

PXR is divergent between the rodent, rabbit, and human as effective activators of human and rabbit PXR have little activity on rodent PXR [12]. The PXR receptor is not very specific as it appears to be activated by many compounds to stimulate expression of Phase I metabolism machinery [99, 106]. During cholestasis, high concentrations of bile salts are thought to activate PXR as a protective mechanism against LCA tissue damage. PXR coordinates drug metabolism through increasing expression of CYP3A and MDR1 [107]. Besides activating expression of the CYP3As, PXR impacts CYP2B through both the adaptive recognition of a phenobarbital response element (PBRE) and through PXR's control over the expression of constitutive androstane receptor (CAR) [108, 109].

1.7.4 CYP Interaction with Bile Salts

In vitro systems indicate that the mechanism for bile salt mediated inhibition of CYP is non-competitive and uncouples the electron transfer mechanism to releases CYP reductase from the microsomal membrane [110]. The potential of bile salts to inhibit hepatic CYPs is inversely proportional to the level of hydroxylation on the steroid nucleus of the bile salt and is positively correlated with taurine conjugation [111]. Bile salts also inhibit specific CYPs as bile-duct

ligated male rats experienced a significant reduction in the male specific CYP2C11 and CYP3A2 [112]. This reduction was much greater than decreases experienced by other microsomal proteins and accounted for most of the loss of total CYPs [112]. The mechanism for the specific reduction is uncertain as the decrease may be due to reduced protein synthesis or increased protein degradation.

Analysis of the bile salt patterns in cholestatic and normal livers indicated elevated levels of CA, CDCA, and LCA levels with impaired sulfation of LCA in the cholestatic livers [68]. Consequently, it was hypothesized that elevated intracellular levels of the hydrophobic CDCA and LCA resulted in the destabilization of membranes through their detergent effects. Besides their predicted non-specific actions, CDCA and DCA are also able to induce apoptosis while UDCA reduces the mitochondrial membrane alterations that lead to apoptosis [113-115].

Increasing the levels hydrophobic bile salts like CDCA, DCA, and LCA are commonly used as experimental methods to induce cholestasis [7, 111, 116]. These bile salts are suspected to be the main cause of hepatic injury as a 30 minute infusion of TCDCA in rats resulted in a significant increase in the release of proteins into the bile [117]. However, coinfusion with TUDCA, a more hydrophilic bile salt, prevented the significant biological changes observed with TCDCA alone [117].

Other hydrophilic bile salts such as UDCA, or tauro- β -muricholate (T β MCA) can also reduce the damage caused by the hydrophobic bile salts [5]. A common treatment for cholestatic patients is bile salt displacement therapy where UDCA is administered to the patients [32].

Besides stimulating biliary bile salt secretion, UDCA administration also affects the hepatic CYP levels [5, 105]. Hydrophobic bile salts tend to cause a reduction in CYP levels while hydrophilic bile salts either increase expression levels or at least, negate the decrease caused by hydrophobic bile salts [118, 119]. Consequently, it is thought that the CYPs help in detoxification of the bile salts.

1.7.5 Bile Salts as CYP Substrates

Cerebrotendinous xanthomatosis (CTX) is linked to mutations in CYP27 in humans. CTX patients experience nervous system dysfunction, tendon and brain xanthomas, and accelerated atherosclerosis [11]. These patients also have reduced levels of CDCA and increased levels of 25-hydroxylated C27-bile alcohols as a result of the microsomal 25-hydroxylation side chain cleavage pathway seen in Figure 4. However, *CYP27*^{-/-} mice did not demonstrate the CTX phenotype [120].

CYP27^{-/-} mice had elevated levels of bile salt synthesis through CYP7A1 and more efficient metabolism of the 25-hydroxylated bile alcohols than the CTX patients [121]. Increased metabolism of the 25-hydroxylated bile alcohols was found to be a result of CYP3A upregulation [11]. Despite the significant increase in CYP3A expression, PXR levels remained constant, suggesting that the upregulation of activity was due to an increase in ligand concentration rather than nuclear receptor levels [109]. Once induced, CYP3A catalyzed side chain hydroxylations of the bile salt intermediates to facilitate their excretion in the bile and the urine [109].

Several toxic bile salt intermediates were activators of mouse PXR but not of human PXR, possibly explaining why humans lacking CYP27 do not display the corresponding increase in CYP3A activity and are stricken with CTX [109]. When the *CYP27*^{-/-} mice were fed a CA or CDCA enriched diet, expression of CYP7A1 was strongly repressed as was CYP3A11 suggesting that bile salt intermediates not bile salts act as PXR activators [109].

As seen in Figure 4, the CYP3A family is also involved in hydroxylation during bile salt synthesis [10, 11]. CYP3A4 hydroxylates CDCA and LCA at the 6 α position, thus making them more hydrophilic [9]. Rifampin, a ligand for human PXR, provides relief in cholestasis by inhibiting the bile salt transport into the hepatocyte and inducing 6 α -hydroxylation of various bile salts by CYPs [122]. Experiments also indicate that prolonged induction of CYP3A is sufficient to hydroxylate hepatotoxic bile salts and prevent cholestasis [99].

The hamster gene product of CYP3A10 hydroxylates LCA at the 6 β position [123]. Expression of the gene appears to be male specific with males expressing 50-fold higher levels than the females. Both mRNA expression levels and enzyme activity were doubled upon CA feeding. It was subsequently assumed that 6 β -hydroxylation of LCA is the male hamsters' major pathway for hepatic detoxification of LCA. It is possible that increased hydroxylation is a response to intra and extrahepatic cholestasis and bile salt overload.

An interesting example of CYPs recognizing bile salts for hydroxylation occurs in pigs. Instead of CA being the major bile salt, pigs synthesize hyocholic acid by 6 α -hydroxylation of CDCA to obtain their tri-hydroxy bile salt. [124]. Although this enzyme recognizes bile salts, the enzyme

was named CYP4A21, due to sequence homology [124]. While the CYP4A family is normally involved in fatty acid hydroxylation, the substrate for CYP4A21 are bile salts. The substrate recognition of CYP4A21 may altered to recognize fatty acids through mutagenesis of three specific amino acid residues in the active site [124]. The impact of a few amino acid differences in the active site suggests the possibility of an enzyme in one species causing tetrahydroxylation while the homologue in another species does not.

1.8 Hypothesis

Bile salt hydroxylation appears to be a major protective mechanism in mice against cholestasis. Protection against the action of bile salts is necessary as bile salt accumulation has toxic effects on cells and solubilizes cellular membranes during cholestasis [99]. While humans lacking *Spgp* experience PFIC2, *spgp*^{-/-} mice experience only mild non-progressive cholestasis. As *spgp*^{-/-} mice have more hydrophilic bile salt pools than the wild-type mice, it was proposed that the *spgp*^{-/-} mice have an active hydroxylation mechanism to produce significant amounts of tetrahydroxylated bile salts. These tetrahydroxylated bile salts are then secreted through an alternative bile salt transport system [3]. Since tetrahydroxylation of bile salts was thought to be a detoxification mechanism, it was proposed that challenging the mice with a 0.5% CA would increase levels of the tetrahydroxylated bile salts.

Focus was placed on the cytochrome P450 super family due to its abundance in the liver and role in the detoxification of many compounds. The focus was narrowed to the CYP3A family as they 6 α -hydroxylate enough bile salt to allow recovery from LCA induced cholestasis [7]. Furthermore, CYP3A upregulation and hydroxylation of bile salt intermediates was identified as

the reason why *CYP27^{-/-}* mice do not display the CTX phenotype demonstrated by *CYP27^{-/-}* humans [11].

2 Materials and Methods

2.1 Mice and Animal Treatment

Mice homozygous (-/-) for the *spgp* gene disruption with the C57BL/6J strain (+/+) as a genetic background has been described by Wang *et al* [3]. Since the FVB/NJ is a widely used strain in the development of transgenic and knockout mice, *spgp^{-/-}* mice were serially crossbred with the FVB strain. All mice used were bred at the BC Cancer Research Centre and used in experiments at 2-4 months of age. They were housed with a 12:12 hour light:dark period, with unlimited access of water and unless otherwise noted, standard mouse diet (Pico Lab[®] Rodent Diet 20, PMI LabDiet[®], Richmond, Indiana). The alternate diet was a 0.5% CA supplemented diet (Pico Lab[®] Rodent Diet 20 supplemented with 0.5% CA) for a period of two days prior to the experiment. Housing conditions and experimental procedures were approved by the Committee on Animal Care, University of British Columbia, according to the Canadian Council on Animal Care guidelines.

Mice were anaesthetized using an i.p. injection of a mixture of Ketamine (112.5 mg/kg) and Xylazine (11.3 mg/kg) after 2 hours of fasting before their abdomen was opened [3]. Distal bile duct ligation was performed followed by cannulation of the gallbladder to collect bile for further analysis [18]. For mRNA expression analysis, the mice were sacrificed using CO₂ and their livers excised and immediately placed in liquid nitrogen.

2.2 High Performance Liquid Chromatography of Mouse Bile

A method for high performance liquid chromatography (HPLC) separation of bile salts was developed to generate biliary bile salt profiles and to monitor levels of the tetrahydroxylated bile salt. Standard solutions were made in HPLC grade MeOH consisting of varying concentrations of T β MC, TUDCA, taurocholic acid (TCA), taurochenodeoxycholic acid (TCDCA), taurodeoxycholic acid (TDCA), tauroolithocholic acid (TLCA), ursodeoxycholic acid (UDCA), cholic acid (CA), chenodeoxycholic acid (CDCA), deoxycholic acid (DCA), LCA, and glyoursodeoxycholic acid (GUDCA) (standards obtained from Sigma and Steraloids). Standards contained 1 mg/mL GUDCA as an internal reference.

Bile samples were collected from the mice through bile duct cannulation and stored at -80°C with minimal freeze-thaw cycles. Prior to analysis, samples were thawed on ice and mixed well. The bile was then diluted 1:4 in MeOH and centrifuged for 2 minutes at 16,000 x g.

HPLC was carried out with a Waters 600 pump and controller and a 486 UV detector. Separation was performed on a Spherisorb S5 ODS2 C-18 (5 μm particle size, 250 mm x 4 mm, Waters) reverse phase analytical column and was preceded by guard column (Nova Pack, Waters). Integration of the peaks was carried out using Millennium 2010 software. The bile salt controls were separated at ambient temperature over 48 minutes at a flow rate of 0.7 mL/min and 3200 psi. The mobile phase consisted of solvent A (MeOH) and solvent B (60:40 MeOH: 0.01 M potassium phosphate, 0.02 M sodium phosphate (pH 5.35 (modified from [125, 126])). Initial conditions were held at 100% B for the first 25 minutes. Over the next 10 minutes, there was a linear gradient to 30% B and conditions were held for another 5 minutes. The conditions then

decreased through a linear gradient to 100% A over 8 minutes. The system was flushed with 100% MeOH followed by equilibration back to the initial conditions. The effluent was monitored at 210 nm. Each metabolite was quantified by interpolation from a standard curve constructed for each metabolite. Some metabolites could not be quantified accurately due to lack of commercially available standards and a first approximation was made with a standard curve of a commercially available bile salt standard with a similar retention time.

In the optimization process, the mobile phase consisted of solvent A (MeOH) and solvent B (50:50 MeOH:0.01 M potassium phosphate, 0.02 M sodium phosphate (pH 5.35)). Initial conditions began with 50%A and 50%B followed by a gradient similar to the one previously mentioned. When unsatisfactory separation was observed, the mixture of the mobile phase was altered by decreasing the percentage obtained from reservoir A by 5%.

During the isolation of tetrahydroxylated bile salts, the gradient was altered slightly. In the modified gradient, the mobile phase consisted of solvent A (MeOH) and solvent C (55:45 MeOH: 0.01 M potassium phosphate, 0.02 M sodium phosphate (pH 5.35)). Separation occurred over 50 minutes. Initial conditions were held at 100%C for the first 25 minutes. Over the next 25 minutes, there was a linear gradient to 100%A followed by a flush through of 100% MeOH then equilibration back to the initial conditions. The effluent was monitored at 210 nm. The desired fractions were collected and shipped on dry ice.

2.3 Identity Confirmation through Mass Spectrometry

Although HPLC separation provides information about characteristics of a compound, it does not provide structural identity. Consequently, liquid chromatography-electrospray mass

spectrometry (LC/MS/MS) was performed by Diane Mignault at the University of Montreal to allow identification of bile salts based on the number of hydroxyl groups and conjugation status [3]. Briefly, the bile salts were extracted with a Bond-Elute C18 reverse phase cartridge where the bile salts were eluted in 5 mL of methanol and evaporated to dryness under nitrogen. The precipitate was dissolved in 1mL of an acetonitrile: water (1: 1) mixture for LC/MS/MS. A Hewlett Packard LC system was operated isocratically at a flow rate of 10 μ l /minute for the purpose of injection. The LC system was connected to a Quattro electrospray tandem mass spectrometer (micro Mass UK) where the negative ion mass spectra between 300 and 800 amu was recorded. The molecular ions for each glycine conjugated bile salts (tetra-, tri-, di-, and mono-hydroxylated bile salts) were; m/z 480.6; 464.6; 448.6; and 432.6 respectively. Taurine conjugated bile salts (tetra-, tri-, di-, and mono-hydroxylated) were; m/z 530; 514.6; 498.6; and 482.6 respectively.

2.4 Northern Blot Analysis

Analysis of the mRNA expression of certain genes was initially performed through northern blot analysis. The probe template was made by PCR of template first strand cDNA with the appropriate primer pair listed in Table 1. The PCR was performed in 50 μ L aliquots in a thermal cycler (GeneAmp 9700, Applied BioSystems) under similar conditions (94°C for 2 minutes, followed by 35 cycles of 94°C for 30 seconds, 58°C for 1 minute, and 72°C for 1 minute, the run was completed by holding at 72°C for 2 minutes). The PCR product was isolated on a 1% agarose gel and extracted using the Quiex II kit (Qiagen). Quantification of the template probe DNA occurred by measurement of the absorbance at 260 nm.

Probe labeling occurred by first denaturing the template probe DNA through heating to 100°C for 5 minutes. Immediately afterwards, the template DNA was placed on ice and the other components of the reaction were added as instructed by the manufacturer (Random Primer DNA Labeling System, Invitrogen). The probes were labeled with [$\alpha^{32}\text{P}$]dCTP during an incubation at 25°C for 2 hours. The labeled probe was purified from the reaction mixture by a spin column that had been pre-equilibrated with TE buffer (10 mM Tris-HCL, 1mM EDTA, pH 7.5). To measure the specific activity of the labeled probe, 1 μL of the mixture was added to 5 mL of scintillation fluid and quantitated using a scintillation counter.

Total RNA was isolated from frozen mouse liver using the TRIzol extraction method (Invitrogen) and its quality was visualized on an electrophoretic gel. Using the total RNA, mRNA was isolated using the Oligotex midi mRNA extraction kit and running it through a spin column (Qiagen). The eluate containing the pure mRNA was quantified at 260 nm.

Electrophoretic samples were made up to 0.75-1.5 μg RNA and the protocol for northern blots was followed [127]. The probe was added to the hybridization buffer to a final concentration of 1×10^6 cpm/mL and left to incubate at 65°C overnight. Following rinsing, the blots were exposed to film for the appropriate length of time at -80°C. Quantification occurred through measurement of the band intensity with a densitometer (Molecular Dynamics). In order to strip the blots for re-

Table 1: Summary of primers designed for probe synthesis in the Northern Blot procedure.

Gene	Accession Number		Primer	Probe Size (bp)	mRNA Size (bp)
CYP3A11	BC010528	5' 3'	GAAACCTGGGTGCTCCTAGCA TAAAAGCTTTTTGGCTTTCTC	606	2070
CYP3A13	NM_007819	5' 3'	AGTATCTAGACATGGTGGTG ATGAAGTGAACATCGGCAGC	690	1881
CYP3A16	NM_007820	5' 3'	ATCGAGATCACAGCCCAGTC GAAGAACTGCAGAACTCC	667	1701
CYP3A25	BC028855	5' 3'	AGAACGCCTTGCTTCAAACC AGAATTCTGAGGCTCTGGC	470	2002
CYP3A41	NM_017396	5' 3'	ATGCCTCTCTTTGTCATCACG TTCCTGCAGTTTCTTCTGGA	768	2070
CYP7A1	L23754	5' 3'	TCACTTGCTCAAGACCGCAC TGGTGTGGCTCTCTACAAGC	749	3099
CYP8B1	AF090317	5' 3'	TTATGATGCTCTGGGCCTCC TTCAGGCGATAGAGGAAGCG	664	1949
Cyclophilin	X52803	5' 3'	CACCGTGTCTTCGACATCA CAGAGATTACAGGACATTGCG	585	736
β -actin	NM_007393	5' 3'	TGGAATCCTGTGGCATCCATGAAA TAAAACGCAGCTCAGTAACAGTCCG	349	1892

Table 2: A BLAST analysis of the probes used for Northern analysis. The identity of the probe and primer pair was compared to the closest gene.

Gene	Closest Gene	Probe identity	Primer Identity
CYP3A11	CYP3A41	90% (548/606)	31% (13/42)
CYP3A13	N/A		
CYP3A16	CYP3A11	94% (627/667)	89% (32/36)
CYP3A25	N/A		
CYP3A41	CYP3A11	94% (719/768)	90% (37/41)
CYP7A1	N/A		
CYP8B1	N/A		

probing, the blots were soaked at 100°C in 1% (w/v) SDS and left to cool to room temperature. These blots were then checked for residual activity through exposure to film for at least 24 hours.

2.5 Real-time PCR

Quantification of mRNA expression was performed using real-time PCR. Primers were designed using the Primer Express software (Applied BioSystems) where the primer length was set to 20 base pairs, an amplicon length between 75 and 100 base pairs, and GC content between 40%-60%. These primers are listed in Table 3. The primers and the regions they amplified were then analyzed using a BLAST search to ensure specificity with the results summarized in Table 4. The primers were diluted in DEPC-treated water to 3 μ M and stored at -20°C. After testing a variety of primer concentrations in the PCR reaction, it was determined that 300nM was the optimal concentration for the genes tested to maximize amplification efficiency and minimize non-specific amplification.

Total RNA was isolated from liver tissue that had been snap-frozen to -80°C. Using a RNeasy kit (Qiagen), total RNA was isolated from 10 mg of tissue. DNase I digestion was performed on 1-2 μ g of the total RNA in a reaction mixture consisting of 20 mM Tris-HCl (pH 8.4), 50 mM KCl, 2 mM MgCl₂, and 0.1 unit/ μ L amplification grade DNase I (Invitrogen). The mixture was held at room temperature for 15 minutes, followed by addition of EDTA to a final concentration of 2.3 mM. In order to inactivate the DNase I, the mixture was heated to 65°C for 15 minutes and then placed on ice for at least one minute. This mixture was directly used in the reverse transcription reaction.

First-strand cDNA was made using a Superscript kit for preparation of cDNA for real-time PCR according to the manufacture's instructions (Invitrogen). Briefly, the DNaseI treated total RNA underwent reverse transcription with oligo(dT)₁₂₋₁₈ and the Superscript II reverse transcriptase. After the reverse transcription, the RNA was degraded using RNaseH. A negative control was prepared at the same time under identical conditions except the negative control lacked the oligo(dT)₁₂₋₁₈ and the Superscript II reverse transcriptase. To confirm that the samples lacked genomic DNA contamination, real-time PCR of the RNA was performed. If any signal was detected, the samples were treated with DNase I again.

The PCR was set-up on a 384-well plate in 15 μ L reactions consisting of 10 ng first-strand cDNA, and 200 nM of the forward and reverse primer, with the remaining components for the reaction being added in a 2 x SYBR green PCR master mix (Applied BioSystems). Each primer pair was analyzed with a positive control known to express the gene and a negative control, with water added instead of the sample. The reaction conditions began with an initial 2 minutes at 50 °C (ABI PRISM 7700HT Sequence Detection System, Applied BioSystems). Activation of the polymerase then occurs by holding the temperature at 95 °C for 10 minutes. There is then 40 cycles of denaturation at 95 °C for 15 seconds and annealing and extension at 60 °C for one minute. After the forty cycles, the temperature is held at 95 °C for 15 seconds, followed by 60°C for 15 seconds. The program ends at 95°C for 15 seconds. Results were quantified using a relative standard curve. Usually the standard was cDNA obtained from a male wild-type mouse on a normal diet, however, for female specific genes, another set of standards was obtained from a female wild-type mouse on a normal diet. The stock was at a concentration of 20 ng/ μ L and

Table 3: Summary of primers designed for real-time PCR analysis.

Gene	Accession Number		Primer	Amplicon Size (bp)
CYP3A11	BC010528	5' 3'	GCTGACAAACAAGCAGGGATG CCAAGCTGATTGCTAGGAGCAC	76
CYP3A13	NM_007819	5' 3'	GAGGCAGGGATTAGGAGAAGGA CAAATGAGGTGGCTGTGATCA	89
CYP3A16	NM_007820	5' 3'	ACCGTGTATTCTTGGCCACT TATTGGGCAGAGCCTCATCG	76
CYP3A25	BC028855	5' 3'	GCTGTCATAGGAGTCCTGCAGA TGGTTCCTGCTGATCTTCAG	81
CYP3A41	NM_017396	5' 3'	CAGGTATGGGACCCGTACACA TGCCTAAAAATGGCAGAGGTG	77
CYP7A1	L23754	5' 3'	GAAGGCATTTGGACACAGAAGC AACACAGAGCATCTCCCTGGA	100
CYP8B1	AF090317	5' 3'	ACGCTTCCTCTATCGCCTGAA GTGCCTCAGAGCCAGAGGAT	101
CYP27	AK004977	5' 3'	ACCATCTGCGTCAGGCTTTG TCGTTTAAGGCATCCGTGTAGA	76
CYP2B10	NM_009998	5' 3'	AAAGTCTGTGGAAAGCGCAT GGATGGACGTGAAGAAAAGGAA	77
FXR	NM_009108	5' 3'	GGAACTCCGGACATTCAAC GTGTCCATCACTGCACATC	111
PXR	AF031814	5' 3'	GTTCAAGGGCGTCATCAACT CAGGGAGATCTGGTCCTCAA	76
LXR α	AF085745	5' 3'	TGCAGGACCAGCTCCAAGTAG TGGGAACATCAGTCGGTCGT	101
LXR β	NM_009473	5' 3'	ATTGCGACTCCAGGACAAGAAGCT ACCACTCTTGGAAGACTCAATGGG	238
PPAR α	NM_011144	5' 3'	GGGCTGAGCGTAGGTAATGC TGCCCATTCAGAAAGGATGTG	51
RPS15	NM_009091	5' 3'	GAGATGATCGGCCACTACCTG CACGGGTTTGTAGGTGATGGA	51
Cyclophilin	X52803	5' 3'	ATCACCATTTCCGACTGTGGA CAGAAGGAATGGTTTGTATGGGT	76

Table 4: A BLAST analysis of amplicons and indicate differences in the primers.

Gene	Closest Gene	Amplicon identity	Primer Identity
CYP3A11	CYP3A41	82% (62/76)	74% (32/43)
CYP3A13	CYP3A25	66% (59/89)	42% (18/43)
CYP3A16	CYP3A11	86% (65/76)	78% (32/41)
CYP3A25	N/A		
CYP3A41	CYP3A11	87% (67/77)	81% (34/42)
CYP2B10	CYP2B13	86% (66/77)	77% (33/43)

was serially diluted down to 0.078 ng/ μ L. The results of the replicates for each sample were obtained from the standard curve, and averaged, followed by normalization to RPS15. The melt profile was analyzed for each reaction and if the DNA melting curve revealed multiple peaks, the real-time PCR of those samples was repeated.

2.6 Statistics

Unless otherwise noted, data points are the mean of three to five mice and values are expressed as the mean \pm SD. PRISM software was used for all statistical analysis (GraphPad, San Diego). The statistical significance of the differences between groups of mice was determined using a two-tailed unpaired Student's *t*-test at a 95% level of confidence. Statistical significance was declared if $p < 0.05$.

3 Results

When fed the normal diet, *spgp*^{-/-} mice still transport bile salts at a level 25% of the wild-type mice. Unlike humans lacking *Spgp* who experience severe cholestasis, *spgp*^{-/-} mice only experience mild cholestasis. One potential mechanism for the difference in severity is increased hydroxylation of the bile salt pool, resulting in a more hydrophilic bile salt pool and the presence of a previously unseen tetrahydroxylated bile salt species. Supplementing the diet with 0.5% CA for several days increases the level of bile salt transport to levels not significantly different than the wild-type mice fed the supplemented diet. An HPLC method was developed to be a rapid and easy method to monitor the tetrahydroxylated bile salt levels. Expression analysis was also performed on the CYP3A subfamily as it is often involved in drug detoxification and hydroxylation of the steroid nucleus.

3.1 High Performance Liquid Chromatography to detect tetrahydroxylated bile salts

Development of an assay to characterize the enzyme involved in bile salt tetrahydroxylation requires a method to monitor the tetrahydroxylated bile salts. Methods considered were MS and HPLC, with both methods having benefits and detriments. MS can accurately determine molecular weight but requires known standards for exact structure determination [128]. A major drawback of MS analysis is that sample preparation and derivatization are required prior to MS analysis. Unnecessary sample processing has the potential to reduce components of the sample and not all components are derivatized with the same efficiency. Although identification in HPLC analysis is also restricted to the comparison of standards, sample preparation is simple, requiring only dilution in methanol. Furthermore, an HPLC machine was readily available to me while MS samples had to be sent to another laboratory for analysis. Consequently, I elected to develop a method for bile salt separation *via* HPLC. To accommodate the limitation of HPLC with structure determination, unknown peaks were collected and sent for MS analysis to confirm the presence of tetrahydroxylated bile salts.

Generation of bile salt profiles of the *spgp*^{-/-} and wild-type mice fed the normal and 0.5% CA diet allowed monitoring of the tetrahydroxylated bile salt levels. These profiles indicated multiple forms of the tetrahydroxylated bile salts, suggesting multiple substrates, multiple reactive centers, or the involvement of multiple enzymes. Furthermore, monitoring the level of tetrahydroxylation provided an indication of the biological impact of additional bile salt levels on the normal and *spgp*^{-/-} mice.

3.1.1 Method Optimization

The HPLC method was modified from an existing procedure due to limitations of the initial procedure and different column chemistries. Limitations of the initial method were due to its initial use in the analysis of human bile. In the initial method, TUDCA was the first bile salt to be eluted with a retention time less than 5 minutes. However, mice possess MCAs that when conjugated to taurine or glycine, elute prior to TUDCA. Another factor making the change in the mobile phase necessary is the production of the tetrahydroxylated bile salt, which when in the conjugated form, eluted prior to the taurine conjugated MCAs.

A gradient was also introduced to allow the hydrophobic bile salts to elute from the column in a reasonable amount of time. Figure 7 demonstrates the baseline shift produced by changing the mobile phase. Further modification of the method was necessary due to differences of column chemistry. The initial method produced baseline separation for the bile salts tested other than T β MCA when the Altrex Ultrex column (reverse phase, C-18, Beckman) was used. However, the initial method using a Spherisorb column did not produce baseline separation of most of the peaks.

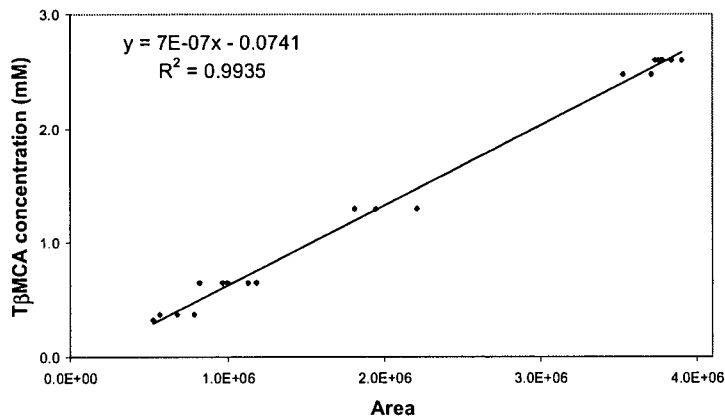
The reverse-phase C18 column was calibrated using a mixture of standard bile salts. The reproducibility of the method was evaluated through 20 μ L injections of the same standard each day over several weeks. The regression equations for the standard curves of the various bile salts are summarized in Table 5(a). In the isocratic portion of the gradient, the Pearson's correlation coefficient was high, ranging between 0.980 and 0.994. Even in the early portion of the gradient, the linear relationship remained high with Pearson correlation coefficient values occurring

Table 5: Quantification of bile salts via HPLC. (a) Linear equations used to calculate amount of bile salt (mM) from the area under the peak. Those that elute after 50 minutes have a poor linear correlation. Bile salts are listed in order of elution (x= area, Y=mM). (b) A representative standard curve (T β MCA) (c) Detection limits of bile salts determined from the standard curves.

(a)

Bile Salt	Equation	R ²
Tauro- β -muricholate	$y = 7E-07x - 0.0741$	0.994
Tauroursodeoxycholate	$y = 8E-07x + 0.025$	0.992
Glycoursodeoxycholate	$y = 6E-07x - 0.1715$	0.985
Taurocholate	$y = 8E-07x - 0.1084$	0.980
Taurochenodeoxycholate	$y = 8E-07x - 0.006$	0.934
Taurodeoxycholate	$y = 8E-07x - 0.2185$	0.982
Ursodeoxycholate	$y = 1E-05x - 0.5531$	0.988
Cholate	$y = 1E-05x - 0.9932$	0.937
Taurolithocholate	$y = 6E-07x + 0.2098$	0.949
Chenodeoxycholate	$y = 1E-05x - 0.2808$	0.744
Deoxycholate	$y = 1E-05x - 0.8222$	0.838

(b)



(c)

	Limit (mM)
Tauro- β -muricholate	0.33
Tauroursodeoxycholate	0.29
Glycoursodeoxycholate	0.53
Taurocholate	0.28
Taurochenodeoxycholate	0.29
Taurodeoxycholate	0.29
Ursodeoxycholate	2.6
Cholate	1.4
Taurolithocholate	0.35
Chenodeoxycholate	2.4
Deoxycholate	1.4

between 0.940 and 0.988. However, by the end of the gradient, determination of the bile salt concentration based on the regression equation was not possible as CDCA possessed an r^2 value of 0.744 and the remaining bile salts, DCA and LCA, were unpredictable in both their run time and peak size.

The modified HPLC method provided a detection limit for taurine conjugated bile salts of approximately 0.3 mM with the exact values summarized in Table 5(b). Although it is possible to visualize bile salt levels below 0.3 mM, these peaks are small and hidden by noise in the baseline or background non-bile salt components. Unconjugated bile salts have a detection limit almost 10-fold higher due to decreased sensitivity to the UV detector.

The average total biliary bile salt concentration of multiple animals produced variation of 25% in wild-type mice on the normal diet and 50% on the 0.5% CA diet. There was slightly less variation in the *spgp*^{-/-} mice as total biliary bile salt levels varied 20% on the normal diet. The variation in the *spgp*^{-/-} mice on the 0.5% CA diet only increased slightly to 25%. Repeated sampling of the same animal resulted a total biliary bile salt level variation of 12%. Analysis of multiple aliquots from the same sample reduced the variability of the HPLC method to 8%. The difference in variation between repeated sampling from the same animal and analysis of different animals suggests that there is a high degree of inter-animal variability.

3.1.2 Biliary Bile Salt Profile

Analysis of the bile salt elution profile from the *spgp*^{-/-} mice in Figure 8(a) indicated the presence of a peak not visible in the wild-type mice. Bile salt elution profiles of *spgp*^{-/-} mice appeared to have multiple peaks comprising the unidentified peak. As a result, the initial

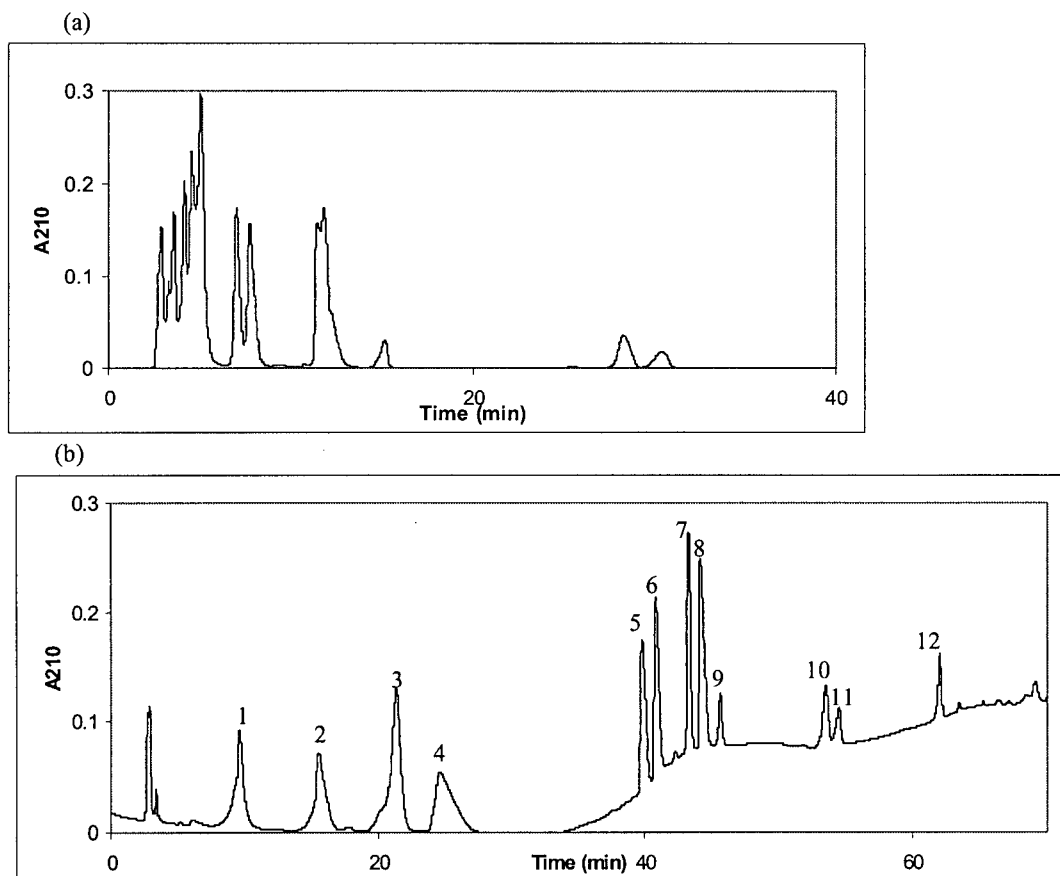


Figure 7: Chromatographs of bile salt separation of commercially available standards on a Spherisorb S5 ODS2 C-18 (5 μ m particle size, 250 mm x 4 mm, Waters) reverse phase analytical column under (a) 75:25 MeOH: 0.01 M potassium phosphate, 0.02 M sodium phosphate (pH 5.35) [126] and (b) a modified method beginning with 60:40 MeOH: 0.01 M potassium phosphate, 0.02 M sodium phosphate (pH 5.35) followed by a gradient (adapted from [129]). Peaks: 1, T β MCA; 2, TUDCA; 3, GUDCA; 4, TCA; 5, TCDCA; 6, TDCA; 7, UDCA; 8, CA; 9, TLCA; 10, CDCA; 11, DCA; 12, LCA.

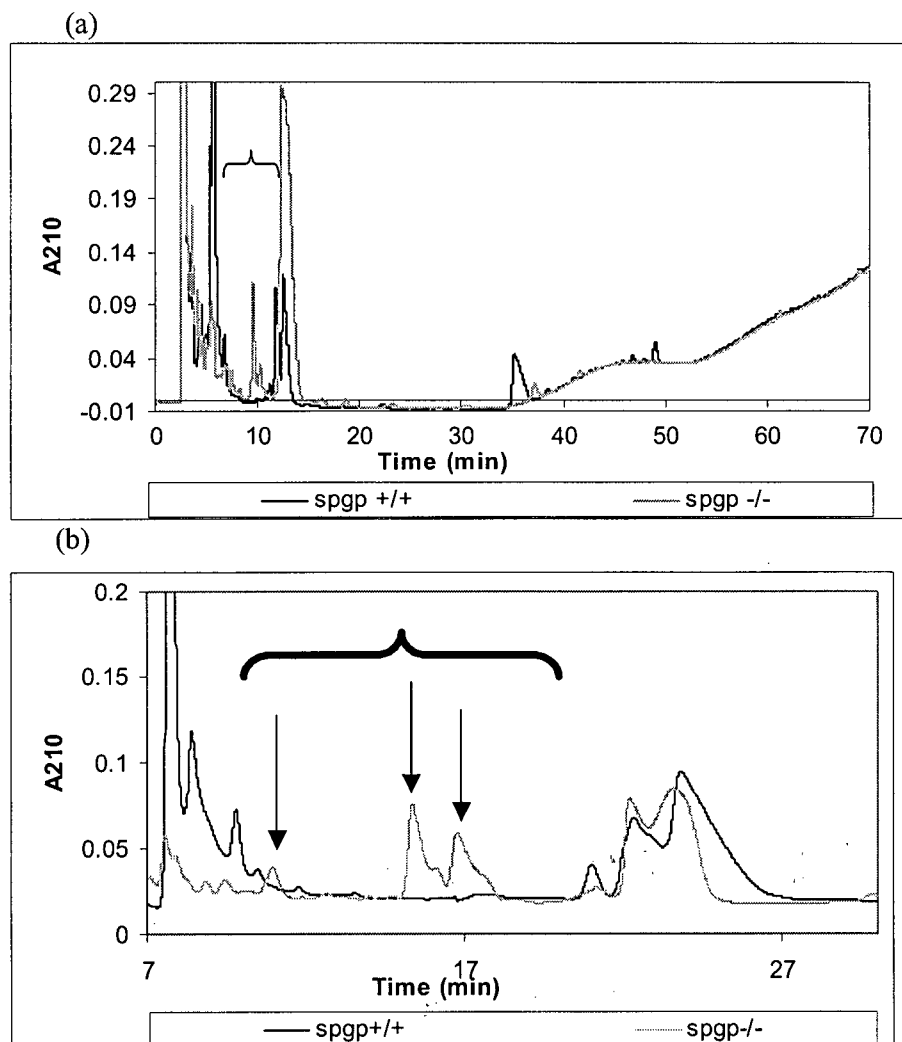


Figure 8: HPLC of *spgp*^{-/-} mouse bile revealed peaks not present in the wild-type mouse bile. The chromatogram in (a) is under standard conditions of 60:40 MeOH: 0.01 M potassium phosphate, 0.02 M sodium phosphate (pH 5.35) while (b) was under the mobile phase conditions of 55:45 MeOH: 0.01 M potassium phosphate, 0.02 M sodium phosphate (pH 5.35) The predicted region for elution of the taurine conjugated tetrahydroxylated bile salts is indicated by a curved bracket. The three peaks in (b) indicated by arrows that did not appear in the wild-type mouse bile samples were collected and sent for MS analysis. Components eluting prior to the taurine conjugated tetrahydroxylated bile salt are unknown and highly variable between samples.

conditions of the mobile phase were further modified to allow baseline separation of the early eluting bile salts present in mice as demonstrated in Figure 8(b).

Table 6 shows the levels of total bile salts obtained by HPLC analysis. Although most of the numbers for the FVB/NJ mice are comparable to values generated by MS for C57BL mice, the value obtained for male *spgp*^{-/-} mice fed the normal diet was not consistent with MS values. The total bile salt levels determined from the HPLC spectrum were higher than the wild-type total bile salt levels. The largest component in the HPLC spectrum of the *spgp*^{-/-} mice was in the region of the T β MCA. This region is a complex region as there may be peaks from T Ω MCA, T α MCA, and 3-sulfo-TCA and tauro-3 α -6 β -dihydroxy-5 β -cholanolic acid within a few minutes of the retention time for T β MCA. Furthermore, there are cholestanes, phospholipids, and fatty acids that elute in this region. However, these compounds do not have much absorbance at 210 nm (results not shown).

Relative levels of tetrahydroxylated bile salts are summarized in Table 6. While the major fraction of tetrahydroxylated bile salts is produced in the *spgp*^{-/-} mice, a small level was found in the bile of one of the wild-type mice fed the normal diet. In comparison, all the wild-type mice fed the 0.5% CA diet for two days produced 20% the amount of tetrahydroxylated bile salts than *spgp*^{-/-} mice on the normal diet did. Levels were not significantly different between the *spgp*^{-/-} mice fed the normal and 0.5% CA diet.

HPLC analysis identified several peaks in the *spgp*^{-/-} mice profiles that were not present in the wild-type profiles (Figure 8). These unknown peaks have retention times consistent with taurine

Table 6: Total biliary bile salt levels and the relative levels of biliary tetrahydroxylated bile salts in FVB/NJ mouse bile as determined by HPLC. The apparent total level of bile salts in the *spgp*^{-/-} mice is higher than in the wild-type mice. The bile salt concentration observed in the *spgp*^{-/-} mice fed the normal diet is mainly due to TMCA transport. The level of transport observed through HPLC contradicts MS data [83]. However, analysis of the TMCA peak from *spgp*^{-/-} mice through MS indicates the peak only consists of TβMCA.

		Normal diet		0.5% CA diet	
Total (mM)	<i>spgp</i> ^{+/+}	28.0	±7.6	40.0	±3.1
	<i>spgp</i> ^{-/-}	50.7	±32.2	32.0	±8.8
tetrahydroxylated bile salts	<i>spgp</i> ^{+/+}	0.1	±0.2	0.2	±0.1
	<i>spgp</i> ^{-/-}	1.0	±0.5	0.7	±0.4

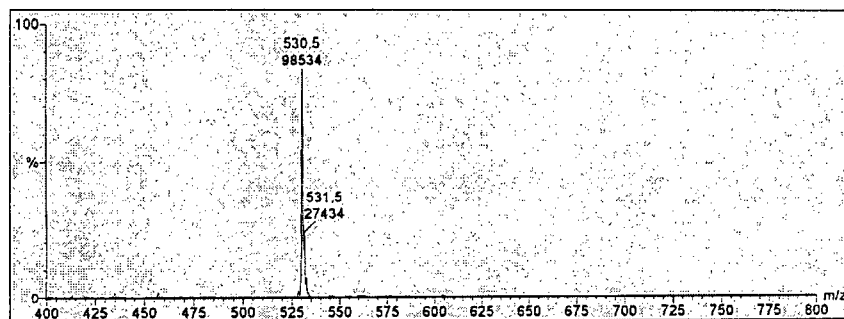
conjugated tetrahydroxylated bile salts and have also had their molecular weight confirmed through MS. In the wild-type mice fed the normal diet, tetrahydroxylated bile salts levels are produced at very low levels compared to the *spgp*^{-/-} mice. While the 0.5% CA diet does not increase tetrahydroxylated bile salt levels in *spgp*^{-/-} mice, the levels do increase slightly in the wild-type mice.

3.1.3 Identification of unknown HPLC peaks using Mass Spectrometry

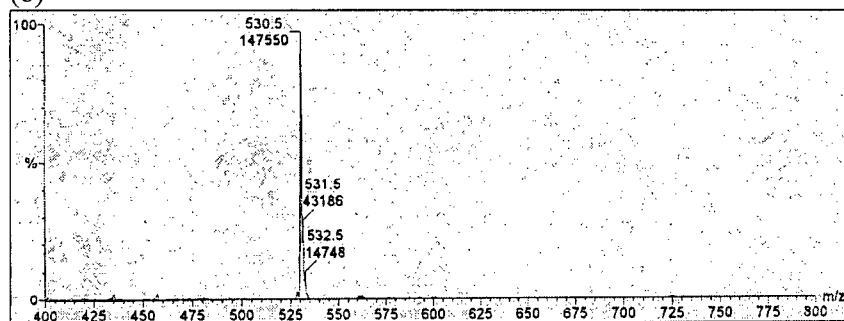
Initial HPLC analysis of *spgp*^{-/-} mouse bile revealed several peaks not present in the control wild-type mice. The retention time of these unknown peaks was in the range predicted for taurine conjugated tetrahydroxylated bile salts. Each of the three peaks identified in Figure 8(b) was isolated and analyzed through MS. Figure 9 provides representative spectra for each peak. The MS spectra confirmed the presence of taurine conjugated tetrahydroxylated bile salt in each of the fractions with the fragment ion at *m/z* 530. The first peak collected also revealed a very small level of tetrahydroxylated bile salt conjugated to glycine at the fragment ion *m/z* 480.6.

Determination of the actual hydroxylation pattern of the tetrahydroxylated bile salt is difficult due to a lack of available standards for tetrahydroxylated bile salts. Analysis of other *spgp*^{-/-} bile samples through GC/MS confirms the presence of four hydroxyl groups and suggests that the major tetrahydroxylated bile salt is 3 α ,6 β ,7 β ,12 α -tetrahydroxy-5 β -cholanic acid [3, 82]. Comparisons were also made to several standard tetrahydroxylated bile salts from humans including 1 β ,3 α ,7 α ,12 α -tetrahydroxy-5 β -cholanic acid, 3 α ,4 β ,7 α ,12 α -tetrahydroxy-5 β -cholanic acid, and 3 α ,6 β ,7 α ,12 α -tetrahydroxy-5 β -cholanic acid although none appeared to correspond to the tetrahydroxylated bile salts in the *spgp*^{-/-} mice [82].

(a)



(b)



(c)

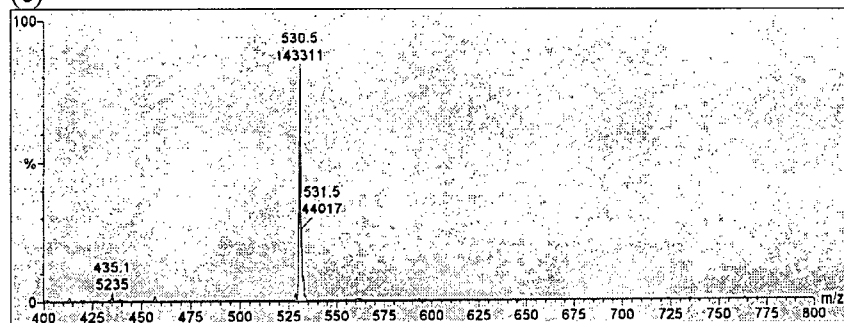


Figure 9: Taurine-conjugated tetrahydroxylated bile salt isolated from *sppg^{-/-}* mice *via* HPLC and detection through LC/MS/MS. (a) peak at 10 minutes (b) peak at 15 minutes and (c) peak at 16 minutes under mobile phase conditions of 55:45 MeOH: 0.01 M potassium phosphate, 0.02 M sodium phosphate (pH 5.35).

HPLC indicates that at least three compounds from the *spgp*^{-/-} mouse bile are confirmed to be taurine conjugated tetrahydroxylated bile salts. Multiple products may be a reflection of common events in the CYP family where an enzyme has the potential to hydroxylate one of multiple positions on the substrate or is capable of hydroxylating multiple substrates. Another possibility is that several enzymes are capable of hydroxylating bile salts.

3.2 mRNA Expression Analysis

One potential method to correlate the production of tetrahydroxylated bile salts to a known gene is to correlate the mRNA expression levels of a candidate gene with the amount of bile salt under different physiological conditions. Many enzymes and transporters involved in cholesterol or bile salt homeostasis have their levels controlled through regulation at the mRNA expression level [130-133]. Besides the gene of the actual hydroxylase, there are often changes in expression of genes in the bile salt synthesis pathway or in one of the nuclear receptors involved in bile salt homeostasis [134-136].

Due to the high degree of homology between CYP3A family members, BLAST searches were performed on the probe regions to ensure they did not recognize regions in other genes (Tables 2 and 4) [137]. Design of the primer set also required careful consideration of the sequence as many of the regions that lacked similarity between the genes were often unsuitable for primer design due to a high level of nucleotide repeats and extreme GC content.

Northern blot analysis was initially used to monitor mRNA expression due to the minimal handling of the samples prior to analysis. Furthermore, following the PCR reaction to generate

the probe, the target sequence may be isolated, eliminating any non-specific fragments, thus reducing background signals in the northern blot.

However, the high degree of homology between CYP3A members appeared to result in errors in the Northern analysis. Northern blot analysis of CYP3A41 demonstrated in Figure 11 indicated that CYP3A41 was present at similar levels in the male and female mice. This data contradicted previously published reports that CYP3A41 was a female specific enzyme [95].

Although there was the potential that the published reports were in error, the possibilities that the CYP3A41 primers listed in Table 1 also amplified CYP3A11 or that the CYP3A41 probes recognized CYP3A11 mRNA could not be eliminated. The CYP3A41 primers had a 90% identity to CYP3A11 mRNA while the probe had a 94% identity to CYP3A11 mRNA. As CYP3A11 and CYP3A41 mRNA was indistinguishable on the Northern blot due to their similar size (2070 bp and 2072 bp respectively), an accurate representation of the contribution of CYP3A11 recognition to the signal associated with CYP3A41 could not be determined. Subsequently, this data decreased the confidence in the other CYP3A analysis.

Further problems arose with the Northern analysis. There was questionable accuracy in the quantification by the densitometer in the analysis of some genes due to large differences in the expression levels in the different groups of mice. Northern analysis did not have the sensitivity to allow accurate quantification of some genes expressed at minimal levels after the 0.5% CA diet. Technical problems were also encountered due to the amount of RNA required and the time consuming process of stripping probes of highly expressed mRNA.

A real-time PCR method was optimized to account for the problems experienced with the Northern analysis. Real-time PCR quantifies mRNA levels by measuring the product after each round of amplification during the early exponential phase of the PCR reaction. A value, C_t , is obtained that reflects the number of amplification cycles required to obtain a threshold level of fluorescence. In combination with the quantitative data obtained from the exponential phase, replicates and samples from multiple animals allow for higher accuracy and precision, even of a poorly expressed mRNA.

SYBR Green binds to double stranded DNA and does not distinguish between the desired product, non-specific products and primer-dimers. Although careful primer design and optimization procedures should reduce the production of non-specific products and primer-dimers, reactions must be monitored to minimize the production of undesired double stranded DNA. The computer program that monitors the threshold fluorescence also monitors the dissociation of the amplicons. Most products or primer dimers will melt at different temperatures and create unique dissociation curves. Monitoring the dissociation curves of each reaction increased confidence of the specificity of the reactions.

3.2.1 Control Gene Choice

Careful normalization is important to accurately compare expression of mRNA between samples and various conditions. As there are no genes expressed at constant levels under all conditions, candidate control genes must be tested under all experimental conditions. Initial Northern blots

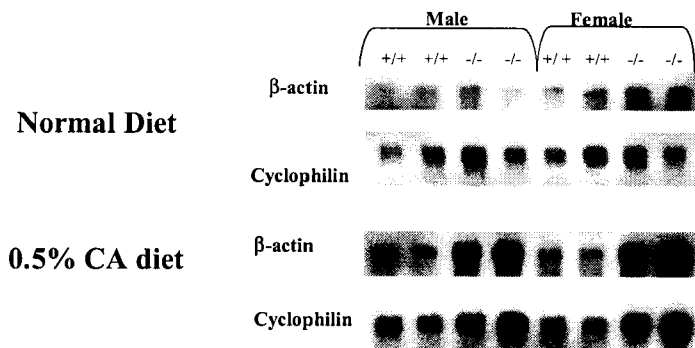


Figure 10: Northern Blot Analysis of β -actin and Cyclophilin mRNA levels of FVB/NJ mice. A diet supplemented with 0.5% CA for two days prior to sacrifice appeared to increase mRNA levels of both β -actin and Cyclophilin. A densitometer was used to quantify the bands and the values are expressed relative to female wild-type mice. Values are the average obtained from two mice in each group.

Table 7: Summary of the frequency of common housekeeping genes as determined from SAGE analysis on 4-day old C57BL mice. Tags numbers have been normalized.

	spgp ^{-/-}	spgp ^{+/+}
β -actin	32	27
GAPDH	60	40
β -2-microglobulin	0	2
15S ribosomal protein	62	56
Cyclophilin	75	72

Table 8: Correlation of RPS15 and Cyclophilin to CYP3A mRNA expression in FVB/NJ mice. Values were taken from the quantification from the real-time PCR. Correlations were calculated using the non-parametric Spearman rank correlation. The significance of the correlation is $p < 0.05$.

	RPS 15	Cyclophilin
Spearman r	0.087	0.562
P Value	0.631	0.002
Significance	No	Yes

used β -actin as the control gene. However, samples from mice fed the 0.5% CA diet indicated β -actin was expressed at much higher levels in the *spgp*^{-/-} mice than in the wild-type mice as demonstrated in Figure 10. Other control genes commonly used for mice with cholestasis were examined through a review of the SAGE data summarized in Table 8. Genes with low or varied expression were not considered as candidates. Cyclophilin initially appeared to be a strong candidate as it was highly expressed at similar levels and has been used as a control gene in the study of cholesterol and bile salt homeostasis in mice [38].

Although Cyclophilin was used as the control gene for the Northern analysis, real-time PCR suggested Cyclophilin was an unsuitable control. Comparison of the expression of Cyclophilin to expression of the CYP3A family indicated a significant correlation as summarized in Table 9. In comparison, there was no significant correlation between the expression of the CYP3A family and RPS15. Consequently, RPS15 was utilized for normalization of the real-time PCR results.

3.2.2 CYP3A mRNA Expression Profile

Expression of most of the CYP3A enzymes is upregulated in the *spgp*^{-/-} mice compared to the wild-type mice, likely reflecting the cholestatic phenotype of the *spgp*^{-/-} mice. However, CA feeding does not affect the expression of most CYP3A members. The lack of induction may reflect a previous report that bile salt intermediates rather than bile salts induce PXR [109]. However, unlike the observations in the *CYP27*^{-/-} mice, CA feeding did not inhibit CYP3A11 induction in the *spgp*^{-/-} mice [109]. This data may indicate that the CYP3A induction observed in *spgp*^{-/-} mice occurs through a different mechanism than in the *CYP27*^{-/-} mice.

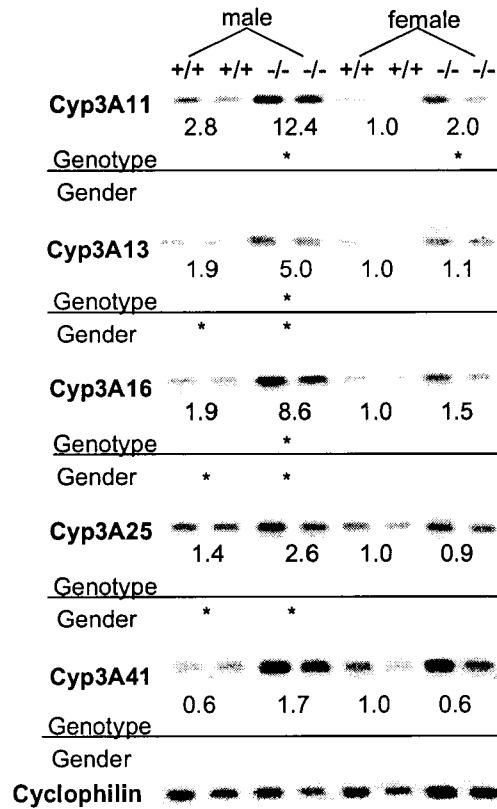


Figure 11: Northern Blot Analysis of hepatic CYP3A mRNA levels from C57BL/6J mice on a normal diet. Samples were obtained from hepatic tissue isolated from wild-type C57BL/6J (+/+) and spgp knockout mice (-/-) fed a control diet and snap frozen to -80°C. A densitometer was used to quantify the bands and the values are expressed as the fold change, after correction for Cyclophilin, relative to female wild-type mice. Values are the average obtained from two mice in each group and asterisks indicate values that are significantly different ($p < 0.05$).

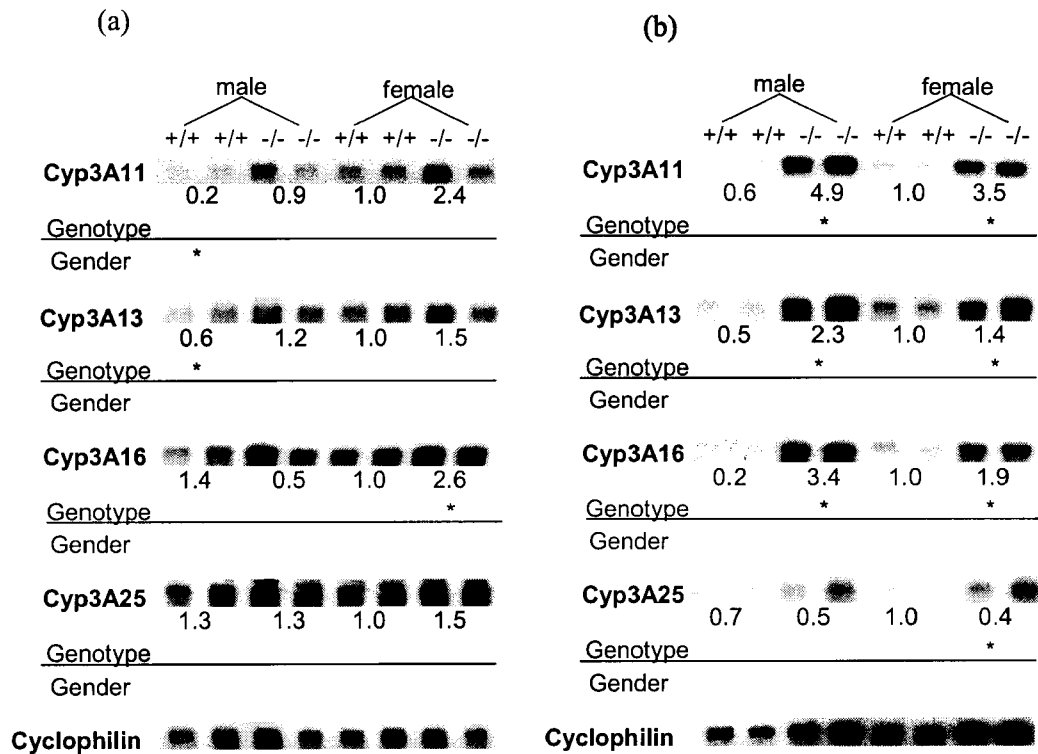


Figure 12: Northern Blot Analysis of hepatic CYP3A mRNA levels from mice of a FVB/NJ background on a (a) normal diet and (b) 0.5% CA diet for two days prior to sacrifice. Samples were obtained from hepatic tissue isolated from wild-type FVB/NJ (+/+) and spgp knockout mice (-/-) fed a control diet and snap frozen to -80°C. A densitometer was used to quantify the bands and the values are expressed as the fold change, after correction for Cyclophilin, relative to female wild-type mice. Values are the average obtained from two mice in each group and asterisks indicate values that are significantly different (p<0.05).

Generally, the real-time PCR data confirmed the trends found in the northern blot results. In several cases, the absolute number for the fold increase was not preserved. However, an increase in expression was still present and the expression was similar between genotypes with the change experienced within the calculated error. One exception to this trend was the expression of CYP3A16 in male mice fed the normal diet as real-time PCR indicated FVB/NJ male *spgp*^{-/-} mice expressed over 2-fold more CYP3A16 than the wild-type mice. While Northern blots indicated C57BL *spgp*^{-/-} mice expressed over 4-fold more CYP3A16 than the wild-type mice, they indicated FVB/NJ *spgp*^{-/-} mice expressed almost 3-fold less CYP3A16 than the wild-type mice. This irregularity may be a result of correlation between Cyclophilin expression and CYP3A expression as β -actin normalization suggested that the male FVB/NJ *spgp*^{-/-} mice expressed 2.6-fold higher levels of CYP3A16 than the wild-type mice, a result more supported by the real-time data.

As a general trend, *spgp*^{-/-} mice expressed higher levels of CYP3A11 than the wild-type mice. Northern blotting indicated that the C57BL *spgp*^{-/-} mice demonstrated a significant 2-6-fold increase in CYP3A11 expression (Figure 11), while the FVB/NJ mice ranged between 2.6-4.5 fold increase (Figure 12) under normal dietary conditions. CA feeding increased the fold increase between *spgp*^{-/-} mice and wild-type as *spgp*^{-/-} mice exhibited a significant 3.5-8 fold increase in CYP3A11 expression. In all cases, the males displayed a larger increase in the CYP3A11 expression of the *spgp*^{-/-} mice when compared to the wild-type mice. Real-time PCR indicated a significant 4-fold increase between *spgp*^{-/-} mice and wild-type mice of both genders fed the normal diet with 0.5% CA feeding not resulting in a significant increase in expression. Although Northern blotting of the FVB/NJ samples indicated wild-type females fed the normal

diet expressed significantly more CYP3A11 than wild-type males, this difference was not observed in the real-time PCR analysis.

In the C57BL mice, Northern Blotting indicated a significant gender difference in the expression of CYP3A16. Male wild-type C57BL mice expressed almost 2-fold higher levels of CYP3A13 than the female wild-type C57BL mice and over 4-fold higher levels in the male *spgp*^{-/-} mice than the female *spgp*^{-/-} mice. The C57BL male *spgp*^{-/-} mice also express CYP3A13 over 2-fold higher than the male wild-type mice. When the genetic background was changed to the FVB/NJ strain, Northern blot and real-time PCR indicated less variation between the mice, with the only the 2-fold difference between the male wild-type and *spgp*^{-/-} mice remaining significant. After the 0.5% CA diet, Northern blot analysis of FVB/NJ mice indicated the male *spgp*^{-/-} mice expressed 4-fold more CYP3A13 than wild-type and females expressed 40% more CYP3A13 than wild-type. Real-time PCR (Figure 13(b)) does not confirm these increases and they may be a result of Cyclophilin and CYP3A correlation of the 0.5% CA diet.

CYP3A16 is expressed in a similar pattern as CYP311. Real-time PCR indicates that *spgp*^{-/-} mice fed the normal diet demonstrate over a 2.6-fold increase in CYP3A16 levels compared to the wild-type mice. Although there is no significant due to the 0.5% CA diet, the 0.5% CA fed *spgp*^{-/-} mice expresses 4-fold more CYP3A16 than the wild-type mice.

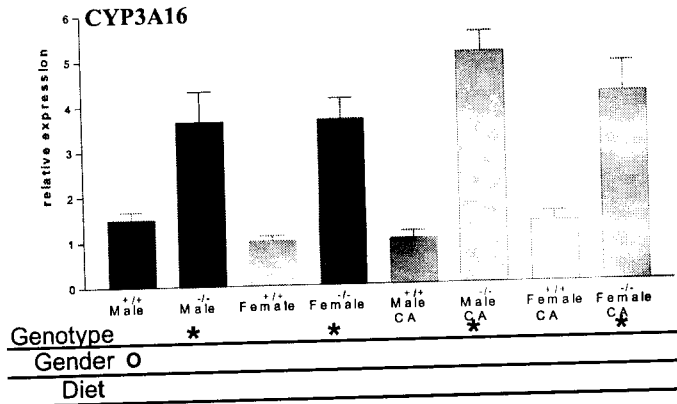
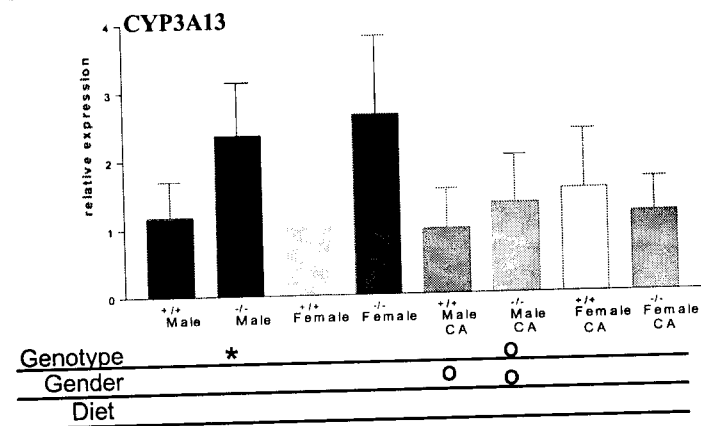
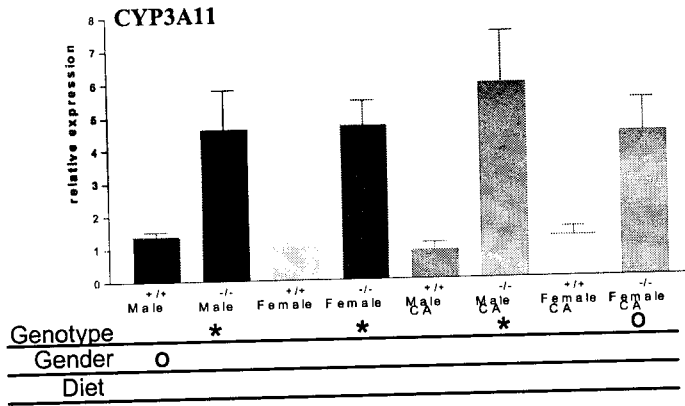
According to Northern blot analysis, CYP3A25 is expressed at similar levels in all the mice fed the normal diet. However, real-time PCR demonstrates a 2-fold increase in the female *spgp*^{-/-} mice compared to the wild-type mice. After the 0.5% CA feeding, CYP3A25 expression in

female *spgp*^{-/-} mice significantly increases by 50%. None of the other mice experience a significant change in expression of CYP3A25 due to the diet change.

Northern blot analysis did not provide an accurate representation of CYP3A41 expression. In comparison, real-time PCR was specific enough to detect this female specific enzyme (Figure 13(e)). CYP3A41 responded differently to the mild cholestasis exhibited by the *spgp*^{-/-} mice as the female *spgp*^{-/-} mice expressed slightly lower levels, but not significantly different than the female wild-type mice. While the 0.5% CA diet resulted in increased or maintenance of the expression of the other CYP3A, expression of CYP3A41 decreased 2-fold in the female wild-type mice and over 7-fold in the female *spgp*^{-/-} mice.

CYP3A41 was not expected to follow the same expression pattern as the other CYP3A enzymes since its expression is hormone regulated and normal CYP3A inducers do not increase expression [95]. Due to the decrease after 0.5% CA feeding, it is unlikely that CYP3A41 is involved in bile salt detoxification. However, expression of CYP3A41 is affected by elevated bile salt levels, possibly through the same elements that can result in pregnancy induced cholestasis [138].

Under the normal diet, CYP2B10 appeared to be female specific as it was expressed at quite low levels in both wild-type and knockout male mice (Figure 13(f)). However, when fed the 0.5% CA diet, the expression of CYP2B10 in male *spgp*^{-/-} mice reached levels comparable to expression in the female mice. However, the 0.5% CA diet did not lead to an induction of



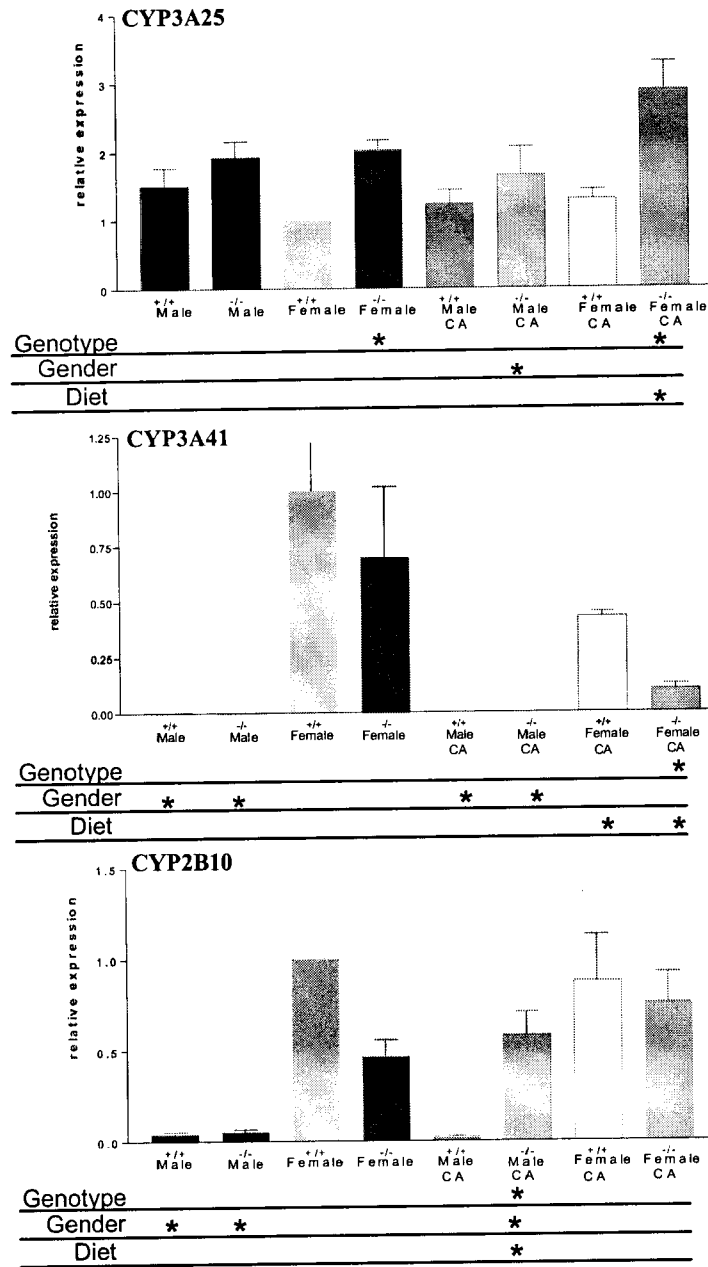


Figure 13: Real-time PCR Analysis of hepatic CYP3A mRNA levels from mice of a FVB/NJ background. Mice were fed either a normal diet or a 0.5% CA enriched diet for two days prior to sacrifice. Samples were obtained from hepatic tissue isolated from wild-type FVB/NJ (+/+) and *spgp*^{-/-} mice (-/-) and snap frozen to -80°C. Values are expressed as the fold changed, after correction for Cyclophilin, relative to female wild-type mice. Values are the average obtained from three to five mice in each group. “*” indicates values that are significantly different at p<0.05 and “o” indicates the values are significantly different at p>0.1.

CYP2B10 in male wild-type mice. The differential expression in CYP2B10 between the male wild-type and male *spgp*^{-/-} mice may be a result of a compensatory mechanism.

The expression patterns of CYP3A11 and CYP3A16 are quite similar. Both are expressed at higher levels in the *spgp*^{-/-} mice than in the wild-type mice. Gender and the two diets tested did not appear to significantly change the expression levels in either genotype. While the CA feeding does not affect the level of tetrahydroxylation in the *spgp*^{-/-} mice, the level does increase significantly in the wild-type mice. Based on the lack of correlation between gene expression and the tetrahydroxylated bile salt levels, it is unlikely that either CYP3A11 or CYP3A16 is involved.

Expression of CYP3A13 and CYP3A25 is similar in the wild-type and *spgp*^{-/-} mice, so it is unlikely that either of these two enzymes is involved. There is the possibility that they could be involved based upon the availability of substrate rather than expression but the major tetrahydroxylated bile salt is suspected to be based upon β MCA and β MCA levels do not change significantly after two day 0.5% CA feeding.

3.2.3 Bile Salt Synthesis CYP mRNA Expression Profile

CYP7A1 is expressed at low levels in male wild-type C57BL mice, and the male *spgp*^{-/-} mice significantly express 6-fold higher levels (Figure 14). There is no significant difference in the expression CYP7A1 in the female wild-type and *spgp*^{-/-} C57BL mice. Northern analysis of FVB/NJ mice fed the normal diet indicates no significant expression difference. In comparison, real-time PCR indicates *spgp*^{-/-} mice express higher levels of CYP7A1 than the wild-type mice with the

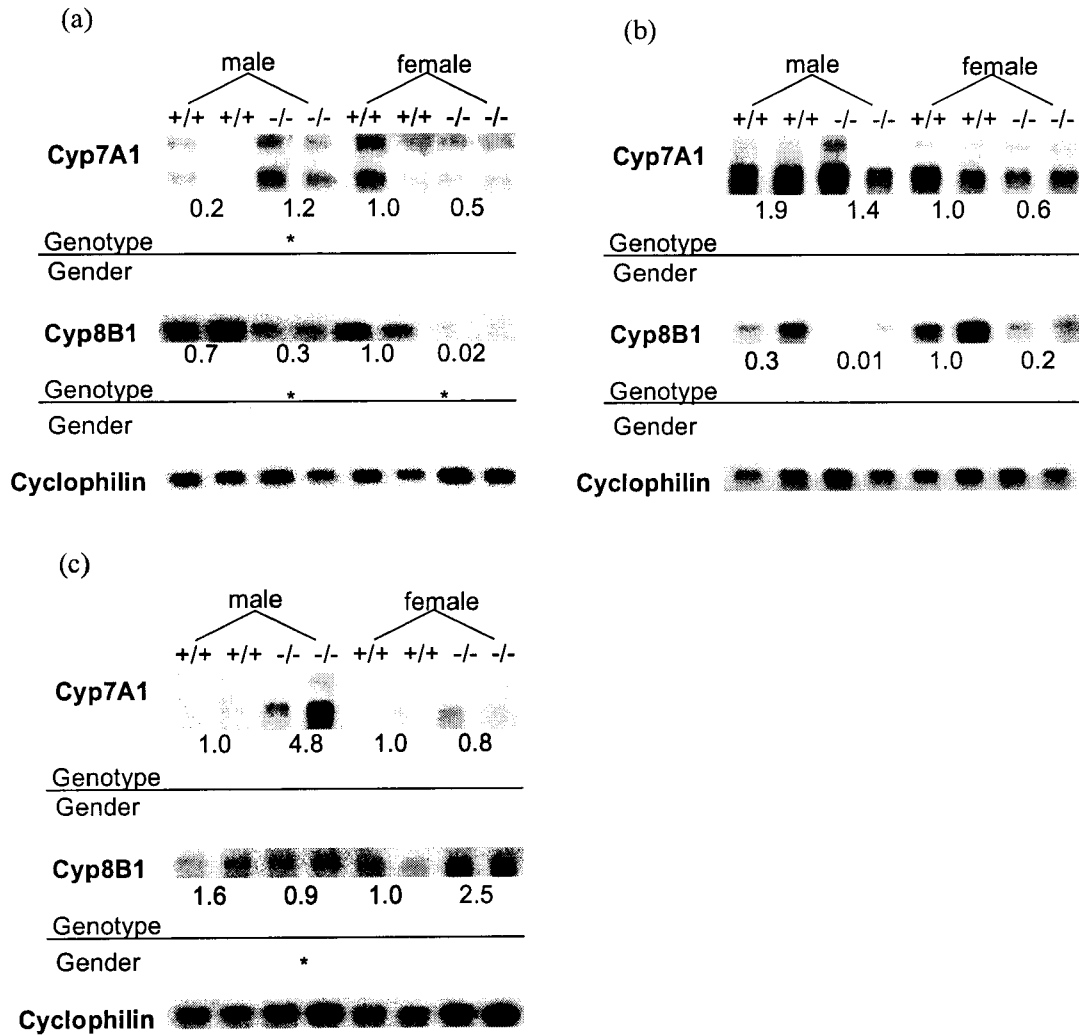


Figure 14: Northern Blot Analysis of hepatic bile salt biosynthesis CYP mRNA levels of (a) C57BL/6J mice on a normal diet, (b) FVB/NJ mice on a normal diet, and (c) FVB/NJ mice fed a 0.5% CA supplemented diet for two days prior to sacrifice. Samples were obtained from hepatic tissue isolated from wild-type (+/+) and spg^g knockout mice (-/-) and snap frozen to -80°C. A densitometer was used to quantify the bands and the values are expressed as the fold change, after correction for Cyclophilin, relative to female wild-type mice. Values are the average obtained from two mice in each group and asterisks indicate values that are significantly different (p<0.05).

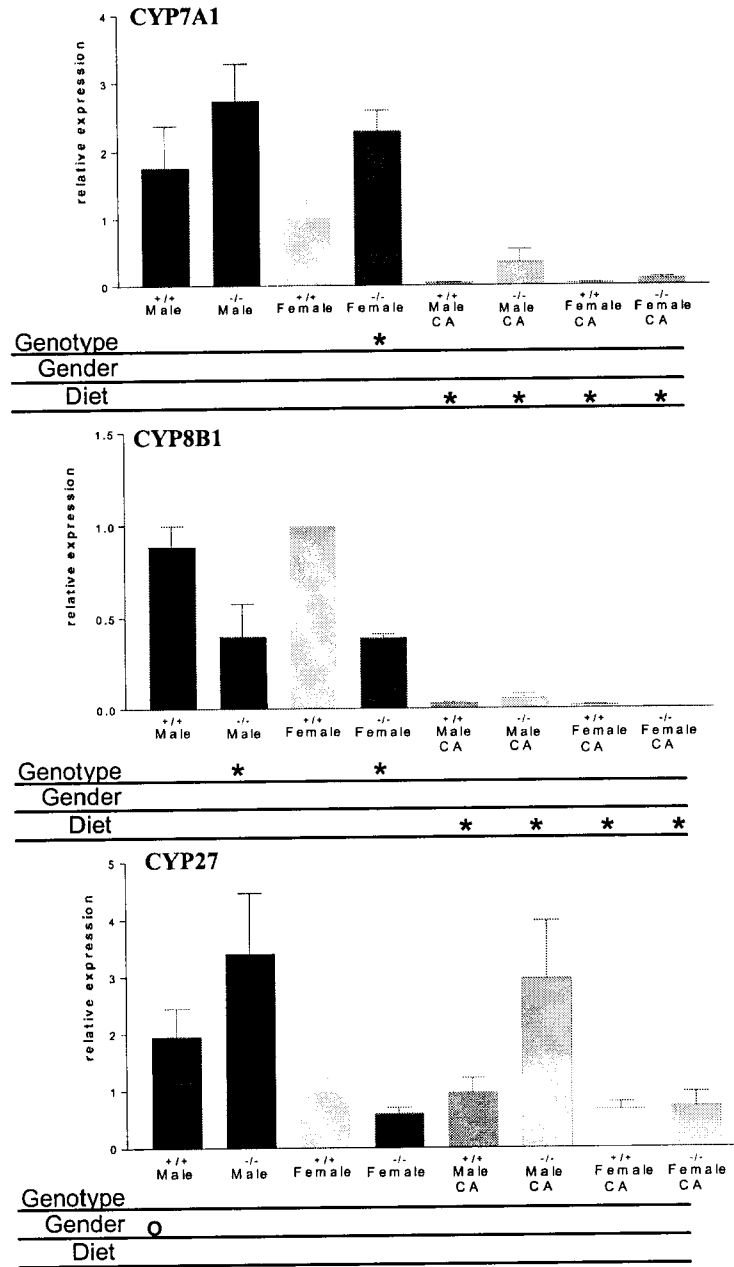


Figure 15: Real-time PCR Analysis of mRNA levels of hepatic enzymes involved in bile salt synthesis from mice of a FVB/NJ background. Mice were fed either a normal diet or a 0.5% CA enriched diet for two days prior to sacrifice. Samples were obtained from hepatic tissue isolated from wild-type FVB/NJ (+/+) and spgq knockout mice (-/-) and snap frozen to -80°C . Values are expressed as the fold changed, after correction for Cyclophilin, relative to female wild-type mice. Values are the average obtained from three to five mice in each group. “*” indicates values that are significantly different at $p < 0.05$ and “o” indicates the values are significantly different at $p > 0.1$.

female FVB/NJ *spgp*^{-/-} mice expressing 2.5-fold higher levels than the female wild-type mice. Both Northern blot analysis and real-time PCR reflected a significant decrease in the CYP7A1 expression of all mice after the 0.5% CA feeding. Although male *spgp*^{-/-} mice fed the 0.5% CA diet appear to express slightly higher levels of CYP7A1 than the other mice in both real-time PCR and Northern analysis, this difference was not significant.

In the C57Bl mice, the wild-type mice significantly expressed at least 2.5-fold more CYP8B1 than the *spgp*^{-/-} mice and no gender difference was observed. In the FVB mice, this trend continued although the significance in the difference between the wild-type and *spgp*^{-/-} mice demonstrated in real-time PCR was only at the 90% confidence level. After the 0.5% CA diet, expression was significantly reduced to barely detectable levels. This decrease is likely due to bile salt activation of FXR [56]. Another possible reason for the reduction of CYP8B1 expression is end-product regulation. CYP8B1 modulates the ratio of CA to CDCA through 12 α hydroxylation of CDCA to produce CA [139]. Since the diet of the mice is enriched in CA, the enzyme that produces more CA may be reduced.

Figure 15 indicates that CYP27, the main enzyme in the alternate pathway, demonstrates a gender difference as the male *spgp*^{-/-} express approximately 4-fold more enzyme than the female *spgp*^{-/-} mice under the normal diet. On the CA diet, the male mice appear to express more CYP27 than the female mice, but this increase is not significant at the 95% level. There was no difference between wild-type and *spgp*^{-/-} mice or between normal and the 0.5% CA diet.

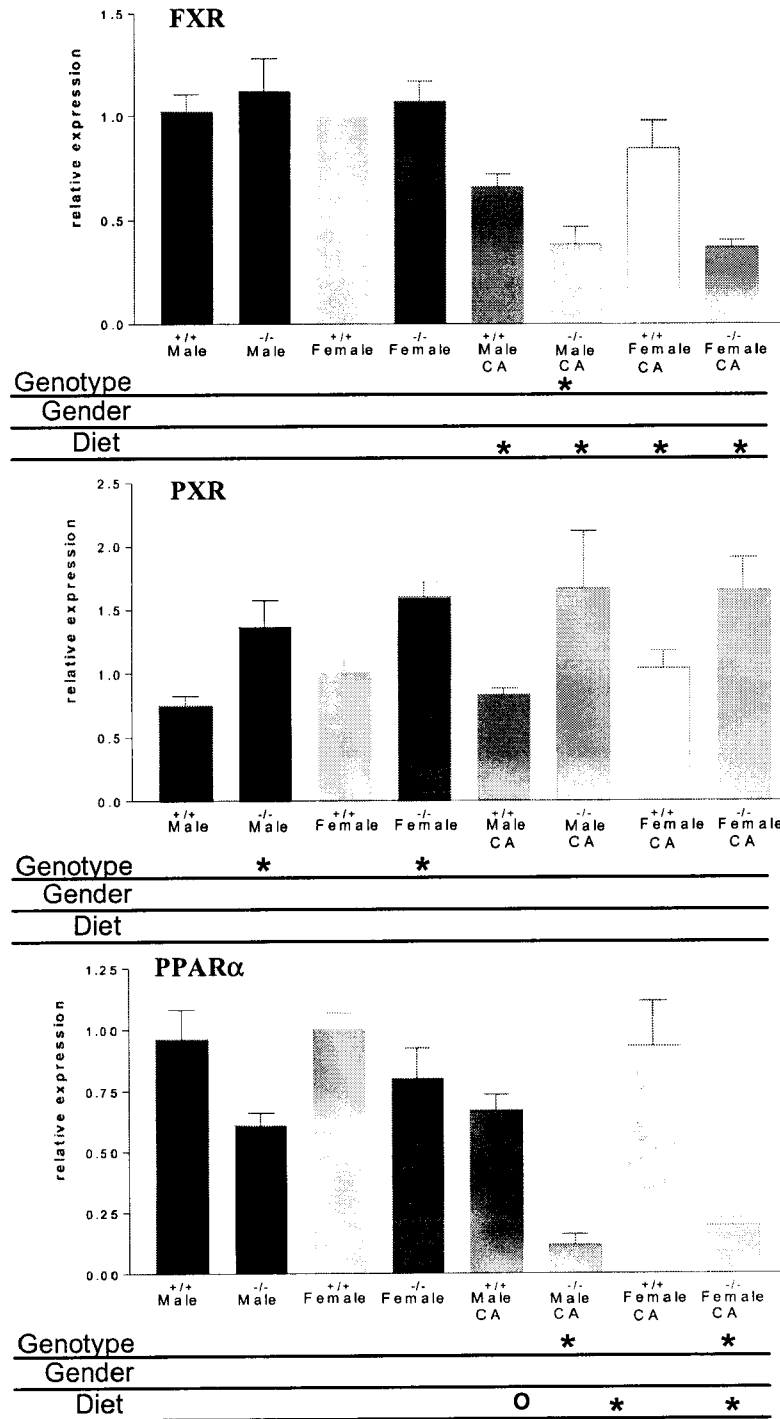
3.2.4 Nuclear Receptor mRNA Expression Profile

Many of the nuclear receptors that control expression of genes involved in detoxification or cholesterol homeostasis were affected by the bile salts present from cholestasis in the *spgp*^{-/-} mice or due to 0.5% CA feeding. Figure 16 summarizes the results of the expression patterns of five nuclear receptors involved in cholesterol and bile salt homeostasis using real-time PCR.

Bile salts such as CDCA and DCA were found to act as ligands for FXR [47, 58, 98]. FXR is involved in the expression of genes like *Spgp*, *CYP8B1*, and *NTCP* [56]. FXR activation also induces expression of *SHP-1*, which represses expression of *CYP7A1* [103]. Consequently, FXR is thought of as a bile salt sensor.

FXR was expressed at similar levels in the four groups of mice fed the normal diet. However, once fed the 0.5% CA diet, all the genotypes experienced a significant decrease in FXR expression levels. The wild-type mice fed the 0.5% CA diet expressed 60% the amount of FXR that the wild-type mice fed the normal diet did. In comparison, the *spgp*^{-/-} mice fed the 0.5% CA diet only expressed 40% the amount of FXR expressed by the *spgp*^{-/-} mice fed the normal diet.

Activation of PXR through ligand binding leads to transcriptional upregulation of many CYP3A members as well as several ABC transporters [101, 106]. Due to the potential for PXR activation to protect against certain liver diseases, PXR agonists may be used to treat cholestatic liver damage [106]. Under normal dietary conditions, there is a significant 50% increase in PXR expression in the *spgp*^{-/-} mice compared to the wild-type mice. The pattern remains the same for the mice fed the 0.5% CA diet. Since PXR regulates the expression of many CYP3A subfamily



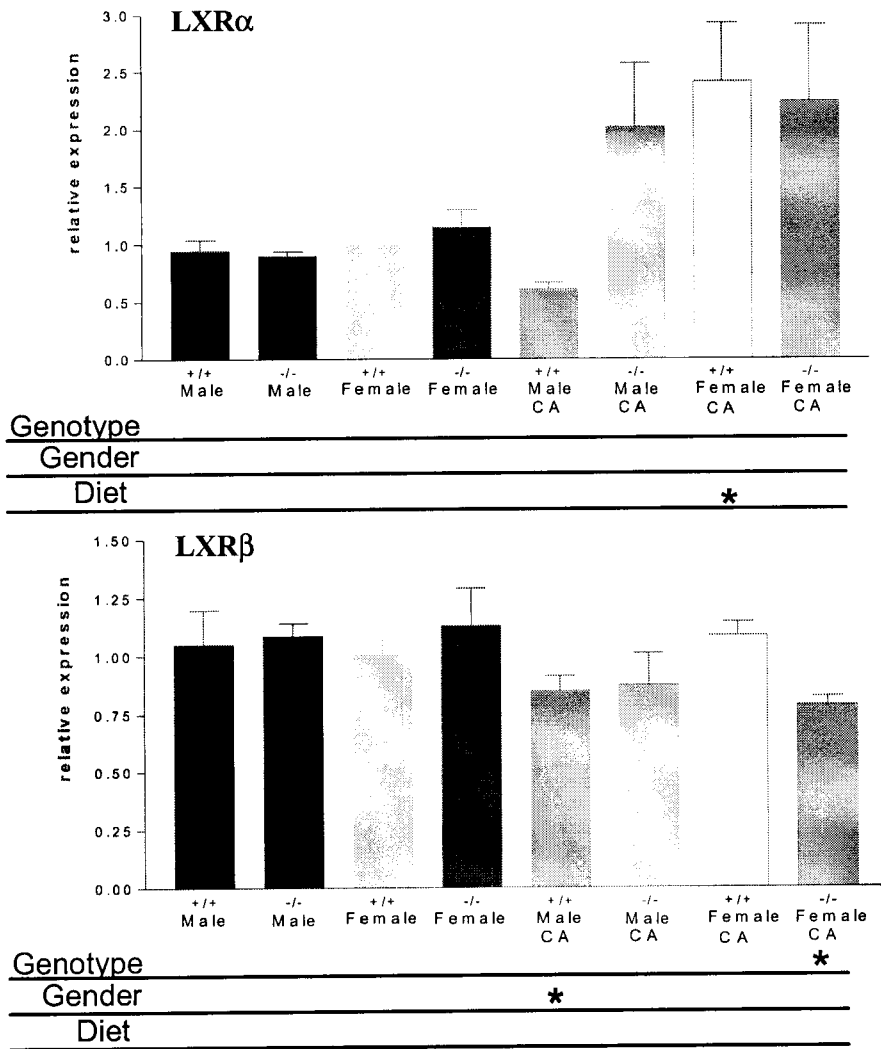


Figure 16: Real-time PCR Analysis of mRNA levels of nuclear receptors affected by bile salts from mice of a FVB/NJ background: (a) FXR; (b) PXR; (c) LXR α ; (d) LXR β ; and (d) PPAR α . Mice were fed either a normal diet or a 0.5% CA enriched diet for two days prior to sacrifice. Samples were obtained from hepatic tissue isolated from wild-type FVB/NJ (+/+) and spgp knockout mice (-/-) and snap frozen to -80°C . Values are expressed as the fold changed, after correction for Cyclophilin, relative to female wild-type mice. Values are the average obtained from three to five mice in each group. “*” indicates values that are significantly different at $p < 0.05$ and “o” indicates the values are significantly different at $p > 0.1$.

members, it is not surprising that expression levels of these CYP3A members did not change in the mice fed the 0.5% CA diet. LXR α and LXR β are nuclear receptors that help regulate the metabolism of cholesterol and bile salts through activation *via* oxysterols or 6 α -hydroxyl bile salts [60, 61]. Characterization of LXR α ^{-/-} mice confirmed the inability to increase CYP7A1 expression and the inability of LXR β to compensate for the loss of LXR α [140].

PPAR α is a nuclear receptor that regulates many genes important for fatty acid β -oxidation. Although bile salts may act as ligands for the other nuclear receptors tested, bile salts do not activate PPAR α . However, during periods of cholestasis, CDCA and CA are capable of antagonizing PPAR α actions through interfering with the recruitment of transcriptional coactivators [55].

When fed the normal diet, wild-type mice expressed slightly higher levels of PPAR than the *spgp*^{-/-} mice did. However, the decrease was only significant in the male *spgp*^{-/-} mice, which expressed 40% less PPAR α than male wild-type mice. When fed the 0.5% CA diet for 2 days, expression of PPAR by the wild-type mice did not change significantly. However, expression of PPAR by the *spgp*^{-/-} mice decreased over 4-fold.

4 Discussion

Cholestatic mouse models in which cholestasis is induced through bile salt administration, indicate that increased bile salt hydroxylation can reduce the severity of the cholestasis [7, 99, 141]. Unlike other cholestatic models in which the role of transport and hydroxylation cannot be tested, our model has the major bile salt export pump knocked out [3]. From results of studies

with *spgp*^{-/-} mice, I conclude that an unknown transport mechanism is capable of transporting the more hydrophilic bile salts. Since the biliary bile salt pool of the *spgp*^{-/-} mice appears to be more hydrophilic than the wild-type mice and contains tetrahydroxylated bile salts, bile salt hydroxylases may be induced as part of a protective mechanism against the damages caused by cholestasis.

HPLC analysis confirmed findings that bile salt transport of the hydrophobic bile salts was impaired in the *spgp*^{-/-} mice. However, transport of the hydrophilic bile salts such as the TMCAs, TUDCA, and tetrahydroxylated bile salts occurred through an alternate mechanism. Supplementing the diet with 0.5% CA diet increased biliary bile salt levels to levels comparable with wild-type mice [83]. Nonetheless, increased transport cannot occur through simply increasing bile salt levels as a CA infusion does not result in elevated levels of bile salt transport in the *spgp*^{-/-} mice [83].

A 2-day 0.5% CA diet was sufficient to induce a small increase in the tetrahydroxylated bile salt levels in the wild-type mice. In comparison, 2-days of 0.5% CA feeding did not lead to a significant increase in the levels of the tetrahydroxylated bile salt already present in the *spgp*^{-/-} mice. However, prolonged feeding for over a week produces an increase in tetrahydroxylated bile salt production indicating the possibility that the hydroxylation system is not completely saturated in the *spgp*^{-/-} mice.

HPLC analysis of the *spgp*^{-/-} mouse bile indicated the presence of three of the taurine conjugated tetrahydroxylated bile salts with structures confirmed through MS analysis. These experiments

demonstrate the feasibility of monitoring tetrahydroxylated bile salts in the *spgp*^{-/-} mice and utilizing this method in future *in vitro* bile salt hydroxylation assays. Identification of the actual hydroxylation pattern is dependent upon the availability of tetrahydroxylated bile salt standards.

One of these peaks is likely the major tetrahydroxylated bile salt, tauro-3 α ,6 β ,7 β ,12 α -tetrahydroxy-5 β -cholanic acid, the major tetrahydroxylated bile salt [82]. Due to the hydroxylation pattern, it is likely that β MCA was hydroxylated in the 12 α position. This pattern is different than the tetrahydroxylation patterns previously identified in human cholestasis. The major tetrahydroxylated bile salt previously identified in cholestatic humans are likely 6 α or 1 β hydroxylated CA [33].

Consequently, it appears the hydroxylation mechanism in humans is based on the production of CA while in mice the hydroxylation pathway is based on the production of MCAs. In humans, only a small percentage of the radiolabeled CDCA was converted into the tetrahydroxylated bile salt fraction. Conversely, 0.5% CA dietary enrichment failed to stimulate increased levels of the tetrahydroxylated bile salt fraction. However, the actual components of the tetrahydroxylated bile salt fraction in the wild-type and the *spgp*^{-/-} mice could be compared to determine if they produce the regio- and stereoisomers at the same frequency. Furthermore, analysis of the small bile salt pool of PFIC2 patients could determine if these patients also produce tetrahydroxylated bile salts.

Induction of the expression of bile salt hydroxylases may be the reason for the increased hydrophilic nature of the biliary bile salt pool of the *spgp*^{-/-} mice. With the exception of

CYP3A41, the CYP3A family members are expressed at higher levels in the *spgp*^{-/-} mice than in the wild-type mice. The level of induction is comparable to the 2-fold CYP3A10 induction in male hamsters in response to CA feeding [123]. Expression of these genes is regulated by the nuclear receptor, PXR. Evidence suggests that PXR is induced by bile salt precursors, which may explain the slightly elevated expression levels of CYP7A1 in the *spgp*^{-/-} mice [109]. While CYP3A11 levels remain relatively constant in *spgp*^{-/-} mice, even after 0.5% CA feeding, *CYP27*^{-/-} mice experienced over a 3-fold decrease in CYP3A11 expression on a 0.1% CA diet. Both knockout mice demonstrated a significant reduction of CYP7A1 on the CA supplemented diet. However, while the *CYP27*^{-/-} mice lack the CYP27 pathway, CYP27 expression is unaffected in *spgp*^{-/-} mice. Consequently, bile salt precursors are available in the *spgp*^{-/-} mice fed the CA supplemented diet that are not available to the *CYP27*^{-/-} mice.

Analysis of the mRNA expression patterns of three of the major enzymes involved in bile salt synthesis indicated that it was unlikely that these enzymes have an important role in bile salt tetrahydroxylation. CYP7A1 appears to be expressed at higher levels in the *spgp*^{-/-} mice fed the normal diet although this difference is only significant in the female mice. Since FXR is activated by bile salts and represses transcription of CYP7A1, there could be some other mechanism like LXR α causing the elevated expression levels [57, 136, 142]. Increased expression of CYP7A1 has been linked to increased degradation of cholesterol and elevated levels of LDLR, ACAT, and cholesteryl ester hydrolase [38]. Elevated levels of CYP7A1 could be one mechanism the *spgp*^{-/-} mice use to eliminate excess cholesterol.

Under the CA enriched diet in the *FXR*^{-/-} mice, CYP8B1 did not experience decreased expression like the wild-type mice. However, in the *spgp*^{-/-} mice and in the wild-type mice, CYP8B1 levels significantly decreased after the CA supplemented diet. The decrease in expression levels for CYP8B1 in the mice fed the 0.5% CA supplemented diet can be attributed to regulation by FXR [56].

CYP27 was expressed at approximately 2-fold higher levels in the male mice than in the female mice fed the normal diet. When fed the 0.5% CA enriched diet, CYP27 expression in the females and the male *spgp*^{-/-} mice remained the same but there was a slight expression decrease in the male wild-type mice. Since CYP27 expression is probably linked to cholesterol levels, it is possible that these changes reflect the cholesterol levels [63]. Male mice expressed more CYP27 than the female mice did. This gender difference may explain why CYP27 overexpressing mice had altered biliary bile salt composition and increased fecal levels of neutral steroids, compared to the wild-type mice, in females but not in males [64].

Previous work by this lab indicated certain requirements for the expression of the gene for bile salt tetrahydroxylation if regulation occurs at the mRNA level. As levels of tetrahydroxylated bile salts are higher in *spgp*^{-/-} mice than in wild-type mice, regulation at the expression should result in higher expression levels in the *spgp*^{-/-} mice. No gender difference in expression would be expected since male and female *spgp*^{-/-} mice produce similar levels of the tetrahydroxylated bile salts. Although the major tetrahydroxylated bile salt appears to be derived from β MCA, there is no significant change in β MCA concentration between wild-type and *spgp*^{-/-} mice.

Furthermore, 2 days of 0.5% CA diet supplementation did not lead to a significant increase in tetrahydroxylation levels in the *spgp*^{-/-} mice. Consequently, expression levels of the gene involved in bile salt tetrahydroxylation after two days of the 0.5% CA diet in the *spgp*^{-/-} mice would not be expected to be elevated. While there is not a significant increase in the relative levels of the tetrahydroxylated bile salts between the normal diet and the 2-day 0.5% CA challenged *spgp*^{-/-} mice, a significant increase is observed during prolonged periods of 0.5% CA feeding [83]. Tetrahydroxylation of bile salts is not restricted to the *spgp*^{-/-} mice as wild-type mice produce minimal levels under the normal diet and levels 30% of the *spgp*^{-/-} mice when fed the 0.5% CA diet [82, 83].

None of the CYP3A family members examined fit the expression requirements to be the bile salt tetrahydroxylase. Consequently, it is unlikely that regulation of the expression of these genes is involved with the regulation of the production of the tetrahydroxylated bile salts. There is the possibility of regulation through the expression of another gene. Since none of the expression patterns of the nuclear receptors tested paralleled the production of the bile salt tetrahydroxylase, expression of the nuclear receptors is unlikely to be the regulatory mechanism. However, the availability of ligands can act as a regulatory mechanism as demonstrated by bile salt intermediates acting as ligands to PXR and regulating CYP3A expression [109].

I had expected the expectation that bile salt synthesis enzymes would be reduced in the *spgp*^{-/-} mice due to their elevated levels of bile salts and the negative-feedback regulation of FXR. However, bile salt synthesis is not impaired in the *spgp*^{-/-} mice on the normal diet. Previous work indicated bile salt feeding inhibited CYP7A1 expression and the production of the bile salt

intermediates, these experiments were performed on *CYP27^{-/-}* mice [109]. However, CYP27 expression is significantly different between genders so it is unlikely that it is involved with the bile salt tetrahydroxylation.

Differential survival patterns of the *spgp^{-/-}* mice fed the 0.5% CA diet were demonstrated [83]. While females are more cholestatic than on the normal diet, they do not appear to be terminally ill. Conversely, most males die within 5-9 days of starting the 0.5% CA diet. Since bile salt tetrahydroxylation levels are not significantly different, there must be another factor contributing to the survival of the female *spgp^{-/-}* mice.

Since this study indicates that regulation of the expression of the CYP3A enzymes does not control the production of the tetrahydroxylated bile salt, there are several possibilities. One important possibility is that the CYP3A is involved, however, regulation occurs at the protein level or through substrate availability, or it is not a rate-limiting enzyme. An alternate possibility is the involvement of some other enzyme. However, due to the nuclear receptor expression analysis, it is likely that even if another enzyme is involved, the other enzyme is not regulated at the transcriptional level. A further consideration is the considerable variation in the expression of some genes, despite the inbred background of the mice. Even the hepatocytes, the cells of interest, exist in a gradient as periportal and perivenous cells have different expression profiles [15, 20]. Furthermore, the expression of many CYPs is affected by hormonal rhythms that vary throughout the day [143-145]. These sources of variation might obscure a change in the expression pattern of the bile salt tetrahydroxylase.

Expression analysis indicates that levels of many of the CYP3A enzymes are elevated in the *spgp*^{-/-} mice compared to the wild-type mice and are not affected by 0.5% CA dietary feeding. This increase provides support for the idea that CYP3A enzymes are involved in bile salt detoxification in the *spgp*^{-/-} mice. The lack of CYP3A increase in the *spgp*^{-/-} mice fed the 0.5% CA diet suggests that this detoxification mechanism can be saturated. While no correlation could be found between the biliary tetrahydroxylated bile salt levels and the mRNA expression of a candidate CYP3A, it is possible that this is a result of the heterogeneity of the liver. Other possibilities include regulation at the protein level or bile salt tetrahydroxylation is the result of a gene not examined.

5 Future Work

Bile salts have been identified as inhibitors of CYPs at both a non-specific level and specific level [110, 112]. The actual mechanism for the specific reduction in the level of certain CYP is unclear and may be due to decreased protein synthesis or increased protein degradation. Hydrophobic bile salts tend to cause a decrease in total CYP levels while the more hydrophilic bile salts either increase CYP levels or at least negate the decrease caused by the hydrophobic bile salts [118]. Preliminary MS data indicates similarity between the biliary bile salt distribution and the liver bile salt distribution [3, 82]. Since the bile salt pool in the *spgp*^{-/-} mice is decreased and more hydrophilic than the wild-type mice, it would be interesting to observe the effect on the total CYP pool.

Measurement of the total CYP pool could be determined through the measurement of the difference spectrum at 450 nm between the CO adduct of the reduced protein and the reduced CYP450 [86, 146]. Consequently, once microsomes are isolated from mice of different

genotypes, genders, ages and diets, the effect of each of the variables on the total CYP levels could be monitored. Preliminary work on C57BL mice indicated that the *spgp*^{-/-} mice have approximately 75% the total CYP levels of the wild-type mice.

The testosterone hydroxylation assay is a well established method for the identification of changes in the CYP profile under various conditions [147]. This assay uses the regio- and stereospecific hydroxylation of the testosterone steroid nucleus to create a sensitive fingerprint. By isolating microsomes from mice of different genotypes, different genetic backgrounds, different genders, different ages, and different dietary conditions, CYP profiles could be created. Some of these trends may correspond to improved or decreased health of the mice, or be related to changes in the bile salt pool.

One additional benefit to testosterone hydroxylation analysis is that production of the 6 β -hydroxytestosterone metabolite is also one of the common methods for the measurement of CYP3A activity [145]. In addition to mRNA expression analysis, an accurate profile of the CYP3A family requires analysis of the enzymatic activity. Further examination of the impact of the various factors on CYP3A activity could provide insight into the detoxification response of the *spgp*^{-/-} mice to their cholestasis. Furthermore, changes in the bile salt pool may be associated with changes in the activity of CYP3A.

Intraperitoneal injection of known murine CYP inducers would provide insight into the effect of increasing expression or activity of a specific CYP family upon the bile salt pool. Although most of the inducers are not specific to one isozyme, *in vivo* determination of the effect of the inducers

could increase the detoxification process by the *spgp*^{-/-} mice. These tests could identify families that play a major role in the detoxification, through the tetrahydroxylation, increasing the hydrophilicity of the bile salt pool, or through some other mechanism. The identification of compounds that increase the level of tetrahydroxylation would prove to be beneficial in the attempt to isolate the enzyme through traditional protein isolation methods.

Furthermore, it would be interesting to see if compounds that increase the level of tetrahydroxylation in the *spgp*^{-/-} mice are capable of increasing the level of tetrahydroxylation in the wild-type mice. The effects of the compounds could aid in the determination of whether it is the presence of the enzyme or substrate that determines the synthesis of the tetrahydroxylated bile salts, *in vivo*. Finally, if a family is identified as being involved in the production of the tetrahydroxylated bile salts, inhibitors of that family could also be tested to determine if preventing the innate detoxification method of the *spgp*^{-/-} mice would produce a phenotype close to PFIC2.

Previous administration of radiolabeled bile salts indicated that most of the bile salts were transported into the liver but few were transported into the bile. Consequently, radiolabeled β MCA, the suspected substrate for the tetrahydroxylation, could be injected into the mice and the bile salt pool could be monitored through HPLC and a scintillation counter or MS. If the tetrahydroxylated bile salt fraction is found to contain radioactivity, it can be assumed that β -muricholic acid is an *in vivo* substrate for the tetrahydroxylation reaction.

One of the most important experiments in the identification of the enzymes involved in tetrahydroxylation of the bile salts is the development of an *in vitro* assay system. Prior to the identification of the numerous CYP isoforms, work was being performed on the *in vitro* tertiary hydroxylation of bile salts using microsomes [40]. This early method could be used as a starting point for the basis of the assay. Furthermore, reproducing those experiments could act as a positive control for the integrity of the initial system. Once the assay system has proven itself, attempts could be made to purify the enzyme. There are many methods available for the isolation of CYPs from the microsomal fraction [148]. By using the assay system, it would be possible to measure the increase in the specific activity and characterize the system.

Besides being used to help in the identification of the protein, development of a bile salt tetrahydroxylation assay could give valuable insight into the preferred substrates and the products. Currently, only the major form of the tetrahydroxylated bile salts has been identified as tauro-3 α ,6 β ,7 β ,12 α -tetrahydroxy-5 β -cholanic acid [82]. Based on its structure, this bile salt could be derived from 12 α hydroxylated β -MCA. However, HPLC analysis revealed the presence of at least three different tetrahydroxylated bile salts. Through the use of commercially available bile salts, the preferred substrate could be determined. Furthermore, identification of the other forms could be aided by the knowledge of the initial substrate.

Besides bile salt tetrahydroxylation as a detoxification mechanism, other factors involved in detoxification need to be considered. The difference in survival observed between the male and female *spgp*^{-/-} mice on the 0.5% CA diet could be initially investigated through changing sex-hormone levels in the mice through hypophysectomy or hormone injection. The gender

difference was interesting as cholestasis may be induced during hormonal changes experienced during pregnancy [138].

The conflict surrounding the T β MCA levels in *spgp*^{-/-} mice also needs to be resolved. While initial MS analysis confirms that the peak only consists of T β MCA, further analysis needs to be performed. If the peak only consists of T β MCA, it could provide a good substrate to use to characterize the unknown alternate transporter. The alternate possibility is that the peak consists of multiple components, including T β MCA. Since the other components only appear significantly in the *spgp*^{-/-} mice, identification of these components may be important in the detoxification mechanism.

6 References

1. Gerloff, T., Stieger, B., Hagenbuch, B., Madon, J., Landmann, L., Roth, J., Hofmann, A.F., and Meier, P.J., *The sister of P-glycoprotein represents the canalicular bile salt export pump of mammalian liver*. J Biol Chem, 1998. **273**(16): p. 10046-50.
2. Childs, S., Yeh, R.L., Georges, E., and Ling, V., *Identification of a sister gene to P-glycoprotein*. Cancer Res, 1995. **55**(10): p. 2029-34.
3. Wang, R., Salem, M., Yousef, I.M., Tuchweber, B., Lam, P., Childs, S.J., Helgason, C.D., Ackerley, C., Phillips, M.J., and Ling, V., *Targeted inactivation of sister of P-glycoprotein gene (spgp) in mice results in nonprogressive but persistent intrahepatic cholestasis*. Proc Natl Acad Sci U S A, 2001. **98**(4): p. 2011-6.
4. Paumgartner, G. and Beuers, U., *Ursodeoxycholic acid in cholestatic liver disease: mechanisms of action and therapeutic use revisited*. Hepatology, 2002. **36**(3): p. 525-31.
5. Tanaka, M., Nakura, H., Tateishi, T., Watanabe, M., Nakaya, S., Kumai, T., and Kobayashi, S., *Ursodeoxycholic acid prevents hepatic cytochrome P450 isozyme reduction in rats with deoxycholic acid-induced liver injury*. J Hepatol, 1999. **31**(2): p. 263-70.
6. Rodrigues, C.M. and Steer, C.J., *Mitochondrial membrane perturbations in cholestasis*. J Hepatol, 2000. **32**(1): p. 135-41.
7. Vu, D.D., Tuchweber, B., Plaa, G.L., and Yousef, I.M., *Pathogenesis of lithocholate-induced intrahepatic cholestasis: role of glucuronidation and hydroxylation of lithocholate*. Biochim Biophys Acta, 1992. **1126**(1): p. 53-9.

8. Chang, T.K., Teixeira, J., Gil, G., and Waxman, D.J., *The lithocholic acid 6 beta-hydroxylase cytochrome P-450, CYP 3A10, is an active catalyst of steroid-hormone 6 beta-hydroxylation*. Biochem J, 1993. **291**(Pt 2): p. 429-33.
9. Araya, Z. and Wikvall, K., *6alpha-hydroxylation of taurochenodeoxycholic acid and lithocholic acid by CYP3A4 in human liver microsomes*. Biochim Biophys Acta, 1999. **1438**(1): p. 47-54.
10. Furster, C. and Wikvall, K., *Identification of CYP3A4 as the major enzyme responsible for 25-hydroxylation of 5beta-cholestane-3alpha,7alpha,12alpha-triol in human liver microsomes*. Biochim Biophys Acta, 1999. **1437**(1): p. 46-52.
11. Honda, A., Salen, G., Matsuzaki, Y., Batta, A.K., Xu, G., Leitersdorf, E., Tint, G.S., Erickson, S.K., Tanaka, N., and Shefer, S., *Side chain hydroxylations in bile acid biosynthesis catalyzed by CYP3A are markedly up-regulated in Cyp27^{-/-} mice but not in cerebrotendinous xanthomatosis*. J Biol Chem, 2001. **276**(37): p. 34579-85.
12. Jones, S.A., Moore, L.B., Shenk, J.L., Wisely, G.B., Hamilton, G.A., McKee, D.D., Tomkinson, N.C., LeCluyse, E.L., Lambert, M.H., Willson, T.M., Kliewer, S.A., and Moore, J.T., *The pregnane X receptor: a promiscuous xenobiotic receptor that has diverged during evolution*. Mol Endocrinol, 2000. **14**(1): p. 27-39.
13. Jones, A.L., *Anatomy of the Normal Liver*, in *Hepatology A Textbook of Liver Disease*, D. Zakim and T.D. Boyer, Editors. 1996, W.B. Saunders: Philadelphia. p. 3-32.
14. Munthe-Kaas, A.C., Berg, T., and Seljelid, R., *Distribution of lysosomal enzymes in different types of rat liver cells*. Exp Cell Res, 1976. **99**(1): p. 146-54.
15. Oinonen, T. and Lindros, K.O., *Zonation of hepatic cytochrome P-450 expression and regulation*. Biochem J, 1998. **329** (Pt 1): p. 17-35.

16. Muller, M. and Jansen, P.L., *Molecular aspects of hepatobiliary transport*. Am J Physiol, 1997. **272**(6 Pt 1): p. G1285-303.
17. Muller, M. and Jansen, P.L., *The secretory function of the liver: new aspects of hepatobiliary transport*. J Hepatol, 1998. **28**(2): p. 344-54.
18. Smit, J.J., Schinkel, A.H., Oude Elferink, R.P., Groen, A.K., Wagenaar, E., van Deemter, L., Mol, C.A., Ottenhoff, R., van der Lugt, N.M., van Roon, M.A., and et al., *Homozygous disruption of the murine mdr2 P-glycoprotein gene leads to a complete absence of phospholipid from bile and to liver disease*. Cell, 1993. **75**(3): p. 451-62.
19. Twisk, J., Hoekman, M.F., Mager, W.H., Moorman, A.F., de Boer, P.A., Scheja, L., Princen, H.M., and Gebhardt, R., *Heterogeneous expression of cholesterol 7 alpha-hydroxylase and sterol 27-hydroxylase genes in the rat liver lobulus*. J Clin Invest, 1995. **95**(3): p. 1235-43.
20. Ugele, B., Kempen, H.J., Kempen, J.M., Gebhardt, R., Meijer, P., Burger, H.J., and Princen, H.M., *Heterogeneity of rat liver parenchyma in cholesterol 7 alpha-hydroxylase and bile acid synthesis*. Biochem J, 1991. **276**(Pt 1): p. 73-7.
21. Fitz, J.G., *Cellular Mechanisms of Bile Secretion*, in *Hepatology A Textbook of Liver Disease*, D. Zakim and T.D. Boyer, Editors. 1996, W.B. Saunders: Philadelphia. p. 362-376.
22. Cooper, A.D. and Ellsworth, J.L., *Lipoprotein Metabolism*, in *Hepatology A Textbook of Liver Disease*, D. Zakim and T.D. Boyer, Editors. 1996, W.B. Saunders: Philadelphia. p. 92-130.

23. Horton, J.D., Goldstein, J.L., and Brown, M.S., *SREBPs: activators of the complete program of cholesterol and fatty acid synthesis in the liver*. J Clin Invest, 2002. **109**(9): p. 1125-31.
24. Nervi, F., Bronfman, M., Allalon, W., Depiereux, E., and Del Pozo, R., *Regulation of biliary cholesterol secretion in the rat. Role of hepatic cholesterol esterification*. J Clin Invest, 1984. **74**(6): p. 2226-37.
25. Tohma, M., Mahara, R., Takeshita, H., Kurosawa, T., Ikegawa, S., and Nittono, H., *Synthesis of the 1 beta-hydroxylated bile acids and identification of 1 beta,3 alpha,7 alpha-trihydroxy- and 1 beta,3 alpha,7 alpha,12 alpha-tetrahydroxy-5 beta-cholan-24-oic acids in human meconium*. Chem Pharm Bull (Tokyo), 1985. **33**(7): p. 3071-3.
26. Albers, J.J., Chen, C.H., and Adolphson, J.L., *Lecithin:cholesterol acyltransferase (LCAT) mass; its relationship to LCAT activity and cholesterol esterification rate*. J Lipid Res, 1981. **22**(8): p. 1206-13.
27. Hernandez, M.L., Martinez, M.J., Lopez de Heredia, M., and Ochoa, B., *Protein phosphatase 1 and 2A inhibitors activate acyl-CoA:cholesterol acyltransferase and cholesterol ester formation in isolated rat hepatocytes*. Biochim Biophys Acta, 1997. **1349**(3): p. 233-41.
28. Sherlock, S. and Dooley, J., *Diseases of the Liver and Biliary System*. 11 ed. 2002, Oxford: Blackwell Science. 706.
29. Vlahcevic, Z.R., Heuman, D.M., and Hylemon, P.B., *Physiology and Pathophysiology of Enterohepatic Circulation of Bile Acids*, in *Hepatology A Textbook of Liver Disease*, D. Zakim and T.D. Boyer, Editors. 1996, W.B. Saunders: Philadelphia. p. 376-417.

30. Carey, M.C., *Bile acids and bile salts: ionization and solubility properties*. Hepatology, 1984. **4**(5 Suppl): p. 66S-71S.
31. Fini, A. and Roda, A., *Chemical properties of bile acids. IV. Acidity constants of glycine-conjugated bile acids*. J Lipid Res, 1987. **28**(7): p. 755-9.
32. Hofmann, A.F., *The continuing importance of bile acids in liver and intestinal disease*. Arch Intern Med, 1999. **159**(22): p. 2647-58.
33. Bremmelgaard, A. and Sjovall, J., *Hydroxylation of cholic, chenodeoxycholic, and deoxycholic acids in patients with intrahepatic cholestasis*. J Lipid Res, 1980. **21**(8): p. 1072-81.
34. Thomassen, P.A., *Urinary bile acids in late pregnancy and in recurrent cholestasis of pregnancy*. Eur J Clin Invest, 1979. **9**(6): p. 425-32.
35. Hofmann, A.F., *Bile Acids: The Good, the Bad, and the Ugly*. News Physiol Sci, 1999. **14**: p. 24-29.
36. Roda, A., Minutello, A., Angellotti, M.A., and Fini, A., *Bile acid structure-activity relationship: evaluation of bile acid lipophilicity using 1-octanol/water partition coefficient and reverse phase HPLC*. J Lipid Res, 1990. **31**(8): p. 1433-43.
37. Axelson, M. and Sjovall, J., *Potential bile acid precursors in plasma--possible indicators of biosynthetic pathways to cholic and chenodeoxycholic acids in man*. J Steroid Biochem, 1990. **36**(6): p. 631-40.
38. Pandak, W.M., Schwarz, C., Hylemon, P.B., Mallonee, D., Valerie, K., Heuman, D.M., Fisher, R.A., Redford, K., and Vlahcevic, Z.R., *Effects of CYP7A1 overexpression on cholesterol and bile acid homeostasis*. Am J Physiol Gastrointest Liver Physiol, 2001. **281**(4): p. G878-89.

39. Chiang, J.Y.L., *Regulation of bile acid synthesis*. Front Biosci, 1998. **3**: p. D176-93.
40. Bjorkhem, I., Danielsson, H., and Wikvall, K., *Hydroxylations of bile acids by reconstituted systems from rat liver microsomes*. J Biol Chem, 1974. **249**(20): p. 6439-45.
41. Kuroki, S., Muramoto, S., Kuramoto, T., and Hoshita, T., *Sex differences in gallbladder bile acid composition and hepatic steroid 12 alpha-hydroxylase activity in hamsters*. J Lipid Res, 1983. **24**(12): p. 1543-9.
42. Hofmann, A.F., *Bile Acids*, in *The Liver Biology and Pathobiology*, I.M. Arias, J.L. Boyer, and N. Fausto, Editors. 1994, Raven Press LTD: New York. p. 677-718.
43. Hardison, W.G., Weiner, R.G., Hatoff, D.E., and Miyai, K., *Similarities and differences between models of extrahepatic biliary obstruction and complete biliary retention without obstruction in the rat*. Hepatology, 1983. **3**(3): p. 383-90.
44. Macdonald, I.A., Sutherland, J.D., Cohen, B.I., and Mosbach, E.H., *Effect of bile acid oxazoline derivatives on microorganisms participating in 7 alpha-hydroxyl epimerization of primary bile acids*. J Lipid Res, 1983. **24**(12): p. 1550-9.
45. MacDonald, I.A., Rochon, Y.P., Hutchison, D.M., and Holdeman, L.V., *Formation of ursodeoxycholic acid from chenodeoxycholic acid by a 7 beta-hydroxysteroid dehydrogenase-elaborating Eubacterium aerofaciens strain cocultured with 7 alpha-hydroxysteroid dehydrogenase-elaborating organisms*. Appl Environ Microbiol, 1982. **44**(5): p. 1187-95.
46. Bertolotti, M., Carulli, L., Concari, M., Martella, P., Loria, P., Tagliafico, E., Ferrari, S., Del Puppo, M., Amati, B., De Fabiani, E., Crestani, M., Amorotti, C., Manenti, A., Carubbi, F., Pinetti, A., and Carulli, N., *Suppression of bile acid synthesis, but not of*

- hepatic cholesterol 7alpha-hydroxylase expression, by obstructive cholestasis in humans.* Hepatology, 2001. **34**(2): p. 234-42.
47. Wang, H., Chen, J., Hollister, K., Sowers, L.C., and Forman, B.M., *Endogenous bile acids are ligands for the nuclear receptor FXR/BAR.* Mol Cell, 1999. **3**(5): p. 543-53.
48. Oude Elferink, R.P., Ottenhoff, R., van Wijland, M., Smit, J.J., Schinkel, A.H., and Groen, A.K., *Regulation of biliary lipid secretion by mdr2 P-glycoprotein in the mouse.* J Clin Invest, 1995. **95**(1): p. 31-8.
49. Chawla, A., Repa, J.J., Evans, R.M., and Mangelsdorf, D.J., *Nuclear receptors and lipid physiology: opening the X-files.* Science, 2001. **294**(5548): p. 1866-70.
50. Repa, J.J. and Mangelsdorf, D.J., *The role of orphan nuclear receptors in the regulation of cholesterol homeostasis.* Annu Rev Cell Dev Biol, 2000. **16**: p. 459-81.
51. Twisk, J., Hoekman, M.F., Muller, L.M., Iida, T., Tamaru, T., Ijzerman, A., Mager, W.H., and Princen, H.M., *Structural aspects of bile acids involved in the regulation of cholesterol 7 alpha-hydroxylase and sterol 27-hydroxylase.* Eur J Biochem, 1995. **228**(3): p. 596-604.
52. Heuman, D.M., Hernandez, C.R., Hylemon, P.B., Kubaska, W.M., Hartman, C., and Vlahcevic, Z.R., *Regulation of bile acid synthesis. I. Effects of conjugated ursodeoxycholate and cholate on bile acid synthesis in chronic bile fistula rat.* Hepatology, 1988. **8**(2): p. 358-65.
53. Heuman, D.M., Vlahcevic, Z.R., Bailey, M.L., and Hylemon, P.B., *Regulation of bile acid synthesis. II. Effect of bile acid feeding on enzymes regulating hepatic cholesterol and bile acid synthesis in the rat.* Hepatology, 1988. **8**(4): p. 892-7.

54. Song, W., Chen, J., Dean, W.L., Redinger, R.N., and Prough, R.A., *Purification and characterization of hamster liver microsomal 7alpha-hydroxycholesterol dehydrogenase. Similarity to type I 11beta-hydroxysteroid dehydrogenase.* J Biol Chem, 1998. **273**(26): p. 16223-8.
55. Sinal, C.J., Yoon, M., and Gonzalez, F.J., *Antagonism of the actions of peroxisome proliferator-activated receptor-alpha by bile acids.* J Biol Chem, 2001. **276**(50): p. 47154-62.
56. Sinal, C.J., Tohkin, M., Miyata, M., Ward, J.M., Lambert, G., and Gonzalez, F.J., *Targeted disruption of the nuclear receptor FXR/BAR impairs bile acid and lipid homeostasis.* Cell, 2000. **102**(6): p. 731-44.
57. Chiang, J.Y., Kimmel, R., and Stroup, D., *Regulation of cholesterol 7alpha-hydroxylase gene (CYP7A1) transcription by the liver orphan receptor (LXRalpha).* Gene, 2001. **262**(1-2): p. 257-65.
58. Parks, D.J., Blanchard, S.G., Bledsoe, R.K., Chandra, G., Consler, T.G., Kliewer, S.A., Stimmel, J.B., Willson, T.M., Zavacki, A.M., Moore, D.D., and Lehmann, J.M., *Bile acids: natural ligands for an orphan nuclear receptor.* Science, 1999. **284**(5418): p. 1365-8.
59. Lala, D.S., Syka, P.M., Lazarchik, S.B., Mangelsdorf, D.J., Parker, K.L., and Heyman, R.A., *Activation of the orphan nuclear receptor steroidogenic factor 1 by oxysterols.* Proc Natl Acad Sci U S A, 1997. **94**(10): p. 4895-900.
60. Janowski, B.A., Grogan, M.J., Jones, S.A., Wisely, G.B., Kliewer, S.A., Corey, E.J., and Mangelsdorf, D.J., *Structural requirements of ligands for the oxysterol liver X receptors LXRalpha and LXRBeta.* Proc Natl Acad Sci U S A, 1999. **96**(1): p. 266-71.

61. Song, C., Hiipakka, R.A., and Liao, S., *Selective activation of liver X receptor alpha by 6alpha-hydroxy bile acids and analogs*. *Steroids*, 2000. **65**(8): p. 423-7.
62. Xu, G., Salen, G., Shefer, S., Tint, G.S., Nguyen, L.B., Chen, T.S., and Greenblatt, D., *Increasing dietary cholesterol induces different regulation of classic and alternative bile acid synthesis*. *J Clin Invest*, 1999. **103**(1): p. 89-95.
63. Pandak, W.M., Ren, S., Marques, D., Hall, E., Redford, K., Mallonee, D., Bohdan, P., Heuman, D., Gil, G., and Hylemon, P., *Transport of cholesterol into mitochondria is rate-limiting for bile acid synthesis via the alternative pathway in primary rat hepatocytes*. *J Biol Chem*, 2002. **277**(50): p. 48158-64.
64. Meir, K., Kitsberg, D., Alkalay, I., Szafer, F., Rosen, H., Shpitzen, S., Avi, L.B., Staels, B., Fievet, C., Meiner, V., Bjorkhem, I., and Leitersdorf, E., *Human sterol 27-hydroxylase (CYP27) overexpressor transgenic mouse model. Evidence against 27-hydroxycholesterol as a critical regulator of cholesterol homeostasis*. *J Biol Chem*, 2002. **277**(37): p. 34036-41.
65. Oude Elferink, R.P., Meijer, D.K., Kuipers, F., Jansen, P.L., Groen, A.K., and Groothuis, G.M., *Hepatobiliary secretion of organic compounds; molecular mechanisms of membrane transport*. *Biochim Biophys Acta*, 1995. **1241**(2): p. 215-68.
66. Forker, E.L., *Mechanisms of hepatic bile formation*. *Annu Rev Physiol*, 1977. **39**: p. 323-47.
67. Jansen, P.L. and Muller, M., *Genetic cholestasis: lessons from the molecular physiology of bile formation*. *Can J Gastroenterol*, 2000. **14**(3): p. 233-8.

68. Fischer, S., Beuers, U., Spengler, U., Zwiebel, F.M., and Koebe, H.G., *Hepatic levels of bile acids in end-stage chronic cholestatic liver disease*. Clin Chim Acta, 1996. **251**(2): p. 173-86.
69. Ballatori, N. and Truong, A.T., *Glutathione as a primary osmotic driving force in hepatic bile formation*. Am J Physiol, 1992. **263**(5 Pt 1): p. G617-24.
70. Nathanson, M.H. and Boyer, J.L., *Mechanisms and regulation of bile secretion*. Hepatology, 1991. **14**(3): p. 551-66.
71. Hoffman, N.E., Iser, J.H., and Smallwood, R.A., *Hepatic bile acid transport: effect of conjugation and position of hydroxyl groups*. Am J Physiol, 1975. **229**(2): p. 298-302.
72. Anwer, M.S., O'Maille, E.R., Hofmann, A.F., DiPietro, R.A., and Michelotti, E., *Influence of side-chain charge on hepatic transport of bile acids and bile acid analogues*. Am J Physiol, 1985. **249**(4 Pt 1): p. G479-88.
73. Meier, P.J., St Meier-Abt, A., Barrett, C., and Boyer, J.L., *Mechanisms of taurocholate transport in canalicular and basolateral rat liver plasma membrane vesicles. Evidence for an electrogenic canalicular organic anion carrier*. J Biol Chem, 1984. **259**(16): p. 10614-22.
74. Wolters, H., Elzinga, B.M., Baller, J.F., Boverhof, R., Schwarz, M., Stieger, B., Verkade, H.J., and Kuipers, F., *Effects of bile salt flux variations on the expression of hepatic bile salt transporters in vivo in mice*. J Hepatol, 2002. **37**(5): p. 556-63.
75. Ananthanarayanan, M., Balasubramanian, N., Makishima, M., Mangelsdorf, D.J., and Suchy, F.J., *Human bile salt export pump promoter is transactivated by the farnesoid X receptor/bile acid receptor*. J Biol Chem, 2001. **276**(31): p. 28857-65.

76. Jones, P.M. and George, A.M., *Symmetry and structure in P-glycoprotein and ABC transporters what goes around comes around*. Eur J Biochem, 2000. **267**(17): p. 5298-305.
77. Lecureur, V., Sun, D., Hargrove, P., Schuetz, E.G., Kim, R.B., Lan, L.B., and Schuetz, J.D., *Cloning and expression of murine sister of P-glycoprotein reveals a more discriminating transporter than MDR1/P-glycoprotein*. Mol Pharmacol, 2000. **57**(1): p. 24-35.
78. Noe, J., Hagenbuch, B., Meier, P.J., and St-Pierre, M.V., *Characterization of the mouse bile salt export pump overexpressed in the baculovirus system*. Hepatology, 2001. **33**(5): p. 1223-31.
79. Byrne, J.A., Strautnieks, S.S., Mieli-Vergani, G., Higgins, C.F., Linton, K.J., and Thompson, R.J., *The human bile salt export pump: Characterization of substrate specificity and identification of inhibitors*. Gastroenterology, 2002. **123**(5): p. 1649-1658.
80. Stieger, B., Fattinger, K., Madon, J., Kullak-Ublick, G.A., and Meier, P.J., *Drug- and estrogen-induced cholestasis through inhibition of the hepatocellular bile salt export pump (Bsep) of rat liver*. Gastroenterology, 2000. **118**(2): p. 422-30.
81. Strautnieks, S.S., Bull, L.N., Knisely, A.S., Kocoshis, S.A., Dahl, N., Arnell, H., Sokal, E., Dahan, K., Childs, S., Ling, V., Tanner, M.S., Kagalwalla, A.F., Nemeth, A., Pawlowska, J., Baker, A., Mieli-Vergani, G., Freimer, N.B., Gardiner, R.M., and Thompson, R.J., *A gene encoding a liver-specific ABC transporter is mutated in progressive familial intrahepatic cholestasis*. Nat Genet, 1998. **20**(3): p. 233-8.
82. Perwaiz, S., Forrest, D., Mignault, D., Tuchweber, B., Phillip, M.J., Wang, R., Ling, V., and Yousef, I.M., *Appearance of atypical 3{alpha},6{beta},7{beta},12{alpha}-*

- tetrahydroxy-5{beta}-cholan-24-oic acid in spgp knockout mice. J Lipid Res, 2003. 44(3): p. 494-502.*
83. Wang, R., Lam, P., Liu, L., Forrest, D., Yousef, I.M., Mignault, D., Tuchweber, B., Phillips, M.J., and Ling, V., *Severe cholestasis induced by cholic acid feeding in knockout mice of Sister of P-glycoprotein. J Clin Invest, 2003. (Submitted).*
84. Nelson, D.R., *Mining databases for cytochrome P450 genes. Methods Enzymol, 2002. 357: p. 3-15.*
85. Gellner, K., Eiselt, R., Hustert, E., Arnold, H., Koch, I., Haberl, M., Deglmann, C.J., Burk, O., Buntfuss, D., Escher, S., Bishop, C., Koebe, H.G., Brinkmann, U., Klenk, H.P., Kleine, K., Meyer, U.A., and Wojnowski, L., *Genomic organization of the human CYP3A locus: identification of a new, inducible CYP3A gene. Pharmacogenetics, 2001. 11(2): p. 111-21.*
86. Omura, T. and Sato, R., *The Carbon Monoxide-binding Pigment of Liver Microsomes. J Biol Chem, 1964. 239(7): p. 2370-8.*
87. Vessey, D.A., *Metabolism of Xenobiotics by the Human Liver, in Hepatology A Textbook of Liver Disease, D. Zakim and T.D. Boyer, Editors. 1996, W.B. Saunders: Philadelphia. p. 257-305.*
88. Matsunaga, E., Umeno, M., and Gonzalez, F.J., *The rat P450 IID subfamily: complete sequences of four closely linked genes and evidence that gene conversions maintained sequence homogeneity at the heme-binding region of the cytochrome P450 active site. J Mol Evol, 1990. 30(2): p. 155-69.*
89. Finta, C. and Zaphiropoulos, P.G., *The human cytochrome P450 3A locus. Gene evolution by capture of downstream exons. Gene, 2000. 260(1-2): p. 13-23.*

90. Sakuma, T., Endo, Y., Mashino, M., Kuroiwa, M., Ohara, A., Jarukamjorn, K., and Nemoto, N., *Regulation of the expression of two female-predominant CYP3A mRNAs (CYP3A41 and CYP3A44) in mouse liver by sex and growth hormones*. Arch Biochem Biophys, 2002. **404**(2): p. 234-42.
91. Watkins, P.B., Wrighton, S.A., Schuetz, E.G., Molowa, D.T., and Guzelian, P.S., *Identification of glucocorticoid-inducible cytochromes P-450 in the intestinal mucosa of rats and man*. J Clin Invest, 1987. **80**(4): p. 1029-36.
92. Shimada, T., Yamazaki, H., Mimura, M., Inui, Y., and Guengerich, F.P., *Interindividual variations in human liver cytochrome P-450 enzymes involved in the oxidation of drugs, carcinogens and toxic chemicals: studies with liver microsomes of 30 Japanese and 30 Caucasians*. J Pharmacol Exp Ther, 1994. **270**(1): p. 414-23.
93. Yanagimoto, T., Itoh, S., Sawada, M., and Kamataki, T., *Mouse cytochrome P450 (Cyp3a11): predominant expression in liver and capacity to activate aflatoxin B1*. Arch Biochem Biophys, 1997. **340**(2): p. 215-8.
94. Nakayama, K., Sudo, Y., Sasaki, Y., Iwata, H., Takahashi, M., and Kamataki, T., *Studies on transcriptional regulation of Cyp3a16 gene in mouse livers by application of direct DNA injection method*. Biochem Biophys Res Commun, 2001. **287**(4): p. 820-4.
95. Sakuma, T., Takai, M., Endo, Y., Kuroiwa, M., Ohara, A., Jarukamjorn, K., Honma, R., and Nemoto, N., *A novel female-specific member of the CYP3A gene subfamily in the mouse liver*. Arch Biochem Biophys, 2000. **377**(1): p. 153-62.
96. Brown, N.P., Leroy, C., and Sander, C., *MView: a web-compatible database search or multiple alignment viewer*. Bioinformatics, 1998. **14**(4): p. 380-1.

97. Mangelsdorf, D.J. and Evans, R.M., *The RXR heterodimers and orphan receptors*. Cell, 1995. **83**(6): p. 841-50.
98. Makishima, M., Okamoto, A.Y., Repa, J.J., Tu, H., Learned, R.M., Luk, A., Hull, M.V., Lustig, K.D., Mangelsdorf, D.J., and Shan, B., *Identification of a nuclear receptor for bile acids*. Science, 1999. **284**(5418): p. 1362-5.
99. Xie, W., Radominska-Pandya, A., Shi, Y., Simon, C.M., Nelson, M.C., Ong, E.S., Waxman, D.J., and Evans, R.M., *An essential role for nuclear receptors SXR/PXR in detoxification of cholestatic bile acids*. Proc Natl Acad Sci U S A, 2001. **98**(6): p. 3375-3380.
100. Forman, B.M., Goode, E., Chen, J., Oro, A.E., Bradley, D.J., Perlmann, T., Noonan, D.J., Burka, L.T., McMorris, T., Lamph, W.W., and et al., *Identification of a nuclear receptor that is activated by farnesol metabolites*. Cell, 1995. **81**(5): p. 687-93.
101. Schuetz, E.G., Strom, S., Yasuda, K., Lecureur, V., Assem, M., Brimer, C., Lamba, J., Kim, R.B., Ramachandran, V., Komoroski, B.J., Venkataramanan, R., Cai, H., Sinal, C.J., Gonzalez, F.J., and Schuetz, J.D., *Disrupted bile acid homeostasis reveals an unexpected interaction among nuclear hormone receptors, transporters, and cytochrome P450*. J Biol Chem, 2001. **276**(42): p. 39411-8.
102. Grober, J., Zaghini, I., Fujii, H., Jones, S.A., Kliewer, S.A., Willson, T.M., Ono, T., and Besnard, P., *Identification of a bile acid-responsive element in the human ileal bile acid-binding protein gene. Involvement of the farnesoid X receptor/9-cis-retinoic acid receptor heterodimer*. J Biol Chem, 1999. **274**(42): p. 29749-54.

103. Lu, T.T., Makishima, M., Repa, J.J., Schoonjans, K., Kerr, T.A., Auwerx, J., and Mangelsdorf, D.J., *Molecular basis for feedback regulation of bile acid synthesis by nuclear receptors*. Mol Cell, 2000. **6**(3): p. 507-15.
104. Chiang, J.Y., Kimmel, R., Weinberger, C., and Stroup, D., *Farnesoid X receptor responds to bile acids and represses cholesterol 7alpha-hydroxylase gene (CYP7A1) transcription*. J Biol Chem, 2000. **275**(15): p. 10918-24.
105. Fickert, P., Zollner, G., Fuchsbichler, A., Stumptner, C., Pojer, C., Zenz, R., Lammert, F., Stieger, B., Meier, P.J., Zatloukal, K., Denk, H., and Trauner, M., *Effects of ursodeoxycholic and cholic acid feeding on hepatocellular transporter expression in mouse liver*. Gastroenterology, 2001. **121**(1): p. 170-83.
106. Staudinger, J.L., Goodwin, B., Jones, S.A., Hawkins-Brown, D., MacKenzie, K.I., LaTour, A., Liu, Y., Klaassen, C.D., Brown, K.K., Reinhard, J., Willson, T.M., Koller, B.H., and Kliewer, S.A., *The nuclear receptor PXR is a lithocholic acid sensor that protects against liver toxicity*. Proc Natl Acad Sci U S A, 2001. **98**(6): p. 3369-3374.
107. Synold, T.W., Dussault, I., and Forman, B.M., *The orphan nuclear receptor SXR coordinately regulates drug metabolism and efflux*. Nat Med, 2001. **7**(5): p. 584-90.
108. Xie, W., Barwick, J.L., Simon, C.M., Pierce, A.M., Safe, S., Blumberg, B., Guzelian, P.S., and Evans, R.M., *Reciprocal activation of xenobiotic response genes by nuclear receptors SXR/PXR and CAR*. Genes Dev, 2000. **14**(23): p. 3014-23.
109. Goodwin, B., Gauthier, K.C., Umetani, M., Watson, M.A., Lochansky, M.I., Collins, J.L., Leitersdorf, E., Mangelsdorf, D.J., Kliewer, S.A., and Repa, J.J., *Identification of bile acid precursors as endogenous ligands for the nuclear xenobiotic pregnane X receptor*. Proc Natl Acad Sci U S A, 2003. **100**(1): p. 223-8.

110. Hutterer, F., Bacchin, P.G., Denk, H., Schenkman, J.B., Schaffner, F., and Popper, H., *Mechanism of cholestasis. 2. Effect of bile acids on the microsomal electron transfer system in vitro.* Life Sci II, 1970. **9**(20): p. 1159-66.
111. Chen, J. and Farrell, G.C., *Bile acids produce a generalized reduction of the catalytic activity of cytochromes P450 and other hepatic microsomal enzymes in vitro: relevance to drug metabolism in experimental cholestasis.* J Gastroenterol Hepatol, 1996. **11**(9): p. 870-7.
112. Chen, J., Murray, M., Liddle, C., Jiang, X.M., and Farrell, G.C., *Downregulation of male-specific cytochrome P450s 2C11 and 3A2 in bile duct-ligated male rats: importance to reduced hepatic content of cytochrome P450 in cholestasis.* Hepatology, 1995. **22**(2): p. 580-7.
113. Rodrigues, C.M., Fan, G., Ma, X., Kren, B.T., and Steer, C.J., *A novel role for ursodeoxycholic acid in inhibiting apoptosis by modulating mitochondrial membrane perturbation.* J Clin Invest, 1998. **101**(12): p. 2790-9.
114. Bernstein, H., Payne, C.M., Bernstein, C., Schneider, J., Beard, S.E., and Crowley, C.L., *Activation of the promoters of genes associated with DNA damage, oxidative stress, ER stress and protein misfolding by the bile salt, deoxycholate.* Toxicol Lett, 1999. **108**(1): p. 37-46.
115. Higuchi, H., Yoon, J.H., Grambihler, A., Werneburg, N., Bronk, S.F., and Gores, G.J., *Bile acids stimulate cFLIP phosphorylation enhancing TRAIL-mediated apoptosis.* J Biol Chem, 2003. **278**(1): p. 454-61.
116. Heuman, D.M., Mills, A.S., McCall, J., Hylemon, P.B., Pandak, W.M., and Vlahcevic, Z.R., *Conjugates of ursodeoxycholate protect against cholestasis and hepatocellular*

- necrosis caused by more hydrophobic bile salts. In vivo studies in the rat.*
Gastroenterology, 1991. **100**(1): p. 203-11.
117. Schmucker, D.L., Ohta, M., Kanai, S., Sato, Y., and Kitani, K., *Hepatic injury induced by bile salts: correlation between biochemical and morphological events.* Hepatology, 1990. **12**(5): p. 1216-21.
118. Paolini, M., Pozzetti, L., Piazza, F., Cantelli-Forti, G., and Roda, A., *Bile acid structure and selective modulation of murine hepatic cytochrome P450-linked enzymes.* Hepatology, 1999. **30**(3): p. 730-9.
119. Paolini, M., Pozzetti, L., Montagnani, M., Potenza, G., Sabatini, L., Antelli, A., Cantelli-Forti, G., and Roda, A., *Ursodeoxycholic acid (UDCA) prevents DCA effects on male mouse liver via up-regulation of CYP and preservation of BSEP activities.* Hepatology, 2002. **36**(2): p. 305-14.
120. Rosen, H., Reshef, A., Maeda, N., Lippoldt, A., Shpizen, S., Triger, L., Eggertsen, G., Bjorkhem, I., and Leitersdorf, E., *Markedly reduced bile acid synthesis but maintained levels of cholesterol and vitamin D metabolites in mice with disrupted sterol 27-hydroxylase gene.* J Biol Chem, 1998. **273**(24): p. 14805-12.
121. Honda, A., Salen, G., Matsuzaki, Y., Batta, A.K., Xu, G., Leitersdorf, E., Tint, G.S., Erickson, S.K., Tanaka, N., and Shefer, S., *Differences in hepatic levels of intermediates in bile acid biosynthesis between Cyp27(-/-) mice and CTX.* J Lipid Res, 2001. **42**(2): p. 291-300.
122. Wietholtz, H., Marschall, H.U., Sjovall, J., and Matern, S., *Stimulation of bile acid 6 alpha-hydroxylation by rifampin.* J Hepatol, 1996. **24**(6): p. 713-8.

123. Teixeira, J. and Gil, G., *Cloning, expression, and regulation of lithocholic acid 6 beta-hydroxylase*. J Biol Chem, 1991. **266**(31): p. 21030-6.
124. Lundell, K., Hansson, R., and Wikvall, K., *Cloning and expression of a pig liver taurochenodeoxycholic acid 6alpha-hydroxylase (CYP4A21): a novel member of the CYP4A subfamily*. J Biol Chem, 2001. **276**(13): p. 9606-12.
125. Hagey, L.R., Schteingart, C.D., Rossi, S.S., Ton-Nu, H.T., and Hofmann, A.F., *An N-acyl glycytaurine conjugate of deoxycholic acid in the biliary bile acids of the rabbit*. J Lipid Res, 1998. **39**(11): p. 2119-24.
126. Rossi, S.S., Converse, J.L., and Hofmann, A.F., *High pressure liquid chromatographic analysis of conjugated bile acids in human bile: simultaneous resolution of sulfated and unsulfated lithocholyl amidates and the common conjugated bile acids*. J Lipid Res, 1987. **28**(5): p. 589-95.
127. Brown, T. and MacKey, K., *Analysis of RNA by Northern and Slot Blot hybridization*, in *Current Protocols in Molecular Biology*, F.M. Ausubel, et al., Editors. 1997, Harvard Medical School: Boston. p. 4.8.1-4.9.16.
128. Perwaiz, S., Tuchweber, B., Mignault, D., Gilat, T., and Yousef, I.M., *Determination of bile acids in biological fluids by liquid chromatography-electrospray tandem mass spectrometry*. J Lipid Res, 2001. **42**(1): p. 114-9.
129. Nichols, J.H., Ellefson, R.D., Hermansen, J., Schifferdecker, K., and Burritt, M.F., *Simultaneous HPLC determination of free, conjugated, and sulfated bile acids*. J Liquid Chrom, 1993. **16**(3): p. 681-97.
130. Vos, T.A., Hooiveld, G.J., Koning, H., Childs, S., Meijer, D.K., Moshage, H., Jansen, P.L., and Muller, M., *Up-regulation of the multidrug resistance genes, Mrp1 and Mdr1b*,

- and down-regulation of the organic anion transporter, Mrp2, and the bile salt transporter, Spgp, in endotoxemic rat liver. Hepatology, 1998. 28(6): p. 1637-44.*
131. Rippin, S.J., Hagenbuch, B., Meier, P.J., and Stieger, B., *Cholestatic expression pattern of sinusoidal and canalicular organic anion transport systems in primary cultured rat hepatocytes. Hepatology, 2001. 33(4): p. 776-82.*
 132. Salphati, L. and Benet, L.Z., *Modulation of P-glycoprotein expression by cytochrome P450 3A inducers in male and female rat livers. Biochem Pharmacol, 1998. 55(4): p. 387-95.*
 133. Stravitz, R.T., Sanyal, A.J., Pandak, W.M., Vlahcevic, Z.R., Beets, J.W., and Dawson, P.A., *Induction of sodium-dependent bile acid transporter messenger RNA, protein, and activity in rat ileum by cholic acid. Gastroenterology, 1997. 113(5): p. 1599-608.*
 134. Vlahcevic, Z.R., Eggertsen, G., Bjorkhem, I., Hylemon, P.B., Redford, K., and Pandak, W.M., *Regulation of sterol 12alpha-hydroxylase and cholic acid biosynthesis in the rat. Gastroenterology, 2000. 118(3): p. 599-607.*
 135. Chen, W., Owsley, E., Yang, Y., Stroup, D., and Chiang, J.Y., *Nuclear receptor-mediated repression of human cholesterol 7alpha-hydroxylase gene transcription by bile acids. J Lipid Res, 2001. 42(9): p. 1402-12.*
 136. Gupta, S., Pandak, W.M., and Hylemon, P.B., *LXR alpha is the dominant regulator of CYP7A1 transcription. Biochem Biophys Res Commun, 2002. 293(1): p. 338-43.*
 137. Altschul, S.F., Madden, T.L., Schaffer, A.A., Zhang, J., Zhang, Z., Miller, W., and Lipman, D.J., *Gapped BLAST and PSI-BLAST: a new generation of protein database search programs. Nucleic Acids Res, 1997. 25(17): p. 3389-402.*

138. Reyes, H. and Sjøvall, J., *Bile acids and progesterone metabolites in intrahepatic cholestasis of pregnancy*. *Ann Med*, 2000. **32**(2): p. 94-106.
139. del Castillo-Olivares, A. and Gil, G., *Alpha 1-fetoprotein transcription factor is required for the expression of sterol 12alpha -hydroxylase, the specific enzyme for cholic acid synthesis. Potential role in the bile acid-mediated regulation of gene transcription*. *J Biol Chem*, 2000. **275**(23): p. 17793-9.
140. Peet, D.J., Turley, S.D., Ma, W., Janowski, B.A., Lobaccaro, J.M., Hammer, R.E., and Mangelsdorf, D.J., *Cholesterol and bile acid metabolism are impaired in mice lacking the nuclear oxysterol receptor LXR alpha*. *Cell*, 1998. **93**(5): p. 693-704.
141. Paolini, M., Pozzetti, L., Piazza, F., Guerra, M.C., Speroni, E., Cantelli-Forti, G., and Roda, A., *Mechanism for the prevention of cholestasis involving cytochrome P4503A overexpression*. *J Investig Med*, 2000. **48**(1): p. 49-59.
142. Davis, R.A., Miyake, J.H., Hui, T.Y., and Spann, N.J., *Regulation of cholesterol-7alpha-hydroxylase: BAREly missing a SHP*. *J Lipid Res*, 2002. **43**(4): p. 533-43.
143. Robertson, G.R., Farrell, G.C., and Liddle, C., *Sexually dimorphic expression of rat CYP3A9 and CYP3A18 genes is regulated by growth hormone*. *Biochem Biophys Res Commun*, 1998. **242**(1): p. 57-60.
144. Jarukamjorn, K., Sakuma, T., Yamamoto, M., Ohara, A., and Nemoto, N., *Sex-associated expression of mouse hepatic and renal CYP2B enzymes by glucocorticoid hormones*. *Biochem Pharmacol*, 2001. **62**(2): p. 161-9.
145. Park, S.H., Liu, X., Hennighausen, L., Davey, H.W., and Waxman, D.J., *Distinctive roles of STAT5a and STAT5b in sexual dimorphism of hepatic P450 gene expression. Impact of STAT5a gene disruption*. *J Biol Chem*, 1999. **274**(11): p. 7421-30.

146. Werringloer, J. and Estabrook, R.W., *Heterogeneity of liver microsomal cytochrome P-450: the spectral characterization of reactants with reduced cytochrome P-450*. Arch Biochem Biophys, 1975. **167**(1): p. 270-86.
147. Arlotto, M.P., Trant, J.M., and Estabrook, R.W., *Measurement of steroid hydroxylation reactions by high-performance liquid chromatography as indicator of P450 identity and function*. Methods Enzymol, 1991. **206**: p. 454-62.
148. Roos, P.H., *Chromatographic separation and behavior of microsomal cytochrome P450 and cytochrome b5*. J Chromatogr B Biomed Appl, 1996. **684**(1-2): p. 107-31.

Appendix

Mouse Diet

Certified PicoLab Rodent 20 (5K75)

INGREDIENTS

Ground corn, dehulled soybean meal, wheat middlings, ground wheat, fish meal, cane molasses, wheat germ, dried beet pulp, brewers dried yeast, dehydrated alfalfa meal, ground oats, dried whey, soybean oil, calcium carbonate, salt, menadione dimethylpyrimidinol bisulfite (source of vitamin K), DL-methionine, choline chloride, vitamin A acetate, pyridoxine hydrochloride, cholecalciferol, dl-alpha tocopheryl acetate, thiamin mononitrate, nicotinic acid, calcium pantothenate, riboflavin, cyanocobalamin, folic acid, manganous oxide, zinc oxide, ferrous carbonate, copper sulfate, zinc sulfate, calcium iodate, cobalt carbonate.

CHEMICAL COMPOSITION

Moisture content is assumed to be 10.0% for the purpose of calculations.

Nutrients (expressed as % of ration except where otherwise indicated)

Protein, % 21.0

Arginine, % 1.26

Histidine, % 0.51

Lysine, % 1.20

Tyrosine, % 0.59

Valine, % 1.06

Glutamic Acid, % 4.54

Taurine, % 0.02

Cystine, % 0.30

Isoleucine, % 1.09

Methionine, % 0.43

Threonine, % 0.80

Serine, % 1.08

Alanine, % 1.23

Glycine, % 0.97

Leucine, % 1.65

Phenylalanine, % 0.94

Tryptophan, % 0.27

Aspartic Acid, % 2.30

Proline, % 1.54

Fat (ether extract), % 4.5 Fat (acid hydrolysis), % 5.4

Cholesterol, ppm 142

Linoleic Acid, % 2.16 Linolenic Acid, % 0.25

Arachidonic Acid, % 0.01 Omega-3 Fatty Acids, % 0.38

Total Saturated Fatty Acids, % 0.97

Total Monounsaturated Fatty Acids, % 0.98

Fiber (Crude), % 4.4

Neutral Detergent Fiber³, % 14.4 Acid Detergent Fiber⁴, % 6.1

Nitrogen-Free Extract (by difference), % 54.4

Starch, % 36.6

Glucose, % 0.20

Sucrose, % 3.20

Fructose, % 0.30

Lactose, % 1.30

Total Digestible Nutrients, % 76.8

Gross Energy, kcal/gm 4.05

Physiological Fuel Value⁵, kcal/gm 3.42

Metabolizable Energy, kcal/gm 3.10

Minerals

Ash, % 5.7

Phosphorus, % 0.58

Potassium, % 0.99

Sulfur, % 0.28

Chlorine, % 0.53

Calcium, % 0.81

Phosphorus (non-phytate), % 0.30

Magnesium, % 0.21

Sodium, % 0.30

Fluorine, ppm 7.1

Iron, ppm 220
Manganese, ppm 79
Cobalt, ppm 0.88
Chromium, ppm 0.68

Vitamins

Carotene, ppm 1.6
Thiamin Hydrochloride, ppm 18
Niacin, ppm 90
Choline Chloride, ppm 1800
Pyridoxine, ppm 8.0

B12, mcg/kg 20
Vitamin D3 (added), IU/gm 2.2
Ascorbic Acid, mg/gm --

Calories provided by:
Protein, % 24.554
Fat (ether extract), % 11.839
Carbohydrates, % 63.607

Zinc, ppm 87
Copper, ppm 12
Iodine, ppm 0.98
Selenium, ppm 0.25

Vitamin K (as menadione), ppm 3.3
Riboflavin, ppm 8.1
Pantothenic Acid, ppm 17
Folic Acid, ppm 1.3
Biotin, ppm 0.2

Vitamin A, IU/gm 26
Vitamin E, IU/kg 100